ABSTRACT

Title of Dissertation: IMMOBILIZATION OF ENZYMES ON NANOPOROUS SILICA COMPOSITES

Allan E. David, Ph.D., 2004

Dissertation Directed By: Associate Professor N.S. Wang, Department of Chemical Engineering
Dr. A.J. Yang, ISTN, Inc.

In this work, the sol-gel process is used to produce a chemically surface modified gel (CSMG) with a high modification density. Sodium silicate, an inexpensive alternative to tetraethoxysilicate, is used as the silica source. The produced N-CSMG material is shown to have a high amino functional group loading of 3.6 mmol/g SiO_2; significantly higher than commercially available matrices.

One aspect of this work deals with retention of an open morphology to provide access of interior surface areas. Activation of N-CSMG, in the wet state, with glutaraldehyde produces GA-N-CSMG which is used for the immobilization of enzymes. Nitrogen adsorption (BET), SEM, and thermogravimetric analysis were used to study material properties.

Invertase was used as a model enzyme to measure the immobilizing character of the GA-N-CSMG material. Using an optimized immobilization protocol, a very high loading of 700 mg invertase per gram GA-N-CSMG is obtained; significantly higher than other published results. The immobilized activity of 246,000 U/g GA-N-

CSMG is also greater than any other in literature. Immobilized invertase showed almost 99% retention of free enzyme activity and no loss in catalytic efficiency.

A major part of this work consists of a scale-up in production of low molecular weight protamine (LMWP), a peptide with possible pharmaceutical applications. Since LMWP is produced by the enzymatic hydrolysis of native protamine, the production of LMWP was improved upon through the immobilization of the enzyme thermolysin. The immobilized thermolysin proved to be quite robust and was integrated into a continuous flow-through system for LMWP production. The purification of LMWP was also improved upon by optimization of a heparin-affinity chromatographic process. Optimization allowed for a scale-up of LMWP production from 5 μg/min to 167 μg/min; a 33-fold increase in production with improved product purity and recovery.

The last part of this work improves on the N-CSMG material by developing particles of controllable size and regular shape. Directions for further improvement of N-CSMG are discussed, including addition of the pH sensitive biopolymer chitosan. The improved surface coverage of mesoporous silica gels will provide significant benefits in the areas of catalysis, water treatment, sensors, drug delivery, and tissue engineering.

IMMOBILIZATION OF ENZYMES ON NANOPOROUS, SILICA COMPOSITES

By

Allan E. David

Dissertation submitted to the Faculty of the Graduate School of the
University of Maryland, College Park, in partial fulfillment
of the requirements for the degree of
Doctor of Philosophy
2004

Advisory Committee:
Associate Professor N.S. Wang, Chair/Co-Advisor
Adjunct Professor A.J. Yang, Co-Advisor (ISTN, Inc.)
Assistant Professor S.H. Ehrman
Associate Professor I. K. Lloyd
Assistant Professor T.R. Pulliam-Holoman

Dedication

To
my wife,

Helen,

for her endless love and patience.

And also to
my parents,

Emerson and Beulah David,

who made all this possible.

"… whatever you do,
do all to the glory of God."
1 Cor. 10:31 (NKJV)

Acknowledgements

This dissertation would not have been possible without guidance from my advisors Dr. Nam Sun Wang and Dr. Arthur Yang. Dr. Wang has always been available when needed and made the process more enjoyable with canoe trips. Our conversations on possible directions of research have stirred the imagination and made me look into areas I had not considered before. Dr. Yang has treated me like a member of his family and has pushed me to maximize my abilities. He has not only given me a better understanding of the fundamentals of science but, more importantly, has shared his lessons of life. I am also indebted to him and the Industrial Science & Technology Network, Inc. (ISTN) for financial support.

The members of my dissertation committee, Dr. Sheryl Ehrman, Dr. Isabel Lloyd, and Dr. Tracey Pulliam-Holoman, have generously shared their time. I would also like to thank Dr. Lloyd for providing access to her labs for BET and TGA analysis. Dr. Doug English very kindly provided access to his confocal fluorescence microscope.

I must acknowledge the support and friendship of everyone at ISTN, Inc as each one has helped me along this journey. Dr. Roman Domszy has been wiling to share his expertise and assist in any way with material characterization. I enjoyed our lunches together.

I very much appreciate Dr. Victor Yang at the School of Pharmacy, University of Michigan, giving me the opportunity to work with and learn from his group. Members of the Yang group have made me feel very much at home and have been fun to work with.

I am grateful to all of my colleagues in the Chemical Engineering Department for their friendship. Darryl, Patricia, Quanzeng, and Tosin were always willing to help and we enjoyed a lot of laughter together. I must also thank Seth and Ellis for the time they spent in the lab as undergraduates.

I have had many uncles, aunts, cousins, and friends who have encouraged me all these years; their prayers and support have carried me through this process and is very much appreciated.

Finally, I would like to thank my wife, my parents, my brother - Allwyn, and my sister - Angie for their support and encouragement. They have always been there when needed and this could not have been accomplished without them.

I have been truly blessed with help and support from this wonderful group of people.

"The boundary lines have fallen for me in pleasant places;
surely I have a delightful inheritance."
Psalm 16:6 (NIV)

Table of Contents

List of Tables

List of Figures

Chapter 1: Introduction

Organic-inorganic composites have generated a significant amount of interest because of their inherent properties. The rigid structure of the inorganic component combined with the functionality of organic groups has yielded advanced materials with improved properties for optics, electronics, protective coatings, sensors, catalysis, and many other fields (Sanchez, Soler-Illia et al. 2001). Silica-based inorganic composites have received much attention since the development of the M41S periodic mesoporous matrix (Kresge, Leonowicz et al. 1992) in the early 1990s. Since then a number of protocols have been developed, using a wide array of conditions, to produce a variety of mesoporous silicas (Sayari and Hamoudi 2001). Two general methods are available for the chemical modification of mesoporous silicas: (1) post-synthesis grafting (Beck, Vartuli et al. 1992) and (2) co-condensation (Burkett, Sims et al. 1996). Post-synthesis grafting involves the reaction of organosilanes with silanol groups present on the matrix surface. Generally this method results in an inhomogeneous surface coverage of the function group with concentration at the outer surface and pore entrances (Lim and Stein 1999).

In the co-condensation process, organosilanes are mixed with the silica sol prior to gelation and condensation between the sol and organosilanes results in a silica matrix with a chemically active surface. A homogenous distribution of functional groups can be achieved with the co-condensation process (Lim and Stein 1999) with higher loading densities (Mori and Pinnavaia 2001; Kruk, Asefa et al. 2002). However, practically all co-condensation processes to date make use of tetraethoxysilane (TEOS) or tetramethoxysilane (TMOS) as the source of silica. Only

recently has a report been published detailing the synthesis of mesoporous organosilicas from sodium silicate in a co-condensation process (Yu, Gong et al. 2004). Yu et. al. vigorously mixed acidified solutions of sodium silicate and organosilanes and allowed hydrolysis to occur for one hour. The solution temperature was then raised to 50 °C and NaF added to induce gelation. With this method methyl, mercapto, and vinyl surface modifications were introduced to mesoporous silica gels.

Although there are many reports using TEOS to produce amino-functionalized silica gels (Lee, Kim et al. 2001; Bois, Bonhomme et al. 2003; Yokoi, Yoshitake et al. 2004), only one reference has been found for a co-condensation process which uses sodium silicate (Shah, Kim et al. 2004). They report a maximum of 50 mol% functionalization of available sites with 3-aminopropyltrimethoxysilane.

While tremendous advances have been made in the fabrication of composites with a high surface area, high functional loading, and controlled morphology, the immobilization of biological specie on these composites has not seen a significant improvement compared to materials of the past. Efficient immobilization of biologics requires not only a matrix with designed properties, but also the proper protocols and processing conditions. Design of such a system requires a proper understanding of the underlying process and an ability to control it.

1.1 Motivation

Advances in biochemistry have made it possible to engineer and produce a variety of proteins. In some cases, these proteins (e.g. insulin, human growth hormone, etc.) are used as medicines to enhance the biological system or to negate a

deficiency (Baker, Meldrum et al. 2003). One exciting and growing area is that of gene therapy. Insight gained in the human genome allows for drugs to be customized for individuals (Gamradt and Lieberman 2004). It could also, someday, provide a means of correcting "mutations" in the DNA structure itself (Pannier and Shea 2004).

Many proteins are also finding their way into industrial processes as catalysts. Enzymes are large protein molecules that significantly increase rates of reaction by lowering the activation energy. An example of this is the decarboxylation of orotic acid, which spontaneously decarboxylates with a half-life of 78 million years at room temperature. The enzyme Orotidine 5'-phosphate decarboxylase increases this rate by 10^{17} fold (Fersht 1999). The ability of enzymes to bind specific substrates and mediate their reaction into stereo-specific products has tremendous potential.

The efficiency of biological enzymes in reaction mediation makes them an attractive tool for use in industrial production processes. Enzymes offer four major advantages:

- **Higher reaction rates**: up to a factor of 10^{12} times greater than the uncatalyzed reactions;
- **Reaction conditions**: enzymes operate at temperatures less than 100^{o}C, atmospheric pressures and near neutral pH;
- **Reaction specificity**: enzyme specificity for both substrate and product produces fewer side reactions;
- **Regulation**: enzyme activity may be regulated by the presence of various molecules.

Because of their ability to improve reaction rates and product specificity, enzymes are a significant part of many industrial processes (Cheetham 1995). They are extensively used in the manufacturing of pharmaceutical drugs and fine chemical production, among many other applications. The use of enzymes in manufacturing processes does possess a few drawbacks; enzymes are a relatively expensive reaction component and therefore increase production costs. They are also extremely sensitive to environment conditions and can be easily denatured. Any manufacturing process must consider the conservation of the enzymes within the reactor while also maintaining their activity.

Where enzymes are used to catalyze a homogenous reaction, protein purification techniques can be used to recover and reuse the enzymes. Several techniques are available for protein separation including chromatographic, electrophoretic, and extractive (Gordon, Moore et al. 1990). Each of these methods has a role in protein purification and they are often used in some combination.

Affinity chromatography is often the method of choice for processes which require high purity (Narayanan 1994). Chromatography methods operate by taking advantage of slight property variations of the proteins. In a broth consisting of the hundreds or thousands of biological molecules present in living systems, these slight property variations often are so small that many molecule types are brought out of solution (Isaacs 1996). Affinity chromatography, on the other hand, works through the specific interaction of one molecule type (ligand) with another molecule type (substrate) (Yan 1996).

Often, the most expensive step in enzyme production is the downstream separation and purification of the desired protein (Conder and Hayek 2000). Therefore, use of these methods for enzyme recovery from a homogeneous catalysis process can significantly increase production costs. One method of lowering these processing requirements is to use a heterogeneous catalyst – an immobilized enzyme (Beck and Suginome 1991; Chitnis and Sharma 1997; Laszlo 1998).

A method that has long been studied, and has been put into some practice, is the immobilization of enzymes on a solid support. There are three basic methods for enzyme immobilization: entrapment, cross-linking and carrier binding (Tischer and Wedekind 1999). Entrapment, as the name suggests, is basically the trapping of the enzyme within a cage-like, porous network that allows the substrate to diffuse through. The relatively large enzymes are unable to, or very slowly, diffuse out of the solid network and are therefore retained. Cross-linking is achieved through intermolecular bonding between enzyme molecules. Carrier binding involves the formation of interactions between enzyme and a support. This method can be further categorized as ionic binding, physical adsorption or covalent binding depending on the method.

There are many advantages to the immobilization of proteins on a solid support (Monsan and Combes 1988; Bergogne, Fennouh et al. 2000; Mateo, Torres et al. 2003):

- Improved enzyme shelf-life (half-life);
- Improved stability in adverse reaction conditions;
- Improved stability in the presence of organic solvents;

- Separation from product stream;
- Allows for continuous flow operations and repetitive usage; and
- Increased enzymatic activity in few cases.

A variety of immobilization materials are available for use in both laboratories and industrial processes with many of these materials based on organic polymers (e.g. agarose, dextran, etc.) which fall under the category of "soft gels" (Abourebyeh, Korber et al. 1991; Camperi, Grasselli et al. 2004). The major drawback of soft gels is their low mechanical strength and in some cases low thermal and chemical stability (Tharakan, Highsmith et al. 1992). Low mechanical strength materials can only sustain a small pressure drop and thus they are limited to low solution flow rates when operated as a packed bed reactor (PBR). This can be a major drawback in industrial processes. The mechanical strength can also limit column size and thereby affect the reactor's efficiency.

The use of silica in enzyme immobilization can provide several benefits:

- **High surface areas** (500 – 1000 m^2/g) provide the possibility of high enzyme loadings on the matrix. This would increase the rate of reaction, measured as the product produced over time.
- **Greater mechanical strength** would allow the use of column reactors at higher flow rates without matrix distortion.
- The silica matrix consists of **surface hydroxyl groups** that can be readily used for a variety of surface modifications. A number of functionalities (thiol, amine, etc) have been introduced on the surface at high loadings (7.5 mmole/g of silica for thiol modification).

- The **hydrophilic silica surface** would minimize fouling problems often encountered with the hydrophobic "soft gels". Organic molecules interact with the surface of these organic gels, creating a film on the surface and interfering with enzyme activity (Amanda and Mallapragada 2001; Li, Wu et al. 2003).
- The **open pore morphology** of silica gels allows substrates to quickly move into the interior regions of the particle.
- Solvents used in the processing of silica materials are **environmentally benign**.

Although enzymes have been immobilized on silica gels, the vast majority of these have been done on pre-formed gels. Immobilization on pre-formed gels involve a number of steps 1) activation of the gel surface, 2) surface modification with a reactive functional group, 3) attachment of a cross-linking agent, and 4) introduction of the enzyme. This method has been successfully used for enzyme immobilization; however the loadings have been limited. When the activated gel is introduced to the enzyme solution, enzyme immobilization first occurs at the pore openings. At higher loadings, the enzymes can effectively block the pores preventing enzyme diffusion into the interior. A more effective method must be developed for the immobilization of enzymes.

1.2 Goals and Objectives

Commercial use of enzymes is limited by their relative high cost. The major goal of this research is to develop methods for the efficient immobilization of enzymes on silica. Ideally, a "one-pot" process would accomplish the enzyme

immobilization and gel formation simultaneously; increasing the loading while reducing the required processing. However, as will be explained further, a "one-pot" process would likely result in enzyme deactivation due to the presence of chemically active small molecules. In this work, we seek to achieve significantly improved loadings while also simplifying the process.

Specific objectives of this work are:

- Surface modification of silica gel with amino functional groups;
- Immobilization of invertase to develop immobilization techniques;
- Compare activity and yield of immobilized enzymes with that of the free enzyme;
- Immobilize thermolysin for Low Molecular Weight Protamine (LMWP) production; and
- Control of silica gel morphology.

The goal of this research is to develop an effective method for the immobilization of bio-molecules onto silica surfaces. An immobilization method will first be developed for invertase, which hydrolyzes sucrose into glucose and fructose. The method will then be applied to the immobilization of thermolysin, a protease used for the production of Low Molecular Weight Protamine (LMWP) from native protamine.

1.3 Relevance and Expected Benefits

Rapid advances in microbiological research have brought about a greater understanding of biological molecule function and much progress in the area of protein engineering. The result is a growing possibility for the use of these biological

molecules as catalysts for commercial processes. However, before any of these molecules can be used commercially, the process must prove to be economically feasible.

Often enzymes are relatively expensive compared to their substrates and are lost in the homogenous reaction process. One method of cost reduction is to recycle and reuse the enzyme from the product stream. This would significantly improve the economics, by optimizing enzyme use, only if the separation can be done efficiently and cost-effectively. Separation can be greatly facilitated by immobilizing the enzyme on a solid matrix. The development of an immobilization technique is proposed for invertase and thermolysin, both on a nanoporous silica matrix.

Potential customers for the product vary from research labs, to academia and large pharmaceutical companies. The market place currently contains a variety of options that can be used for the immobilization of biological molecules. These materials have considerable limitations when it comes to large-scale processing. The engineered, silica based material would provide some property improvements and could be ideal for large-scale processes. Such materials can find use in heterogeneous catalysis, affinity chromatography, membrane reactors, bio-sensors and drug delivery, among many others.

Chapter 2: Silica Gel Synthesis

2.1 Sources of silica

Silicon is the second most abundant element on earth, after oxygen, making-up approximately 25 percent of the earth's crust by weight; largely found in the form of oxides such as sand and clay (Winter 2003). Sodium silicate, of formula Na_2SiO_3, is commercially produced by the reaction of soda ash and sand in a furnace. Also know as "water glass", sodium silicate is used as an adhesive (Suleman and Hamid 1997), detergent (Keeley 1983), and fire-retardant (Nassar, Fadali et al. 1999). In addition to sodium silicate, several organic silica precursors are available, such as tetraethoxysilane (TEOS), of formula $Si(OC_2H_5)_4$, and tetramethoxysilane (TMOS), of formula $Si(OCH_3)_4$.

The advantages and disadvantages of each of these precursors must be carefully considered when designing a sol-gel protocol to produce porous silica gels. TEOS and TMOS present the advantage of relatively high purity. However, the organic precursors have low solubility in water, prior to hydrolysis, and require the addition of alcohol as a co-solvent (Brinker and Scherer 1990). Sodium silicate, on the other hand, is inexpensive and highly soluble in water. However, it has a high ionic strength, which may be problematic, and the gel must be extensively washed to remove the considerable amount of salt which forms. Reagent grade TEOS can be purchased from Sigma-Aldrich at a cost of $38.90 per liter (Cat. No. 131903, 2004). Sodium silicate of the same grade has a cost of $22.70 per liter (Cat. No. 338443,

2004). This gives a savings of more than 40 percent, compared to TEOS, which can be significant on an industrial scale.

In this work, sodium silicate is used as the initial source of silica. However, in order to reduce the solution ionic strength, a cation-exchange Amberlite™ resin is used to exchange sodium ions for hydrogen. A column filled with the ion-exchange resin is activated by flowing through an acid (e.g. hydrochloric acid) to introduce hydrogen ions onto the resin surface, which is sulfonic acid-functionalized and negatively charged. The column is then washed with deionized water before the sodium silicate solution is passed through. Since the silicate solution is sodium-rich, relative to the resin, at any given point along the column, there is an exchange of sodium and hydrogen such that sodium silicate (pH>12) is transformed into silicic acid (pH<3):

$$Na_2SiO_3 \xrightarrow[ion\ \ exchange]{} H_2SiO_3 \qquad (1)$$

Silicic acid can be used to fabricate silica gels in a sol-gel process by simply adjusting the solution pH to neutral with a base.

2.2 The sol-gel process

A sol, by definition, is a suspension of solid particles, with size between 1-1000 nm, in a liquid continuous phase. The sol-gel process refers to the creation of a continuous, solid network through a change of interactions between the colloidal particles; changing the systems characteristics from that of a liquid to that of a gel. The result is a bi-continuous system composed of the continuous, interpenetrating solid and liquid phases. Using a patent-pending process from the Industrial Science and Technology Network, Inc. (ISTN), silicic acid, $Si(OH)_{4,}$ is obtained without the

alcohol generation associated with hydrolysis of TEOS and TMOS. In many cases, a high alcohol content results in protein denaturation (Berman and Boyer 1972; Schellman and Hawkes 1979; Alonso and Dill 1991; Stepuro, Lapshina et al. 1991). Compared with other sol-gel processes that start directly from a colloidal silica, ISTN's process using silicic acid starts with a much lower ionic strength. The low ionic charge is critical to the modification reaction because of an improved solubility for the organic ligand components (Cserhati and Illes 1991; Tasleem, Durani et al. 2004). Freshly prepared silicic acid is composed of silica particles with very small particle size (2 - 10 nm) and, thus, a very large surface area and plenty of active silanol groups. A silane coupling reagent may be used to incorporate ligand groups on the particle surface and the modified silica sol can be gelled quickly with an adjustment of pH.

The sol-gel process consists of three basic steps: 1) gelation; 2) ageing; and 3) drying. During gelation, the synthesis of silica polymers occurs through the simultaneous hydrolysis and condensation reactions (Figure 2-1):

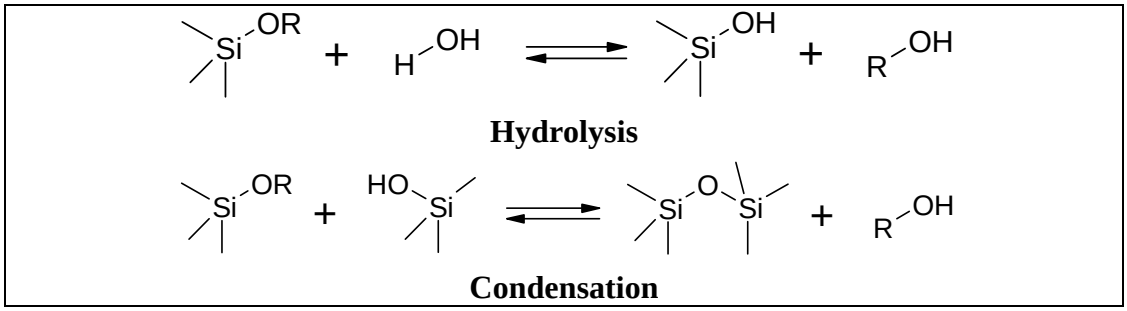

Figure 2-1 Hydrolysis and Condensation reactions during the sol-gel process

The synthesis of silica gel is easily carried out through either an acid or base catalyzed reaction. Under these conditions the silicate undergoes polymerization to form a stable and ordered mesoporous silica gel (Khushalani, Ozin et al. 1999).

Hydrolysis, through an S_N2 mechanism, occurs by nucleophilic substitution. Condensation between the precursors results in the formation of a 3-dimensional network, or gel, which grows to encapsulate the solvent phase. It is the relative rates of hydrolysis and condensation that determines the properties of the silica gel formed. Acidic conditions favor hydrolysis leading to the growth of silica filaments, while basic conditions favor condensation and yields colloidal silica (Brinker and Scherer 1990). Gelation can be accomplished by a one-step process which involves the use of a single base or acid as catalyst. In addition, a two-step process can also be used by initiating hydrolysis with an acid catalyst and following this with base-catalyzed condensation. A number of factors, including the precursor, temperature, pH, catalyst, and water content, can be manipulated to effect a variation in the reaction rates (Boonstra and Bernards 1989; Coltrain and Kelts 1990; Bernards, Vanbommel et al. 1991). In this work, a two-step process is used in the making of silica gels as detailed in later sections.

After gelation, the next phase in sol-gel fabrication is the ageing process. Although the gel formed in the initial phase entraps the entire solvent volume, the hydrolysis and condensation reactions continue to occur within the gel (Scherer 1988). During this phase, some gel shrinkage is seen along with a corresponding expulsion of solvent. Gels of desired densities can be obtained by simply varying the ageing time (Kistler 1937).

Typically, an application for silica gel requires the removal of the solvent phase and this is the final stage of the sol-gel process – the drying step. Drying conditions can have a significant effect on the final gel properties (Harris, Cooke et

al. 1998). In drying, as the liquid is removed from the gel, a liquid-vapor interface is developed within the gel and this creates significant capillary pressures as described by the LaPlace equation:

$$\Delta p = \frac{2\gamma(\cos\theta)}{r} \qquad (2)$$

where Δp is the capillary pressure difference, γ is the specific surface energy of the liquid-vapor interface, θ is the contact angle, and r is the pore radius. With a pore radius on the nanometer scale, the large stresses generated can result in permanent shrinkage of the gels. In the following section we discuss methods for alleviating gel shrinkage.

2.3 Control of Morphology

Over the past decade, a great deal of research has focused on the development of mesoporous materials due to their remarkable properties. These ordered mesoporous structures have shown improved mechanical behavior and also optical, electrical and biological properties (Ober and Wegner 1997). With such an array of properties available, the possible applications of this material are vast ranging from insulation, to optical wave-guides, chromatography packing and even gas separation and membrane reactors (Nair, Elferink et al. 1996; Pajonk 2003). A significant barrier in the processing of such materials is control of the silica gel morphology.

Silica gels with a mesoporous structure and high surface areas were first reported in the preparation of aerogels by Steven Kistler in 1931. In this work, silica gels were prepared by reacting sodium silicate with hydrochloric acid. After extensive washings, to remove salts, water is replaced with an alcohol and the gels dried in an autoclave at supercritical conditions (T^c_{EtOH} = 216 °C, P^c_{EtOH} = 956 psi).

Kistler's purpose for using supercritical conditions was to, in his words, "replace the liquid with air by some means in which the surface of the liquid is never permitted to recede within the gel" (Kistler 1931). Prior to this work, xerogels were prepared by the air drying of silica gels and yielded void volumes between 30-50%. With the use of supercritical drying, Kistler was able to produce aerogels with void volumes up to 99% and he stated that the gel morphology could be tuned by a variation of the drying conditions (Kistler 1937). This method, however, is not commercially viable because it is time consuming and requires a great deal of capital investment. The washing and solvent exchange process is very tedious and time consuming. In addition, the high temperatures and pressures required to obtain supercritical conditions creates a potentially explosive situation. The 1980s saw the development of a supercritical drying process using liquid CO_2 at much lower temperature and pressure (T_c = 31.5 °C, P_c = 1072 psi) (Tewari, Hunt et al. 1985) which is the current standard used in aerogel production.

Wet silica gel contains a considerable amount of silanol groups along its surface (Perry and Li 1991; De, Kundu et al. 1993). These groups provide a valuable resource for surface modification, but can also destroy gel porosity by undergoing condensation reactions with each other (Duffours, Woignier et al. 1996). This problem is magnified further during the drying process when capillary stresses created by the vapor-liquid interface of the escaping solvent crack and collapse the porous structure. Condensation of surface silanol groups can then result in an irreversible loss of porosity (Woignier, Despetis et al. 2000).

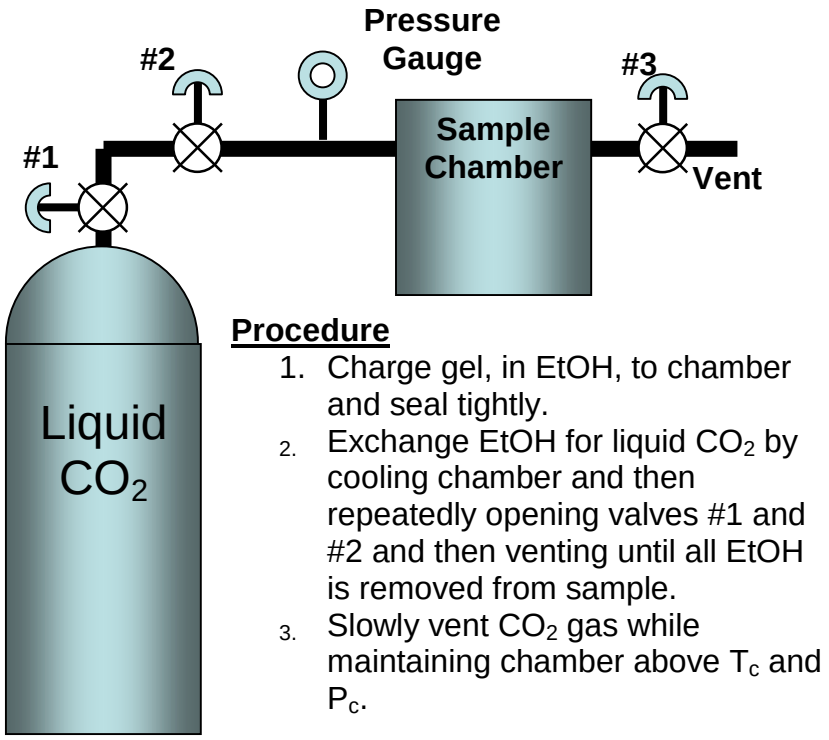

Figure 2-2 Sample apparatus design for supercritical CO_2 drying.

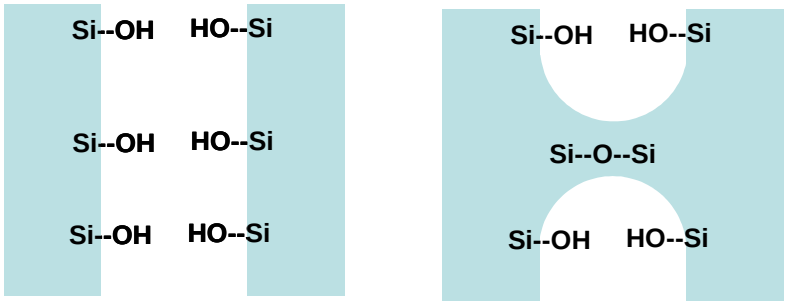

Figure 2-3 Collapse of pores due to condensation of surface hydroxyl (silanol) groups.

Permanent shrinkage of silica gels occurs due to condensation that occurs between the surface hydroxyl groups (see Figure 2-3). This can obviously result in the collapse of pores and degradation of material properties (i.e. surface area, porosity). However, shrinkage also serves to increase the mechanical strength of the silica gel. It is therefore important that the degree of condensation be carefully controlled to obtain gels of desired morphology.

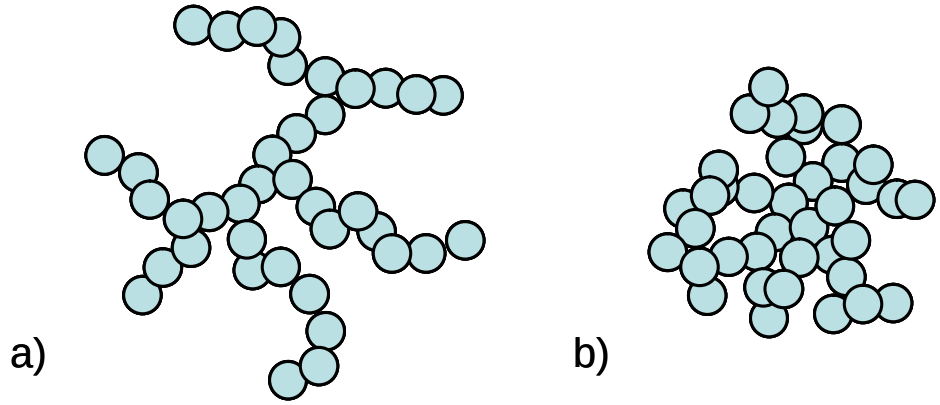

Figure 2-4 Silica gel network formation by (a) acid and (b) base catalyzed hydrolysis and condensation.

Adjusting the reaction conditions and reactant concentrations also changes the sol-gel morphology. One factor which can have significant effect on silica morphology is the solution pH (Chao, Lin et al. 2004). In acidic conditions, the hydrolysis reaction occurs at a faster rate than condensation; a low degree of crosslinking due to steric crowding results in silica polymers which are weakly branched (Klemperer, Mainz et al. 1988). As the pH is increased, the rate of condensation increases relative to the hydrolysis rate until, under basic conditions, the relatively fast condensation rate results in the formation of highly branched polymers which are of colloidal nature. The structure and packing efficiency of these polymers determine the structure of the gel, with the highly branched systems leading to mesoporous gels due to inefficient packing and the more linear, weakly branched polymers yielding a highly dense, microporous structure (Handy, Walther et al. 1991; Nair, Elferink et al. 1996). Ying and co-workers indicate that the acid-catalyzed silica gels contain higher concentrations of adsorbed water, silanol groups, and unreacted alkoxy groups than the base-catalyzed counterpart (Ying, Benziger et al. 1993). They also discovered that upon heating, significant densification was seen with the acid-catalyzed gels while the base-catalyzed silica gels maintained a high

surface area of 100 m^2/g. The high silanol content of acid-catalyzed silica gels is desirable in order to achieve a high surface modification density, as discussed in the next section. However, the high silanol content also leads to a significant reduction in surface area and pore volume upon drying. The understanding of this process has allowed us to develop a process which significantly improves the loading capacity of surface-modified, silica gels.

In this work, we begin with the silica precursor in acidic conditions (pH <3). As stated above, this condition leads to increased hydrolysis, compared to condensation, and weakly branched polymers that contain a large amount of silanol groups. The addition of a basic catalyst increases the condensation rate and within a few minutes results in the formation of a gel. This process has allowed for the significant improvement in the surface modification of silica gels with various functional groups while also minimizing the shrinkage observed after drying. These results are presented in the following sections.

Another variable that can be adjusted to vary gel structure is the reaction temperature. An increase in reaction temperature leads to a greater degree of branching and therefore a less densely packed structure (Brinker and Scherer 1990). Room temperature was used for the fabrication of all silica gels in this work. The water and catalyst content also determines the rates of hydrolysis and condensation and these, in turn, vary the polymer structure from linear to weakly branched (Hench and West 1990).

Controlling reactant concentrations and reaction temperature are a few of the tools available for the customization of silica gels. Another available tool is the use

of surfactants. The use of surfactants as templates for porous silica gels has received considerable attention since the development of ordered mesoporous structures (M41S materials) by Mobil Corporation in the early 1990s (Beck, Vartuli et al. 1994). With a variety of surfactants available, control of pore size at the nanometer level is attained through the proper selection of a surfactant (Kickelbick 2004). In addition to differences in molecular size, surfactants also vary with anionic or cationic heads or with variations in the hydrophobic tail. This vast array of properties allow for the customization of mesoporous structure through the judicial choice of a surfactant. Preparing ordered solid-state structures using polyelectrolyte-surfactant complexes as building blocks provides even more exciting and versatile routes for morphology creation (Li, Bhosale et al. 2004). The engineered nanopore structure achieved by scientists at Mobil is one example of such an application.

Growing silica particles in a precursor system behave as a polyelectrolyte. The strong interaction of silica with the oppositely charged, self-assembled surfactants leads to the morphology creation by surfactant template. The Coulombic interaction, much stronger than van der Waals interaction, can be used favorably to stabilize the composite morphology. With an intelligent selection of the solvent system, plus appropriate fine-tuning of pH, an ordered nanostructure can be formed by design.

2.4 Surface Modification

Organic-inorganic composites combine the rigidity of the silica network with the reactivity of organic functional groups. These composites have been pursued for use in various applications, such as catalysis, bioreactors, membranes, and sensors.

Sulphonic acid modified silica gels have been used for the concentration of scandium, zirconium, hafnium, and thorium based on a cation-exchange process (Alimarin, Fadeeva et al. 1987). Various modified silicas have also been used for removal of trace Cd(III), Cu(II), Co(II), Hg(II), Ni(II), Pb(II), Zn(II), and Mn(II) ions for purposes of water purification (Nakagawa, Haraguchi et al. 1998; Bowe and Martin 2004; Mahmoud, El-Essawi et al. 2004; Mahmoud, Masoud et al. 2004). Modified silicas have also been investigated for the recovery of precious metals, such as silver, gold, platinum, and palladium (Tong, Akama et al. 1990; Tikhomirova, Fadeeva et al. 1991; Barboiu, Luca et al. 1997).

The sol-gel process allows for the introduction of a variety of surface modifications and also provides the capability for morphology control (Hench and West 1990). The organo-functionalization of mesoporous silica gels can be accomplished by two general routes: (1) the post-modification of gels through the reaction of organosilanes with surface silanol groups, and (2) the co-condensation of organosilanes with the silica precursor during gel formation. In many instances, the silica gels used in the first method lack reactive surface silanol groups and must first be activated, typically using a strong acid, to break siloxane bonds and form silanol groups. The organosilane modifier is then introduced for surface modification. The degree of surface modification is typically low when using this post-modification method.

The co-condensation approach is preferred because it requires fewer processing steps and the material obtained has a more uniform, controlled distribution of the functional group (Burkett, Sims et al. 1996; Walcarius and Delacote 2003).

Although both synthesis routes have been used to prepare ordered, mesoporous silica gels, the co-condensation process has generally been shown to yield higher degrees of surface modification (Mori and Pinnavaia 2001).

Table 2-1. Loading of amino functional groups on silica gels made by the post-synthesis and co-condensation processes.

Surface Area (m^2/g)	Amino loading (mmol/g)	Reference
Post-synthesis of silica gel		
390	1.35	(Etienne and Walcarius 2003)
662	2.01	(Yokoi, Yoshitake et al. 2004)
Co-condensation with TEOS		
0.5	5.34	(Sartori, Bigi et al. 2004)
65	2.2	(Bois, Bonhomme et al. 2003)
328	2.42	(Lee, Kim et al. 2001)
525	2.3	(Etienne, Lebeau et al. 2002)
721.7	1.7	(Huh, Wiench et al. 2003)

The published work that most closely resembles our approach to silica gel fabrication was done by Shah and co-workers (Shah, Kim et al. 2004). In their work, the authors used sodium silicate as the silica sources in making organo-functionalized mesoporous molecular sieves. The surface modifying organosilane was first introduced to a solution of ethanol, acetic acid, and the non-ionic surfactant, Brij 56 and allowed to hydrolyze for one hour. The sodium silicate solution was then introduced to the hydrolyzed organosilane and then aged at 65°C for 24 hours. Using this method, the researchers introduced a variety of functional groups (amino, thio, phenyl, and nitrile) into silica structure with hexagonal and wormhole morphologies.

Specific surface areas for the material ranged from 515 – 1190 m^2/g and pore volumes from .53 – 1.15 cm^3/g.

This work begins with a solution of sodium silicate which is ion-exchanged to produce silicic acid. In order to accomplish the surface modification, 3-aminopropyltriethoxysilane (APTES) is introduced to the system at a ratio of 1.1 mols per mol silicic acid and the system stirred with a magnetic stir bar. APTES, with its basic amino group, acts as a base-catalyst to induce gelation of the system while it also undergoes the hydrolysis and condensation reactions to be introduced into the network of the forming gel. This simple process produces chemically surface-modified gels (CSMG) with high loadings and uniform distribution of the amino functional group (N-CSMG). In addition, this process can be easily scaled-up by simply increasing the amount of reactants and can be used to produce gel monoliths of desired shapes with the use of an appropriate mould.

2.5 Material Characterization

2.5.1 Nitrogen Adsorption

The surface area and pore size characterization of silica gels is often accomplished by means of physical gas adsorption. In this technique, the amount of gas adsorbed onto the solid surface is directly correlated to the material's surface area and pore structure (Groen, Peffer et al. 2003). Often the gas of choice is, but not limited to, nitrogen at 77 K – the boiling temperature of liquid nitrogen. The construction of an adsorption isotherm over a range of partial pressures (p/p_0), the ratio of system pressure to the saturation pressure, provides information on the specific surface area, pore size distributions, and pore volumes of the material.

Brunauer, Emmett, and Teller first realized that gases at the boiling point adsorb in multilayers as the pressure is gradually increased (Brunauer, Emmett et al. 1938). By extending the Langmuir monomolecular adsorption to multilayers, they determined the surface area with the BET equation (3), where W is the weight of adsorbed nitrogen at a relative pressure of (p/p_0), W_m is the gas weight of monolayer surface coverage, and C is a constant related to the heat of adsorption.

$$\frac{1}{W\left[\left(p_0/p\right)-1\right]} = \frac{1}{W_m C} + \frac{(C-1)}{W_m C}\frac{p}{p_0} \tag{3}$$

Generally the adsorption isotherm is linear in the (p/p_0) range of 0.05 – 0.30 (see Figure 2-5), in which case the BET equation can be used to determine the monolayer weight of adsorbed nitrogen and the constant C from the slope and y-intercept (4). The specific surface area can then be determined from the monolayer weight and the cross-sectional area of the gas molecule, 16.2 $Å^2$ per molecule for nitrogen (N_2).

$$\begin{aligned} slope &= \frac{(C-1)}{W_m C} \\ y-\text{int} &= \frac{1}{W_m C} \end{aligned} \tag{4}$$

Pore size distribution is determined by the model developed by Barret, Joyner and Halenda (BJH model) based on the Kelvin equation, corrected for multilayer adsorption (Barrett, Joyner et al. 1951). The pore sizes are divided into three categories based on diameter: micropores (< 2 nm), mesopores (2 – 50 nm), and macropores (> 50 nm). Mesopores of size >30 nm are ideal for materials used in

enzyme immobilization due to improved access of the interior surfaces (Tischer and Wedekind 1999).

As mentioned earlier, a significant issue in working with mesoporous materials is shrinkage and the corresponding pore collapse. With the realization that permanent gel shrinkage occurs due to the condensation of surface silanol groups, we proposed that the shrinkage of gels can be minimized through modification of the silica gel while it is in the wet state. In the wet state, the pore size and specific surface areas are at their maximum. Any attempt to dry the gel, even partially, leads to shrinkage. To minimize the mass transfer limitations, by taking advantage of the fully open pores, all surface modification reactions were conducted with the wet gel. To test this hypothesis, we produced N-CSMG gels according to the procedure outlined in Section 2.4 . A portion of the N-CSMG was further reacted with glutaraldehyde, as will be detailed in Chapters 3 and 4, to produce GA-N-CSMG. Samples taken from both N-CSMG and GA-N-CSMG were then air dried at room temperature, freeze dried, or supercritically dried. Air dried samples, in 50 mL centrifuge vials covered with filter paper, were placed in a fume hood for 48 hours. Freeze dried samples, also in 50 mL centrifuge vials, were first frozen in liquid nitrogen and then lyophilized, at -40 °C for 24 hours, with a Labconco Freeze Dry System (Model: Freezone 4.5). Samples for supercritical drying were repeatedly washed with ethanol and then freeze dried using the protocol specified in Figure 2-2. Each sample was then further, dried under vacuum, at 100 °C for a minimum of 2 hours until all adsorbed moisture was removed and then analyzed for surface area. The air dried and supercritically dried samples were analyzed using a NOVA 1200,

Version 6.0 High Speed Gas Sorption Analyzer from Quantachrome Corporation (Boynton Beach, USA). Analysis of freeze dried samples was conducted by Quantachrome Corporation on an Autosorb Automated Gas Sorption System.

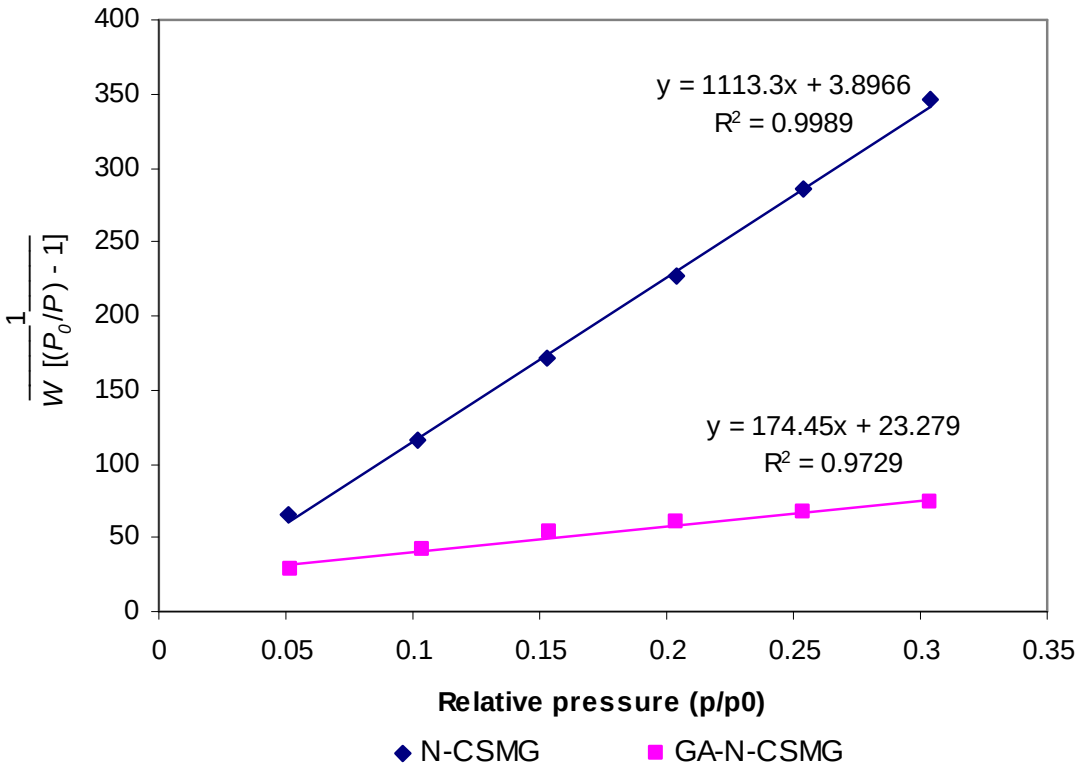

Figure 2-5 N_2 adsorption isotherms for air dried silica gel samples.
N-CSMG and GA-N-CSMG samples were air dried at room temperature for 72 hours and then degassed under vacuum for a minimum of two hours at 100 °C prior to measurement of N_2 adsorption.

Figure 2-5 shows the nitrogen adsorption isotherms for the air dried N-CSMG and GA-N-CSMG samples. Because the y-axis contains the term (1/W), materials that adsorb a higher nitrogen weight, W, show a smaller slope value but posses greater surface areas. From the plot it is clear that a significant difference is seen in the nitrogen adsorption isotherms of the unmodified N-CSMG and GA-N-CSMG upon air drying. Figure 2-6 shows a similar difference between N-CSMG and GA-N-CSMG when the samples are freeze dried. When comparing the results of the freeze

and air dried samples, it must be noted that the y-axis in Figure 2-6 is only half the scale of that shown in Figure 2-5.

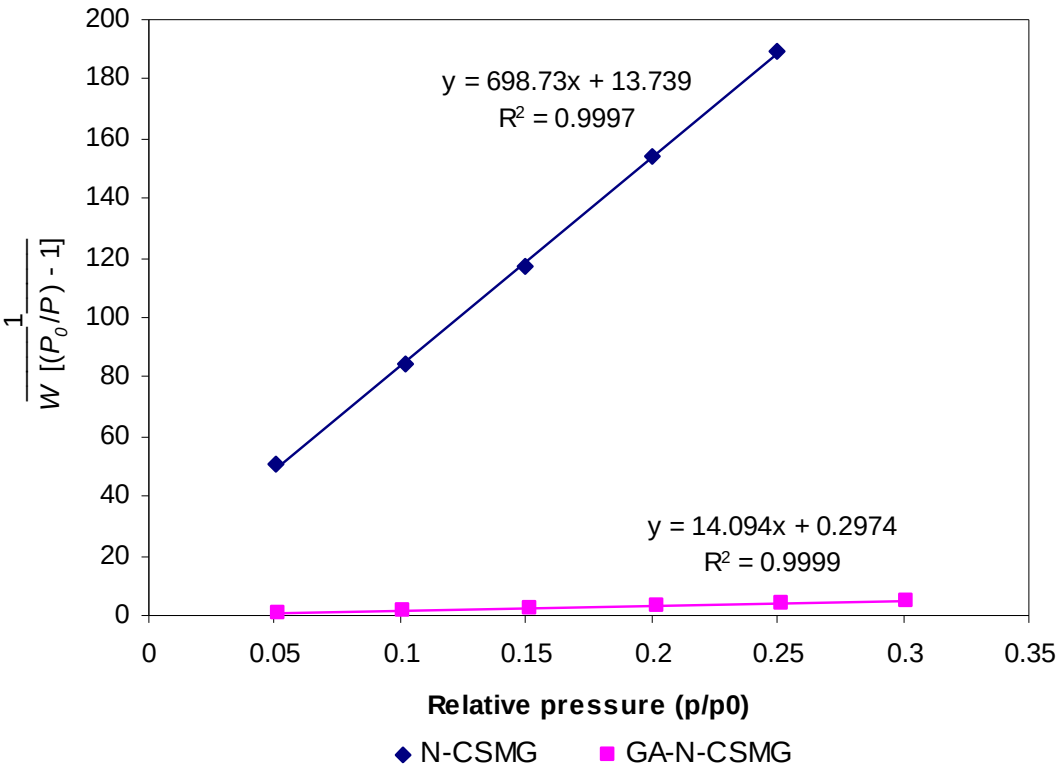

Figure 2-6 Nitrogen adsorption isotherms of freeze-dried silica gels.
N-CSMG and GA-CSMG suspensions in deionized water were frozen in liquid nitrogen and then lyophilized. Samples were degassed under vacuum at 100 °C until adsorbed moisture was removed prior to analysis.

Table 2-2 Specific surface area of N-CSMG and GA-N-CSMG after air drying, freeze drying, and supercritical drying as determined by the BET method.

	Air Dried (m^2/g)	Freeze Dried (m^2/g)	Supercritical Dried (m^2/g)
N-CSMG	3	5	--
GA-N-CSMG	18	242	649

Surface area analysis of the material before and after modification has shown considerable difference in material properties. The air dried GA-N-CSMG has a surface area five times greater than the corresponding N-CSMG while the freeze

dried GA-N-CSMG shows an almost 50-fold increase in surface area compared to N-CSMG. It is also interesting to note that freeze drying only slightly improves the N-CSMG surface area, compared to air drying, while an increase greater than 13-fold is seen for GA-N-CSMG. An improvement against shrinkage is clearly seen when the N-CSMG is modified in the wet state. It is likely that the glutaraldehyde works similar to the templating agents commonly used for control of pore morphology in sol-gel processes. Since glutaraldehyde is a bi-functional molecule, it is also possible that it binds to the silica matrix on both ends and braces the gel against the collapsing stresses. Pore-size analysis for freeze-dried GA-N-CSMG is shown in Appendix A-5.

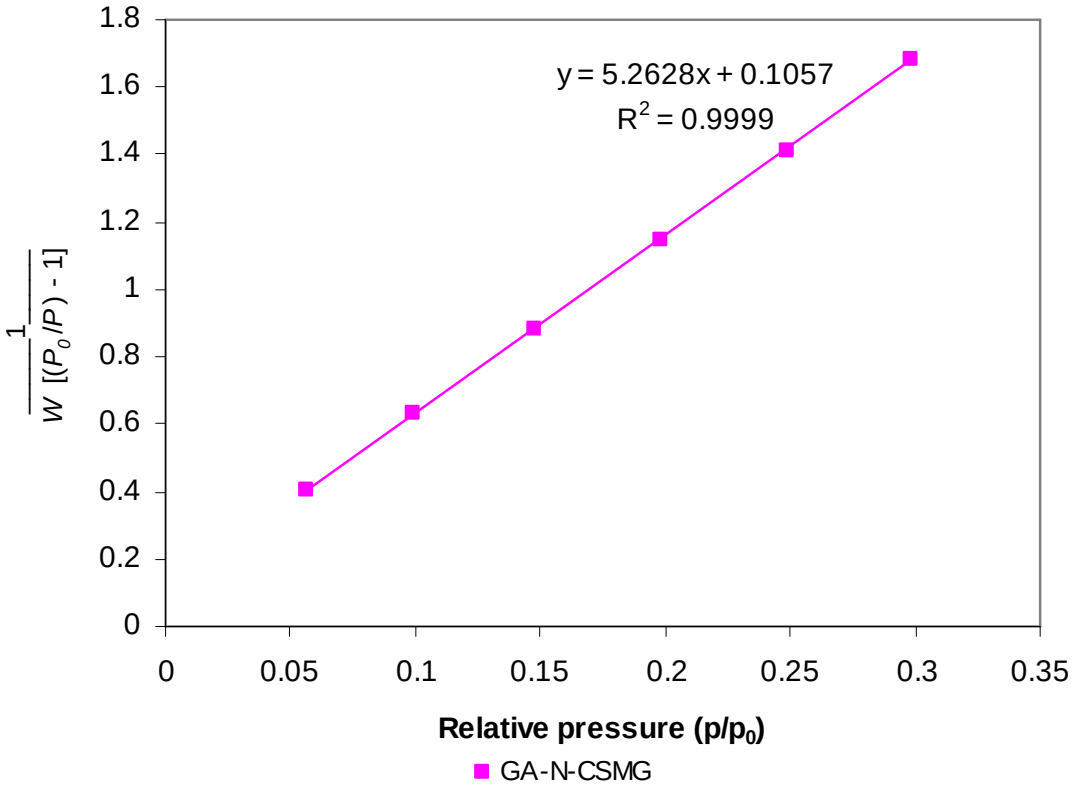

Figure 2-7 Nitrogen adsorption isotherm of silica gel dried with supercritical CO_2.

GA-CSMG suspensions in deionized water were washed with 60% ethanol (3X), 80% ethanol (3X), and absolute ethanol (3X). Ethanol was then exchanged for liquid CO_2 and then the system pressure and temperature raised to supercritical conditions (T > 32 °C, P > 1170 psi) and sample dried by venting the supercritical CO_2. Samples were degassed under vacuum at 100 °C until adsorbed moisture was removed prior to analysis.

For comparison purposes, a sample of the modified gel was supercritically dried and the surface area measured (see Figure 2-7). The obtained specific surface area of approximately 649 m^2/g-GA-N-CSMG is likely close to the surface area of the gel in its wet state.

2.5.2 Thermogravimetric Analysis

Thermogravimetric analysis (TGA) is the measure of change in sample weight with increasing temperature. This measurement allows us to determine the degree of surface modification through comparison of the percent weight loss. All samples were held at 100 °C for ten minutes for removal of any adsorbed water. The temperature was then increased at a rate of 10 °C per minute with simultaneous recording of weight measurements.

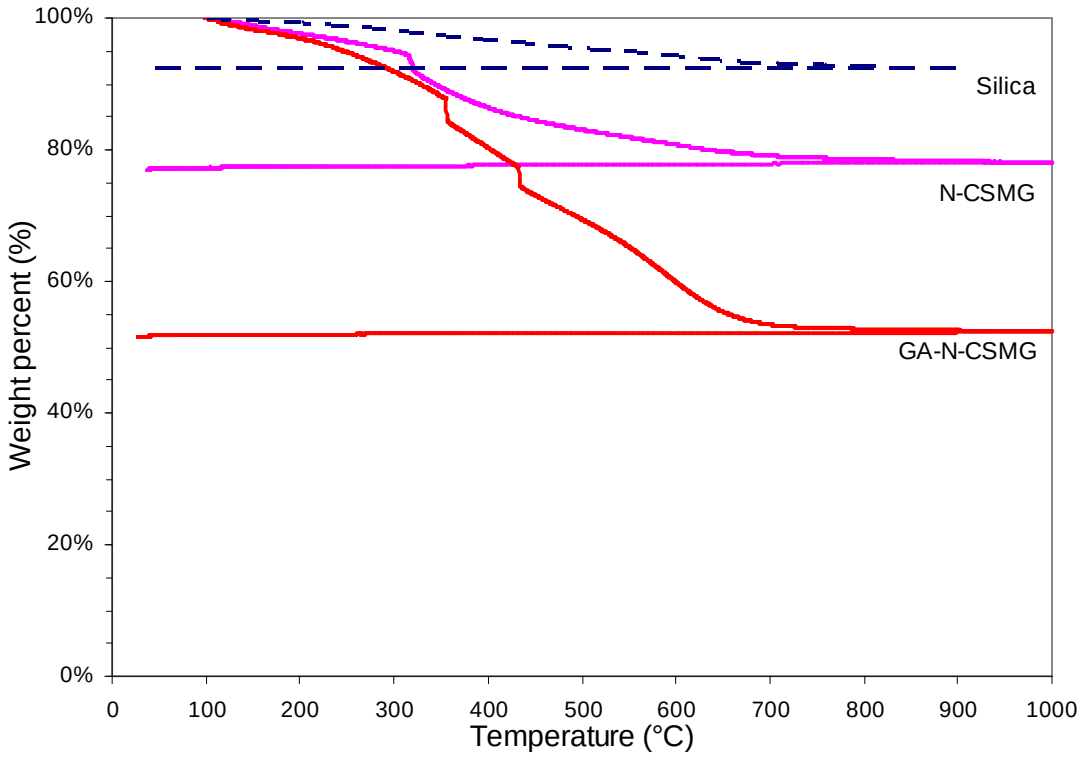

Figure 2-8 Thermogravimetric analysis (TGA) of N-CSMG and unmodified silica gel.

The TGA profiles of unmodified silica, N-CSMG, and GA-N-CSMG are shown in Figure 2-8. The unmodified silica gel was made using the same recipe as N-CSMG, with APTES replaced by 6 M NaOH as the gelling agent. Since no APTES is added, the resulting gel has active silanol groups but no amino-modification of the surface. The unmodified silica gel shows a decrease in weight of approximately 8.2 percent. Increasing the temperature induces condensation between silanol groups; resulting in the formation of water, which is vaporized, and decreasing the sample weight.

N-CSMG shows a weight loss of approximately 23 percent according to the TGA data. The approximately 15% difference in weight loss, compared to unmodified silica, is directly related to the degree of APTES modification of the gel. With the TGA weight loss profiles, the silanol and APTES in the silica gels can be quantified and the loading densities calculated, assuming homogenous distribution with a surface area of 1250 m^2/g-SiO_2 determined from the surface area of supercritical dried GA-N-CSMG (see Table 2-2). The results are summarized in Table 2-3 with the loading expressed based on the amount of residual SiO_2, sample weight remaining at the end of TGA, to allow for comparisons.

Table 2-3 Quantity of silanol and amino groups as determined by TGA.

Functional Group	Loading (mmol/g SiO_2)	Loading Density (μmol/m^2)
Silanol (Si – OH)	4.54	3.63
Amino (APTES)	3.64	2.91
Glutaraldehyde	7.54	6.03

The loading densities of silanol and APTES indicate that a large fraction of the active surface area has been amino-modified (approximately 80%) with this sol-gel protocol. Also, with an APTES footprint of 50 $Å^2$ (Vansant, van der Voort et al. 1995), the surface loading of 3.64 mmol/g SiO_2 is almost 88% of the maximum theoretical APTES loading of 4.16 mmol/g SiO_2 (see Equation 5).

$$APTES_{\max} = 1250 \frac{m^2}{g\ SiO_2} \times \frac{1 molecule}{.50 nm^2} \times \frac{\left(1 \times 10^9\ nm\right)^2}{1 m^2} \times \frac{1000 mmol}{6.02 \times 10^{23}\ molecules} \qquad (5)$$

$$APTES_{\max} = 4.16 \frac{mmol}{g\ SiO_2}$$

Table 2-4 Typical loadings of APTES in silica gels in (a) two-step and (b) co-condensation processes.

Precursor	APTES Loading (mmol/g)	Reference
Silica[a]	1.7	(Etienne and Walcarius 2003)
Silica[a]	2.0	(Yokoi, Yoshitake et al. 2004)
TEOS[b]	5.3	(Sartori, Bigi et al. 2004)
TEOS[b]	1.7	(Huh, Wiench et al. 2003)

Some of the typical loadings of APTES in silica gels made by the post-modification and co-condensation methods are shown in Table 2-4. The N-CSMG amino loading of 3.6 mmol/g is significantly higher than most published results and should show improved capacity for enzyme immobilization.

While the TGA data shows an APTES loading of 3.64 mmol/g SiO_2, the glutaraldehyde loading is more than twice this amount at 7.54 mmol/g SiO_2. This higher loading is likely due to the presence of polymerization between glutaraldehyde molecules (Aso and Aito 1962; Overberger, Ishida et al. 1962; Rasmusse.Ke and

Albrecht.J 1974). Dinitrosalicylic acid was used to determine the presence of the aldehyde groups by their reducing power (Miller 1959) according to a standard curve (see Appendix A-3). The measured reducing power of GA-N-CSMG is equivalent to 3.12 ± 0.5 mmol glutaraldehyde per gram of GA-N-CSMG.

Confocal fluorescence microscopy (Olympus FV-500 with a HeNeG laser) was used to image the fluorescence of the Schiff-base formed when glutaraldehyde reacts with the N-CSMG surface. As seen in Figure 2-9, the Schiff-base is homogenously distributed throughout the GA-N-CSMG particles indicating both an even distribution of the amino surface modification and the glutaraldehyde crosslinker. A homogenous distribution of the reactive groups is important in achieving a good distribution of the immobilized enzyme and it also maximizes the immobilized activity by taking advantage of a larger surface area for immobilization.

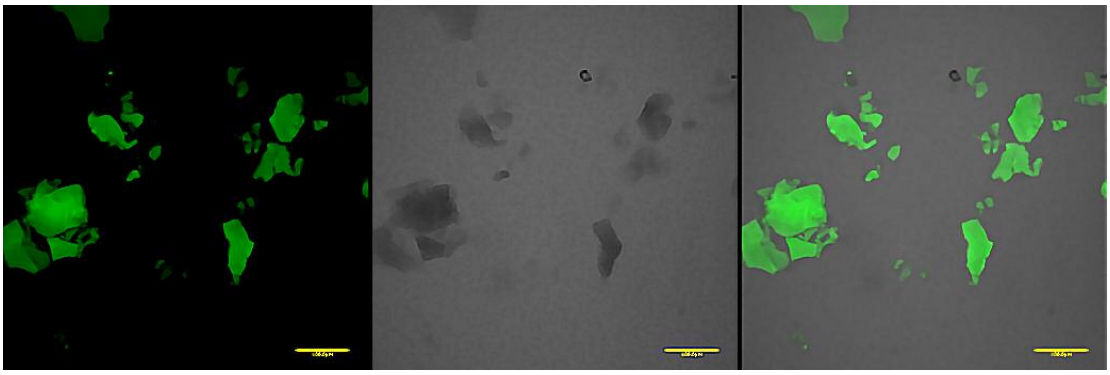

Figure 2-9. Confocal fluorescence microcopy image showing the homogenous Schiff-base distribution of GA-N-CSMG. The fluorescence image is to the left and the bright-field image in the center. The image to the right is a superimposition of the first two images. Scale bar = 100 μm.

2.5.3 Scanning Electron Microscopy

Scanning electron microscopy (SEM) allows the visualization of materials at very high magnifications. Depending on the instrument and materials properties, it is capable of providing resolutions down to the nanometer scale and is used to obtain images of a gel's pore structure.

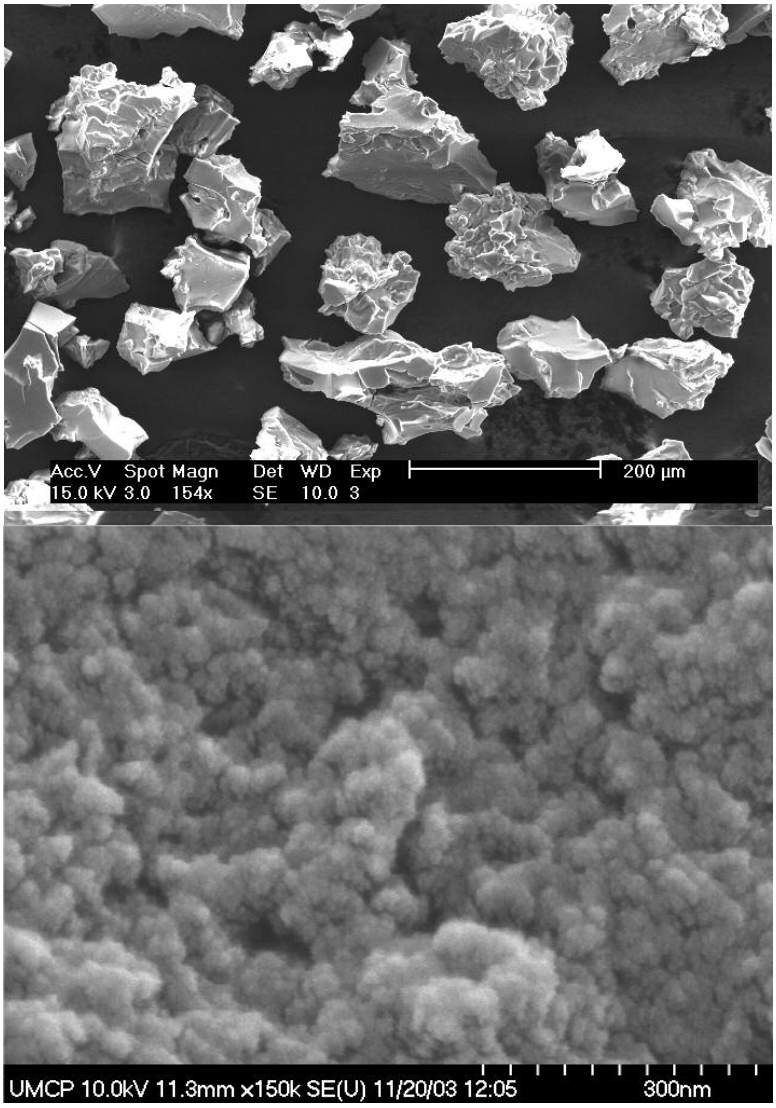

Figure 2-10 Visualization of N-CSMG morphology by SEM under low and high magnification.

SEM images of N-CSMG dried with supercritical CO_2 in Figure 2-10 show that the material contains a distribution of pore sizes with the largest pores greater than 30 nm in size. Also seen is the rough surface texture which provides the high surface area.

In the following chapters, we will discuss how the properties of N-CSMG material are ideal for enzyme immobilization (Chapter 3) and provide the results of invertase (Chapter 4) and thermolysin (Chapter 5) immobilization.

Chapter 3: Enzymes

With new enzymes being discovered and even developed by genetic technologies, many fine chemicals and pharmaceutical products will likely be produced by biological reactions. A recent example is the synthesis of phenylglycidate ester (Stinson 2000). The traditional method starting from a Darzens reaction of methyl chloroacetate took eight steps, six isolations of solid substances, and two vacuum distillations; resulted in 15% overall yield; and would have needed 50 weeks to make the 19 kg desired at a cost of $90,000 per kg. Dow Contract Manufacturing Services devised a two-step process involving enzyme-catalyzed hydrolysis of the methyl ester in 28% overall yield to make 19 kg in 14 weeks at a cost of $25,000 per kg. The high-value commercial opportunities are considerable for the immobilization of novel enzymes.

Furthermore, the proposed technology has plenty of room for additional innovations. The surface modification scheme developed here can be used for attaching many other biological entities such as antibodies and many target-specific groups (Wang, Narang et al. 1993; Zuhlke, Knopp et al. 1995). A series of microorganism or cells can also be encapsulated within a surface-modified structure to perform functions other than catalysis (Branyik, Kuncova et al. 1998; Bergogne, Fennouh et al. 2000; Carturan, Dal Toso et al. 2004).

3.1 A short history of enzymes

Enzymes had been used for thousands of years without a clear understanding of their nature. The first records of enzyme use involve the production of cheese

from the stomach linings of calves, which contain chymosin. Apparently ancient travelers used to carry milk in pouches made from sheep stomach. The action of chymosin, a coagulating enzyme present in the stomach which induces gelation of the protein casein, changed the milk to curd and whey. The gel is cut and drained to remove the whey and the remaining solid, the curd, pressed to produce cheese. This process was first detailed by the Romans who brought it into Europe (EUFIC 2004).

It was not until the 1800s that the nature of enzymes was understood. Kirchhoff saw in 1814 that a component of wheat was capable of producing sugar from starch. Then in 1833, Payen and Persoz obtained a malt extract – amylase, which hydrolyzed starch into sugar. Dubonfout, in 1846, saw the activity of invertase and Berthelot observed the same activity in an alcohol precipitate from yeast. It was not until 1878 that the word enzyme, meaning "in ferment", was proposed by Kühne. And in 1893, Ostwald first classified enzymes as a catalyst.

The next leap in the understanding of enzymes came in 1894 when Emil Fischer first proposed the "lock-and-key" theory to explain the specificity of enzymes. In 1913, Michaelis and Menton published theoretical work on enzyme kinetics (Michaelis and Menton 1913) that led to the development of the Michaelis-Menton equation, discussed in Section 3.2.2 . The protein nature of enzymes was first shown by Sumner through the crystallization of urease from jack bean (Sumner 1926). In 1967, the 3-D structure of an enzyme, lysozyme, was determined by X-ray crystallography (Blake, Johnson et al. 1967; Blake, Mair et al. 1967; Phillips 1967).

3.2 Enzymes as catalysts

Proteins are heteropolymers constructed from 20 different amino acids, as the monomer units, linked together by peptide bonds. They vary dramatically in size, with the smallest often called peptides, and are the major functional molecules of life. Enzymes are specialized proteins which are able to catalyze reactions with a very high substrate and product specificity. They occur widely in animals, plants, yeast, bacteria, and fungi. Based on the reaction catalyzed, all enzymes can be placed into six basic groups: hydrolases, isomerases, ligases, lyases, oxidoreductases, and transferases. According to the recommendations of the International Union of Biochemistry and Molecular Biology (IUBMB), each enzyme is assigned to an enzyme class (EC 1 – 6) based on the reaction catalyzed (Moss 2004).

Oxidoreductases (EC 1) catalyze oxido-reductions with the oxidized substrate considered to be an electron donor. This class of enzymes is further divided into 22 sub-classes based on the function group (e.g. sulfur, aldehyde, heme, etc.) acted upon. The transferases (EC 2) are named for their ability to transfer groups from a donor compound to an acceptor compound. They are further separated into nine sub-classes according to the group transferred.

The third class of enzymes, the hydrolases (EC 3), catalyzes the hydrolysis of various bonds including C – O, C – N, and C – C bonds. Depending on the bond that is hydrolyzed, hydrolases are further divided into 13 sub-classes. Hydrolases, at approximately 80% of all industrially used enzymes, are the most abundant in industrial processes – used mainly in food processing (Krishna 2002). Invertase (EC 3.2.1.26), also known as β-D-Fructofuranoside fructohydrolase, and thermolysin (EC

3.4.24.27), or Thermophilic-bacterial protease, are both hydrolases that will be discussed further in Chapters 4 and 5, respectively.

Lyases (EC 4), which make up the fourth enzyme class, catalyze the cleavage of various bonds by means other than hydrolysis or oxidation. They are separated into seven sub-classes depending on the bond cleaved. Lyases are often called "synthase" when the reverse reaction is the more desirable. The fifth enzyme class, isomerases (EC 5) with six sub-classes, contains enzymes which are able to catalyze changes within a single molecule. Some of these enzymes change molecular geometry while other transfer groups from one position in the molecule to another. The final class of enzymes, also with six sub-classes, is the ligases (EC 6). These enzymes catalyze the joining of two molecules along with the hydrolysis of ATP diphosphate bonds.

It is this vast variety in function that makes enzymes attractive for many industrial processes. More than 4300 enzymes have been classified by IUBMB, as of July 2004, but the vast majority present in nature is yet to be characterized.

3.2.1 Thermodynamics of enzyme catalysis

Although many reactions in biochemistry are thermodynamically favored and occur spontaneously, the rate of reaction can be very slow. Many of these reactions are under kinetic control and require an input of energy to proceed. This can be explained clearly in terms of free energy. The thermodynamics of a reaction is described in terms of the change in free energy (ΔG), change in enthalpy (ΔH), and change in entropy (ΔS) according to Equation 6.

$$\Delta G = \Delta H - T\Delta S \tag{6}$$

Thermodynamics tells us that a reaction is spontaneous only if ΔG is negative. From Equation 6 we can see that any exothermic reaction, $-\Delta H$, will always result in a spontaneous process, $-\Delta G$. An endothermic reaction is spontaneous only if $T\Delta S$ is greater than ΔH. In Figure 3-1 we show a system that is exothermic and, therefore, spontaneous. However, there are many reactions with a similar profile which do not proceed at a significant rate. One example is the oxidation of glucose to produce carbon dioxide and water ($\Delta G \approx -2900$ kJ/mol). Although this reaction is spontaneous, glucose is quite stable because the reaction is kinetically slow.

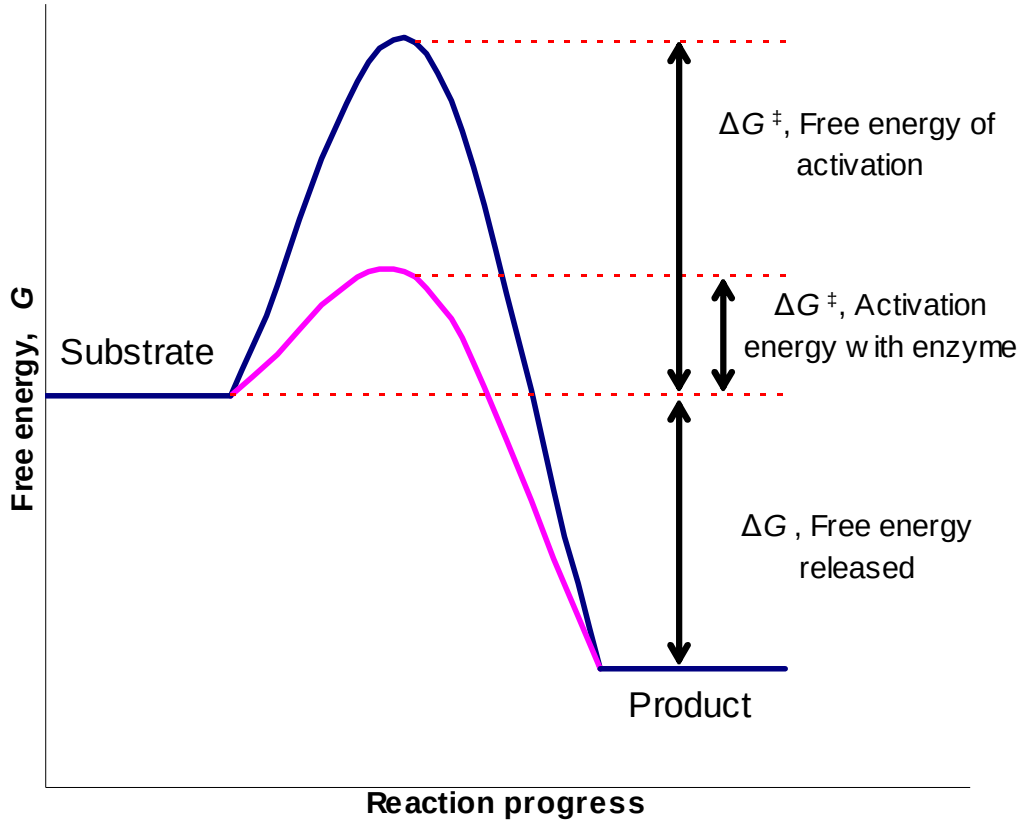

Figure 3-1 Free energy of activation of uncatalyzed and catalyzed reactions.

In order for the reaction to progress from substrate to product, it must cross an energy barrier corresponding with an unstable transition state. The energy required to

cross this barrier is called the free energy of activation, or activation energy ($\Delta G^{\ddagger}$). According to transition state theory, the rate constant of a reaction, *k*, is exponentially and inversely related to the free energy of activation (7). The rate of reaction can be increased by two methods: increase temperature to increase substrate free energy; and lower the activation energy. Enzymes increase the reaction rates by lowering the energy of activation.

$$k = \frac{k_B T}{h} e^{-\Delta G^{\ddagger}/RT} \tag{7}$$

k_B = Boltzmann constant, h = Planck's constant, R = gas constant, and T = temperature

It must be noted that, although enzymes increase reaction rates, enzymes do not affect the equilibrium of the reaction. Take for example the hydrolysis of sucrose (S) to glucose (G) and fructose (F) by invertase:

$$S \xleftrightarrow[Invertase]{} G + F$$

The reaction equilibrium can be written, with respect to the concentrations, as

$$K_{eq} = \frac{[G][F]}{[S]} \tag{8}$$

Because the enzyme reduces the activation barrier for both the forward and reverse reactions, the overall equilibrium is unaffected but the system does reach equilibrium more rapidly.

3.2.2 Michaelis-Menten Kinetics

Michaelis-Menten kinetics is one way to describe the rate of production in an enzyme catalyzed reaction. Let us derive the Michaelis-Menten equation by considering the following reaction:

$$E + S \underset{k_{-1}}{\overset{k_1}{\rightleftarrows}} ES \xrightarrow{k_{cat}} E + P \tag{9}$$

The Michaelis-Menten derivation assumes that the substrate is present in much greater excess than the enzyme ([*S*]>>[*E*]). This is often true because of the high catalytic efficiency of enzymes. A second assumption is that the forward reaction rate of product formation, k_{cat}, is much greater than the reverse of product depletion. Also, since the enzyme concentration is conserved through the reaction, the enzyme concentration balance is written as,

$$[E_0] = [E] + [ES] \tag{10}$$

[E_0] = enzyme introduced to system; [E] = free enzyme;
[ES] = enzyme-substrate complex

We also write the rate equation for the change in product concentration with time,

$$\frac{d[P]}{dt} = k_{cat}[ES] \tag{11}$$

A steady-state approximation for the rate of change in the enzyme-substrate complex concentration can also be written,

$$\frac{d[ES]}{dt} = k_1[E][S] - k_{-1}[ES] - k_{cat}[ES] \approx 0 \tag{12}$$

This equation can be rearranged to obtain,

$$\frac{[E][S]}{[ES]} = \frac{k_{-1} + k_{cat}}{k_1} = K_M \tag{13}$$

Solving (13) for [E] and substituting into equation (10) and rearranging gives,

$$[ES] = \frac{[E_0][S]}{K_M + [S]} \tag{14}$$

This is finally substituted into equation (11) to obtain the Michaelis-Menten rate equation,

$$\frac{d[P]}{dt} = \quad v = \frac{k_{cat}[E_0][S]}{K_M + [S]} \tag{15}$$

As seen in Figure 3-2, the Michaelis-Menten equation follows saturation kinetics in terms of the substrate concentration. At very low concentrations, the rate of reaction increases linearly with increasing substrate concentration. As the substrate concentration is further increased, the reaction rate goes toward a limiting maximum value, V_{max}. The substrate concentration, [S], at which the reaction rate is one-half of V_{max} is called the Michaelis constant, K_M.

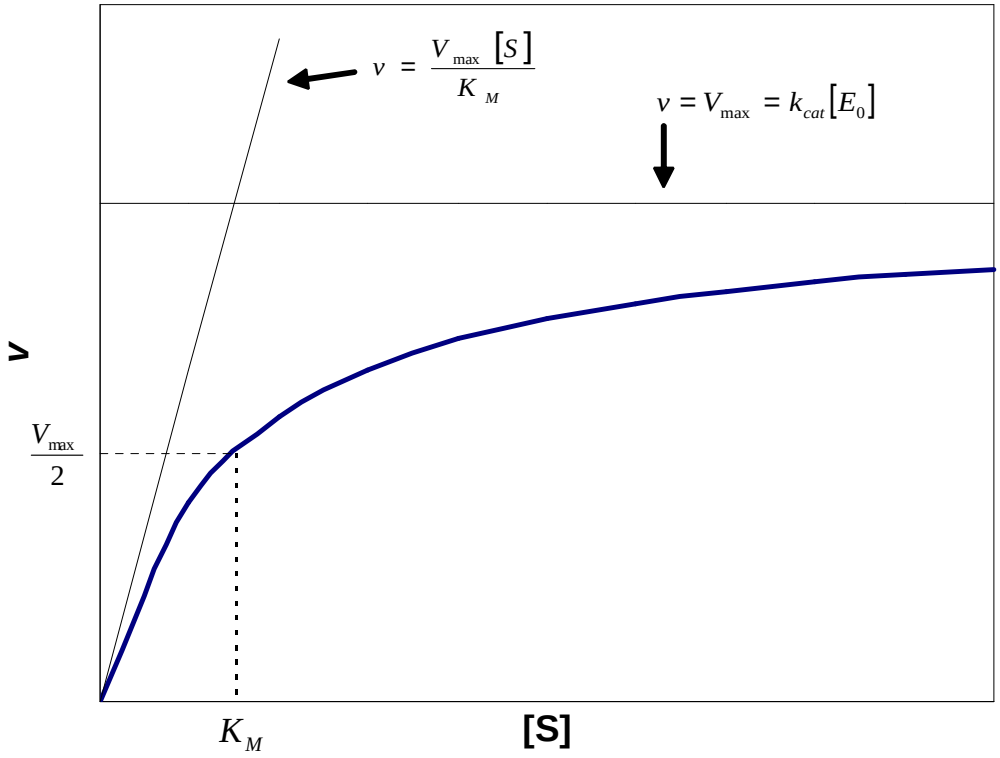

Figure 3-2. Plot of reaction rate, *v*, against substrate concentration, [*S*], for a reaction obeying Michaelis-Menten kinetics.

Both of the Michaelis-Menten kinetics parameters, K_M and V_{max}, were determined for free and immobilized invertase to provide some insight into the effect

immobilization on N-CSMG has on enzyme activity. In addition, the catalytic efficiency of the enzyme is determined by the ratio V_{max}/K_M.

3.3 Immobilization of Enzymes

Invertase, which hydrolyzes sucrose into glucose and fructose, was the first enzyme to be used commercially in immobilized form during World War II when sulfuric acid, used in the traditional process, was unavailable (Cheetham 1995). Although enzyme immobilization has been performed for over 50 years, its use in industrial processes has been limited due to high enzyme cost and limited enzyme stability and specificity.

Recent developments have made the use of enzymes in industrial processes much more feasible (Ikehata, Buchanan et al. 2004). Advancements in bioengineering have allowed for the over-expression of selected enzymes in fermentations and, coupled with improved purification techniques, lowered the cost of enzymes (Kim, Kang et al. 2004; Koizumi 2004). In addition, the developments in protein engineering and advanced screening techniques have introduced a large variety of designed enzymes: providing greater selection for the improvement of particular reactions (Selber, Tjerneld et al. 2004). Most recently, the development of non-aqueous enzymatic processes has drawn interests from many groups due to improved product and enzyme recovery (Gupta 1992; Braco 1995; Krishna 2002).

Today there are some examples of enzymes in industrial processes, some of which are listed in Table 3-1. Universal Oil Products (UOP) has successfully used immobilized glucose isomerase in the production of high fructose syrups. The high demand for semi-synthetic antibiotics has led to the use of immobilized penicillin

amidohydrolase, and several other enzymes, for the production of the precursor 6-Aminopencillanic acid (6-APA).

Table 3-1. Some enzymes in industrial applications.

Enzyme	Substrate	Product	Scale (tons/year)	Company
Glucose isomerase	Glucose	Fructose	$>10^6$	UOP
Penicillin amidohydrolase	Penicillin	6-Aminopencillanic acid	1,000	DSM
Lipase	Triglycerides	Cocoa butter	$>10^6$	Unilever
Aspartic acid ammonia lyase	Fumaric acid	L-Aspartic acid	1,000	DSM
Subtilisin carlsberg	--	(*S*)-Phenylalanine	--	Coca-Cola

Immobilization of enzymes involves certain costs associated with the cost of materials (e.g. polymer matrix, cross-linkers) and processing time. The two major driving concerns in an industrial scale process are to lower the unit cost and to increase the unit production per fixed time. Immobilization becomes economically feasible only if it allows the repetitive use of enzyme in multiple batches to reduce the unit production cost. Further, immobilized-enzyme beads can be packed into a bed or a column for continuous flow-through reactions, if applicable, to reduce costs associated with otherwise labor intensive processes. Such a reactor also simplifies the separation of enzyme from product: alleviating some down-stream processing costs.

The appropriate immobilization matrix is chosen based on several different properties which affect the production process (Tischer and Wedekind 1999):

- Surface area and porosity: It is desirable to have materials with high surface areas (> 100 m^2/g), for high enzyme loadings, and high porosity to provide enzyme access for the substrate. Pore sizes >30

nm are ideal for the diffusion of enzymes during the immobilization process.

- Surface functional groups: The degree of enzyme loading onto a carrier matrix also depends on the loading density of functional groups on the surface and its distribution. Choice of functional groups also affects the activity yield and material stability.
- Mechanical and chemical stability: Many immobilized enzyme operations are conducted as a stirred-tank or packed-bed reactor. To prevent enzyme loss, the matrix integrity must be maintained under the shear-stresses or back-pressures present in these reactors. In addition the matrix must be resistant to chemical degradations which will also result in the loss of enzyme.
- Size and shape: To simplify handling of the immobilized enzyme (i.e. stirring, filtration) it is ideal to have particles of uniform shape and size. For this reason, the use of a uniform spherical matrix is preferred and also results in the reduction of back-pressures in column reactors. In addition, spherical particles are also more easily characterized for modeling purposes.
- Microbial resistance: A major concern of any immobilized enzyme process is the presence of microbes. The durability of the carrier is often determined by its resistance to microbial degradation.
- Hydrophobic/hydrophilic nature: The compatibility of the support with the liquid phase is important to insure the free exchange of

substrate and product between the matrix and bulk phase. It can also determine the life-time of the matrix due to the surface adsorption of materials through non-specific interactions.

Immobilization allows the enzyme to be used in a continuous-flow mode which provides several benefits: 1) continuous removal of products from the reactor, which can be beneficial for systems that suffer from product inhibition; 2) product separation through column retention, reducing the burdens for downstream purification by affinity columns; and 3) increased enzyme stability will allow the enzyme to maintain activity for longer periods of use and in more extreme conditions.

3.3.1 Methods of enzyme immobilization

Enzyme immobilization, the restriction mobility, can be accomplished in a variety of ways, by entrapment, cross-linking, or physical attachment (Tischer and Kasche 1999). Enzyme entrapment is accomplished through the polymerization of a matrix from a solution containing both the monomer and enzyme. As shown in Figure 3-3a, entrapment results in the physical entrapment of enzymes within a cage-like matrix. Enzyme entrapment generally does not involve any modification of the enzyme and therefore may not adversely affect activity. However, this method can be susceptible to leaching of enzymes out of the matrix by diffusion when pore diameters are larger than the enzyme.

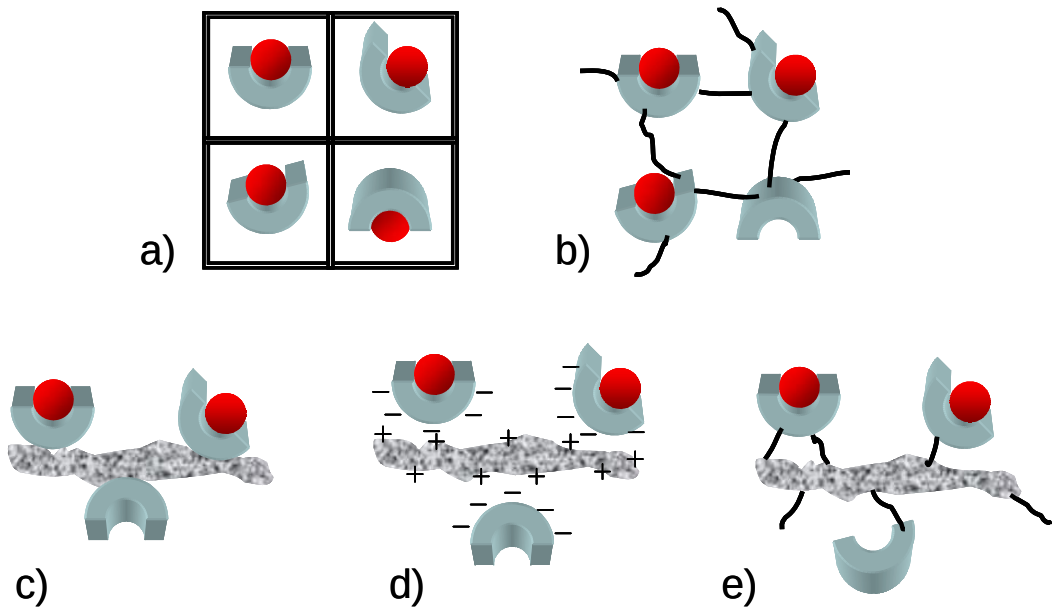

Figure 3-3 Methods of enzyme immobilization include a) entrapment, b) cross-linking, and physical attachment by c) adsorption, d) ionic interaction, and e) covalent binding.

Cross-linking, which involves the attachment of enzymes to each other (see Figure 3-3b), is another method used to immobilize enzymes (Tyagi and Gupta 1998). However, in many cases the extensive interactions required, whether electrostatic, chemical, or physical in nature, tend to significantly reduce enzyme activity by hindering formation of the enzyme's optimum folding conformation. In addition, because the material properties are governed by the enzyme, which is the major component in the cross-linked beads, mechanical strength can be fairly low: limiting the cross-linked enzymes to low system pressure reactors.

The physical attachment of enzymes to a solid matrix, by adsorption, ionic, or covalent interaction (see Figure 3-3c, d, and e, respectively), provides several advantages compared to entrapment and cross-linking. Due to the stronger interactions with the matrix, physical attachment provides greater material stability against leaching when compared to entrapment. However, if the immobilization is accomplished by adsorption or ionic interactions, leaching may still occur depending

on system conditions (i.e. pH, temperature, and solution ionic strength). The covalent attachment of enzymes to the matrix is preferred because of its inherent stability. Covalent immobilization is accomplished through the binding of reactive groups on the enzyme with a chemically-active surface. Covalently immobilized enzymes can be used in a variety of reaction environments with no significant increase in leaching due to the strong binding. However, the strong binding may also inhibit enzyme movement and thus reduce its activity by preventing conformational changes.

Enzymes are composed from a selection of 20 different amino acids with the majority of these acids having relatively inert side chains composed of hydrocarbons. However, as seen in Figure 3-4, nine of the amino acids have chemically active functional groups (i.e. amino, thiol, hydroxyl) on their side chains. The configuration of an enzyme is determined by the interaction of these side groups among themselves and with the environment (e.g disulfide binding, amide bonds, and hydrophobic/hydrophilic interactions). It is also through these interactions that enzymes can be attached to a solid surface.

Although the thiol group of cysteine is the more potent nucleophile, the amino groups are the more important target because of their relative abundance in proteins. Additionally, sulfhydryl groups are generally found in pairs that form disulfide bonds and have some influence on protein structure. Modification of these sulfide bonds may have detrimental effects on enzyme activity. Therefore, the preferred binding site is the amino residue on lysine side chains (Tischer and Wedekind 1999).

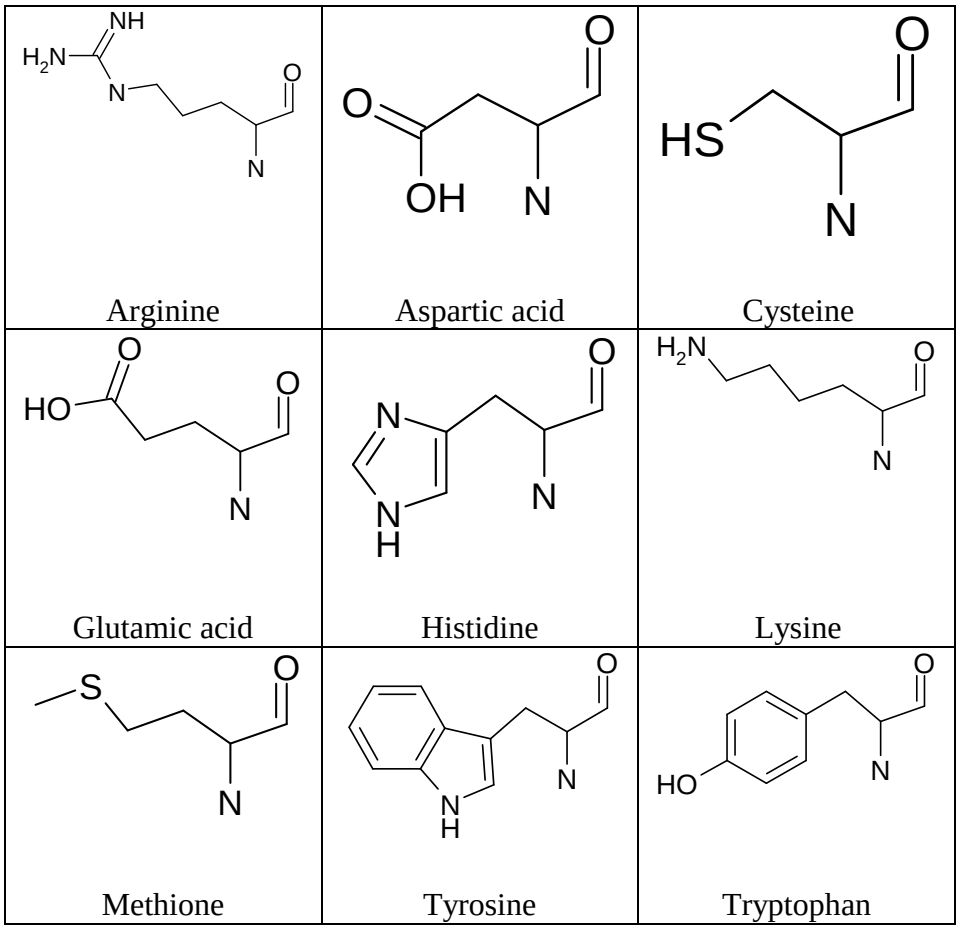

Figure 3-4 Amino acids with chemically active side chains.

Many enzyme immobilization techniques involve S_N2-type, nucleophilic substitution reactions. A typical enzyme immobilization system can consist of four different parts: the matrix; a surface modifying agent, if the matrix does not posses reactive functional groups; a cross-linking agent, which attaches the enzyme to the matrix; and, the enzyme. An ideal situation would allow immobilization to occur by simply mixing all matrix and reactive precursors together with the enzyme. Polymerization of the matrix would then allow for enzyme immobilization at high loadings and even distribution. This is not possible in the vast majority of cases because non-specific interactions between the reactive groups can result in the formation of undesirable bonds.

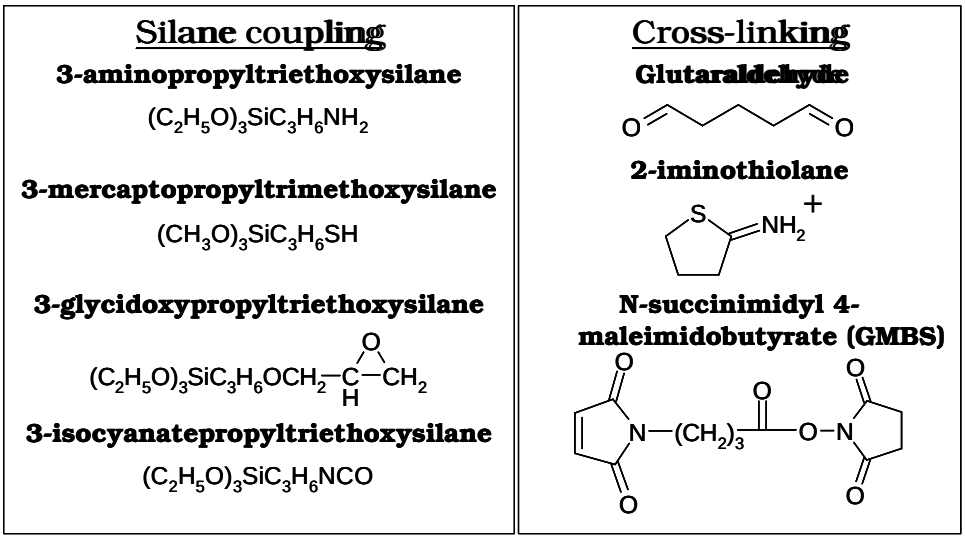

Figure 3-5. Commonly used silica gel modifying, organosilane agents and enzyme cross-linkers.

Several of the surface modifying silane agents and cross-linkers available for the immobilization of enzymes on silica gels are shown in Figure 3-5. A commonly used cross-linking agent, which reacts with amino groups, is the homo-bifunctional molecule - glutaraldehyde. The aldehyde reacts with amine groups to produce imines, or Schiff-bases, as shown in Figure 3-6.

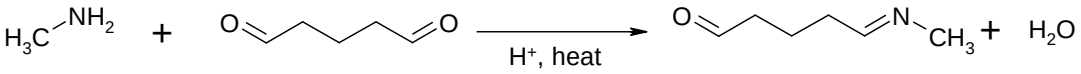

Figure 3-6. Reaction of glutaraldehyde with a primary amine.

In the presence of enzyme and an amino-modified surface, glutaraldehyde can immobilize the enzyme by attaching to an enzyme amino group with one hand and to the amino surface with the other (see Figure 3-3e). However, if each species were in solution prior to matrix formation, the non-specific nature of the aldehyde reaction will create cross-linked enzymes (Figure 3-3b) and also the cross-linking of two amino groups on the surface modifying agent. In addition, the interaction of enzymes with small, reactive molecules can lead to enzyme deactivation (Tischer and

Wedekind 1999). Although a "one-pot" process is preferable, a serial processing method, by introducing the reactive groups one at a time, is used because it minimizes these side-reactions.

3.3.2 Immobilization of enzymes on silica gels

A variety of matrixes have been used as carriers of immobilized enzymes. Many of these carriers fall under the category of "soft gels" because of their low mechanical strength. Silica gels offer a number of advantages over these "soft gels" for use in industrial processes. Silica's higher mechanical strength allows a much wider range of operating pressures as evidenced by their preferential use in High Performance Liquid Chromatography (HPLC) (Majors 2003; Cabrera 2004; Xu, Feng et al. 2004). Additionally, silica also has relatively higher thermal and chemical stabilities, except at extreme pH which is rarely experienced in enzymatic reactions, and is resistant to microbial degradation (Nefedov 1992; Pang, Qiu et al. 2002). Silica gels also provide high surface areas and high porosity which can be used to increase enzyme loadings and accessibility.

An array of functionally active proteins and other biological entities, including catalytic antibodies, antigens, live cells, and plant spores have been encapsulated by sol-gel silica and its hybrids. A thorough review paper provides a clear picture of the current status of the bioencapsulation technology (Gill and Ballesteros 2000). According to the review, significant advantages of silica encapsulation are: excellent optical and mechanical properties, high resistance to (biological, chemical, and thermal) degradation, simple fabrication, enhanced activities, long and stable shelf

life, and application versatilities. However, this review also highlights some substantial hurdles for future technology development. These hurdles include:

- Identificantion of biocompatible precursors/protocols to prevent denaturation during encapsulation;
- Shrinkage and pore collapse during xerogel formation; and
- Porosity and mechanical stability improvement.

Covalent immobilization of enzymes, including onto silica surfaces, has been done for a number of years (Weetall 1993). These methods commonly involve the use of pre-fabricated silica gels that have chemically inactive surfaces (Hossain and Do 1985). The gel surface must be activated, with strong acids, to produce the reactive surface hydroxyl groups. The activated surface is then modified with silane couple reagents, such as aminopropyltriethoxy-silane (APTES), which link functional groups (e.g. amino) to the silica surface via siloxane bonds (Moreno and Sinisterra 1994). The cross-linking agent (e.g. glutaraldehyde) is then introduced to react with the modified surface and finally the enzyme is added. In addition to being process intensive, these methods have been limited to relatively low enzyme loadings.

Since pre-fabricated silica gels are used, they depend upon diffusion for introduction of the surface modifying agent, cross-linking agent, and the enzyme into the gel interior. A problem that arises, particularly when attempting to obtain a high loading, is the blockage of pores by the diffusing species (Pizarro, FernandezTorroba et al. 1997; Baruque, Baruque et al. 2001). Naturally, reactions first occur on the gels outer surface and at pore entrances. At high loadings, the buildup of enzymes at pore

entrances can effectively clog the pore preventing further immobilization in the interior regions.

In this work, much higher invertase loadings have been achieved in comparison to previously published results. Immobilization of enzymes onto a matrix requires compatibilization of the enzyme in the presence of all precursors. To test the retention of enzymatic activity, alpha-amylase, an enzyme that hydrolyzes starch, was entrapped within a silica matrix. Alpha-amylase, in 100 mM acetate buffer (pH 7), was mixed into the silicic acid and the silicic acid quickly gelled to form a cage around the α-amylase, entrapping the enzyme. Enzyme activity was followed with the use of an iodine solution which, in coordination with starch molecules, results in a distinct blue color. As the starch is hydrolyzed, its ability to coordinate with iodine is hampered reducing the color intensity. The starch concentration can be determined through spectroscopic absorbance measurements at a wavelength of 620 nm according to the standard curve (see Appendix A-1). To two 10 g/L starch solutions, 8.4 mg of amylase was added in free and entrapped form. As seen by the plot in Figure 3-7, enzymatic activity of α-amylase was retained after entrapment. Although the hydrolysis action of the entrapped enzyme is delayed due to diffusion effects, both the free and entrapped enzymes show a similar maximum activity indicating that entrapment by sol-gel silica resulted in no significant activity loss of the enzyme.

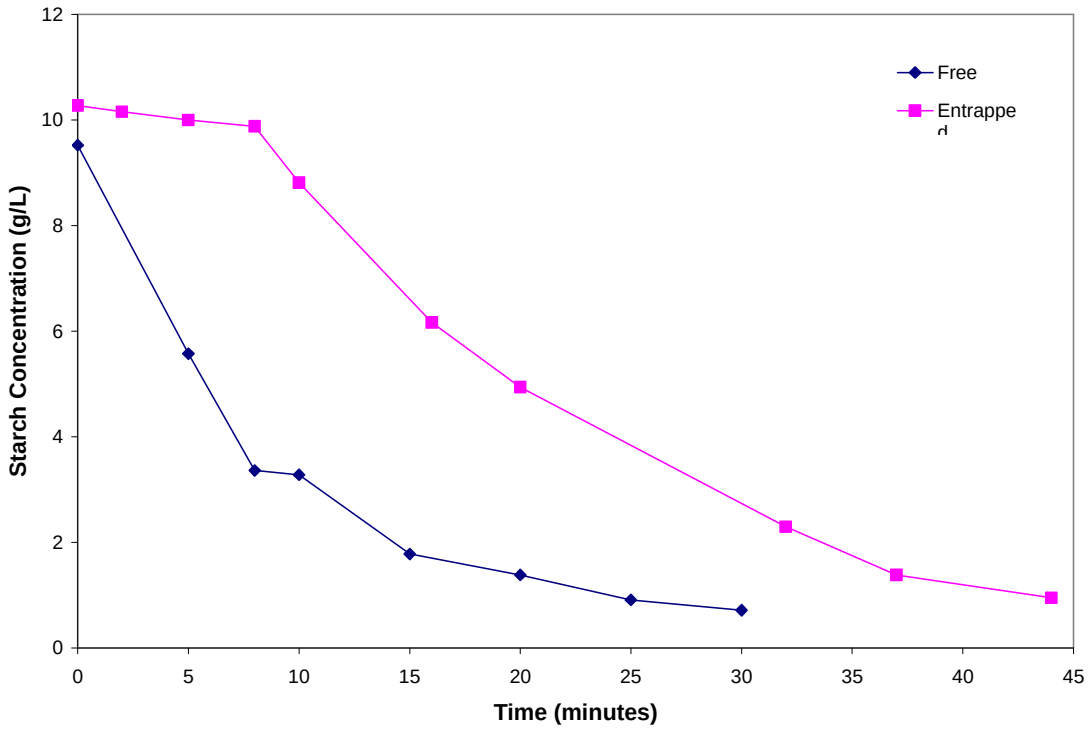

Figure 3-7. Comparison of starch hydrolysis by alpha-amylase entrapped within silica gel.

A leaching test was done to determine the degree of enzyme that entered into solution. Two equal amounts of the enzyme-entrapped gel were tested using slightly different recipes. In the first test, the entrapped gel was added to a buffered starch solution and the starch concentration measured over time. In the second "leaching" test, the entrapped gel was added to a buffer solution (no starch) and stirred for a period of one hour. At this time, the gel was removed from the buffer and a starch solution added to the buffer. Starch hydrolysis would then proceed if any enzyme had leached out of the gel. The two data sets show very similar behavior and so indicate that much of the enzyme activity of the entrapped gel is obtained through leaching of the enzyme. This makes sense, intuitively, considering the much greater size of starch molecules as compared to the enzyme; the enzymes encounter a smaller resistance to diffusion than starch. No activity was retained by the silica gel.

Although the leaching of enzymes would invalidate this system for use in industrial production processes, it can be of considerable value in applications where a controlled-leaching rate would be desirable (e.g. controlled drug release).

3.4 Characterization of immobilized enzymes

A number of measures, such as the rate of reaction, are used to determine the success of immobilization methods. The rate of reaction is proportional to the enzyme concentration or loading, as mentioned earlier, and also to the enzyme activity. Increased reaction rates would imply that either the system has a high loading of immobilized enzymes or that immobilization has increased enzymatic activity, both of which are desirable. Another measure would be the enzyme's reusability. This would involve the measurement of enzyme activity in repeated batch experiments. Immobilization systems that are able to maintain activity over many batches have greater value that those which lose activity.

In addition to the above measurements, the enzyme system's activity must be characterized over varying pH and temperatures. Enzymes typically show maximum activity at a particular pH and temperature with drop-offs on either side of the maximum. These maximums do not necessarily correspond to the maximums of the free enzymes. The immobilization of enzymes can have slight or drastic effects on enzyme conformation, shifting the activity maximum. These curves are used to determine the optimum operating conditions.

Chapter 4: Immobilization of Invertase

Invertase is a highly used enzyme in the food industry for the production of sweeteners used in beverages, jams, and as artificial honey (Cheetham 1995). As an enzyme, invertase catalyzes cleaving of the α-1,4 glycosidic bonds of sucrose to produce glucose and fructose (Khobragade and Chandel 2002) by the following reaction:

$$\textbf{Sucrose} + H_2O \rightarrow \textbf{Glucose} + \textbf{Fructose}$$

Invertase has a molecular weight of 270 kDa (Lampen 1971; Kupcu, Sara et al. 1991) and an isoelectric point between 3.4 – 4.4 (Righetti and Caravaggio 1976). No co-factors are required for activation of invertase while its activity is inhibited by the presence of iodine, Ag^{+}, Zn^{2+}, and Hg^{2+} (Lampen 1971; Goldstein and Lampen 1975; Huttl, Oehlschlager et al. 1999). Invertase is a multimeric enzyme with a minimum active state as a dimer but it also exists as larger multimers under certain pH and concentration conditions (Torres, Mateo et al. 2002).

Invertase has been immobilized on a number of carriers including methacrylate-based polymers (Bayramoglu, Akgol et al. 2003; Cirpan, Alkan et al. 2003), Sepabeads (Torres, Mateo et al. 2002), celite and polyacrylamide (Mansour and Dawoud 2003), menthyl ester (Kiralp, Toppare et al. 2003), organosilanes (Airoldi and Monteiro 2003), and agarose (Fuentes, Maquiese et al. 2004), just to name a few.

The invertase-sucrose system was chosen as an ideal model to study the immobilization capacity of the GA-N-CSMG material. The product formation is followed using the 3,5-dinitrosalicylic acid (DNS) method (Miller 1959). Unlike sucrose, glucose and fructose are both reducing sugars. The reduction of DNS by glucose and fructose results in a color change which can be measured spectraphotometrically to determine the product concentration.

4.1 Materials and Methods

Materials. Invertase (Grade VII) from baker's yeast, glutaraldehyde (25 wt. % in water), (3-aminopropyl)triethoxysilane (min. 98%), and sucrose were purchased from Sigma-Aldrich and used as supplied. Sodium silicate ("N" type) was purchased from PQ Corporation, PA. All other reagents were of analytical grade.

Synthesis of amino-chemically surface modified gel (N-CSMG). Silicic acid was produced from sodium silicate using an ion-exchange process developed at ISTN, Inc. The ion-exchange, accomplished with anionic Amberlite resin, exchanges sodium ions for hydrogen to produce a low ionic strength, silica sol with reactive silanol groups (- Si-OH). Formation of N-CSMG was done by addition of ethanol and 3-aminopropyltriethoxy-silane (APTES) to the silicic acid. Addition of the basic APTES to silicic acid increases the solution pH and induces the gelation. Gelation occurs through the condensation of silanol groups. Co-condensation between silica sol and APTES produces silica gels with amino surface modification. The monolithic gel was mechanically broken into particles of 11μm average diameter (range of 7 – 38 μm) as measured on a CEDEX particle size analyzer with a 40 μm measurement limit. The particles were washed with ethanol, vacuum filtered, and

washed extensively with deionized water. The final filtered gel was stored at 7°C until used for a maximum of 2 weeks.

Glutaraldehyde (GA) activation of N-CSMG to produce glutaraldehyde-activated silica gel (Ga-N-CSMG). To activate N-CSMG with glutaraldehyde, the gel was suspended in glutaraldehyde solution at a ratio of 20 mL solution per gram N-CSMG. The suspension was magnetically stirred at room temperature for 24 hours. Then, the suspension was vacuum filtered, to remove the GA solution, and washed extensively with deionized water. The final filtered gel was stored at 7°C until use.

Immobilization of invertase on Ga-N-CSMG. To immobilize invertase, 500 mg of Ga-N-CSMG was weighed into a 50 mL centrifuge vial. Then, 20 mL of invertase, in 50 mM acetate buffer at pH 4.5, was introduced to the vial and the suspension magnetically stirred at 7°C for a minimum of 48 hours. The suspension was then centrifuged at 10,000g for 10 minutes and the supernatant removed.

The invertase-immobilized gel was washed three times with 20 mL of 100 mM acetate buffer (pH 4.5) and centrifuged between each wash. Three washes were found to be adequate for removal of non-immobilized enzymes, through activity measurement of the supernatants, as shown in Figure 4-1. The final wash was carried out for 4 days with vigorous stirring and less than one percent of the initial activity remained in the supernatant. This indicates that the immobilization method is stable and no significant leaching has occurred. The washed gel was suspended in 20 mL of 100 mM acetate (pH 4.5) and stored at 7°C until use.

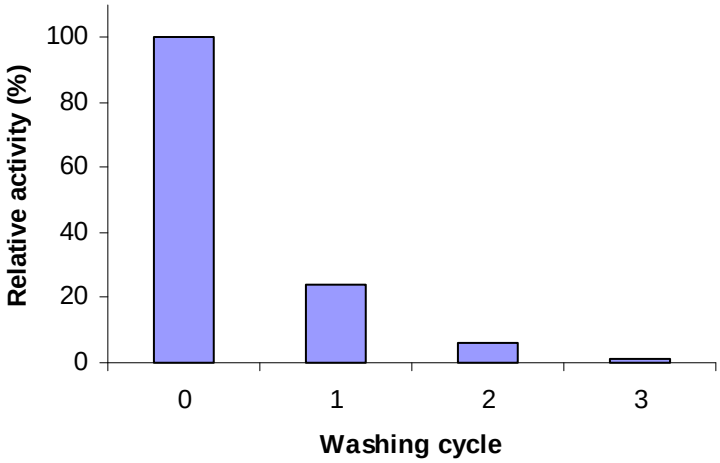

Figure 4-1. Invertase activity in supernatant after succesive washing of gel with buffer solution. The first bar indicates the enzyme activity of the invertase solution added to GA-N-CSMG for immobilization. After 3 washing cycles, only 1 percent of the initial activity remained in the supernatant.

Determination of Enzyme Activity. Invertase activity was determined by monitoring the hydrolysis of 30 mL 50 g/L sucrose in 50 mM buffer in a magnetically stirred, thermostatized vessel. The activity was measured by the dinitrosalicylic acid (DNS) method (Miller 1959). At various times, 500 μL of reaction solution were withdrawn and introduced to 5 mL of 10 g/L DNS solutions which stopped the reaction. The sample vials were capped and heated in boiling water for 30 minutes prior to addition of 1 mL sodium tartrate (40 wt. %) to stabilize the color. Absorbance was measured at 575 nm on a Gilford Response spectrophotometer and the glucose concentration determined by comparison with a standard curve (see Appendix A-2). Glucose concentration is plotted against time and invertase activity determined from the reaction profile as the initial activity. Enzyme activity is expressed in units per gram (U/g) where a unit is defined as the production of 1 μmole glucose product per minute (μmole/minute). All activity tests were conducted in triplicate.

Optimization of glutaraldehyde concentration. The optimum glutaraldehyde concentration was determined by adding 20 mL of glutaraldehyde and one gram N-CSMG (wet weight) to a 50 mL centrifuge vial. After allowing the reaction to take place for 24 hours at room temperature, the gel was thoroughly washed with deionized water. To 500 mg of each sample, 20 mL of 2 g/L invertase in 50mM acetate (pH 4.5) is added and immobilization is allowed to take place at 7 °C for 48 hours. The gel is then washed several times, suspended in 100 mM acetate buffer (pH 4.5), and measured for invertase activity at room temperature. Glutaraldehyde concentration was varied from 0 to 10 weight percent.

Optimization of invertase concentration. The optimum concentration for immobilization of invertase was determined by adding 20 mL of buffered, invertase solution to 500 mg of the optimized GA-N-CSMG. Invertase concentration was varied from 0 to 20 g/L.

4.2 Results and Discussion

Compared with other sol-gel processes that start directly from colloidal silica, this process using silicic acid ($Si(OH)_4$) starts with a much lower ionic strength. The low content of charges is critical to the modification reaction because of improved solubility for the organic ligand components. The freshly prepared silicic acid (silica sol) is composed of silica particles with very small particle size (2 - 10 nm) and, thus, a very large surface area and plenty of active silanol groups. A silane coupling reagent may be used to incorporate ligand groups on the particle surface. This modified silica sol can be gelled quickly with an adjustment of pH.

Compared to other methods, this process differs in the following categories: (1) Ionic strength and alcohol contents can be easily controlled to enhance the miscibility; (2) Composition - much higher loading; (3) Morphology - open channels connecting micro- and mesopores; (4) Adsorption – high efficiency: majority of the loaded ligands are accessible; (5) Processing – high efficiency: significantly reduced processing time; (6) Solvent systems for processing - environmentally benign solvents.

4.2.1 Characterization of N-CSMG material

As determined by thermogravimetric analysis, our N-CSMG material contains a functional group loading of approximately 3.6 mmol amino per gram of silica. This loading is significantly higher than the 1.0 mmol/g loading of commercially available products (e.g. Sigma-Aldrich #364258) and allows for much higher loadings of protein. In order to covalently immobilize enzymes on the N-CSMG, the amino-modified silica is first activated with glutaraldehyde and then, after extensive washing, added to a buffered enzyme solution. Each of these immobilization steps were optimized by using invertase, a well studied enzyme that hydrolyzes the disaccharide sucrose into glucose and fructose.

One advantage that nanoporous silica materials provide, compared to other immobilization matrices, is a high surface area. The surface area of the optimized Ga-N-CSMG was determined using BET analysis based on nitrogen adsorption on a Quantachrome Nova (Model 1200). Silica based materials experience a significant amount of shrinkage upon drying which would also affect the surface area. One method, developed initially by Steve Kistler, is to use supercritical drying to avoid the

liquid/vapor interface which causes the shrinkage. Supercritical CO_2 was used to dry the optimized Ga-N-CSMG material prior to surface area analysis. This treatment allowed us to obtain a truer surface area measurement of the material in its wet state. After outgassing, under vacuum for 2 hours at 100°C, the surface area of the optimized Ga-N-CSMG was measured at approximately 650 m^2/g.

4.2.2 Optimization of glutaraldehyde concentration

Glutaraldehyde is a common crosslinker used to activate supports with aldehyde functionality. This homobifunctional molecule can react with the amino groups located along the silica surface. Ideally the second aldehyde on each crosslinker molecule will then be available for reacting with amino groups present on protein molecules – immobilizing the protein to the silica surface.

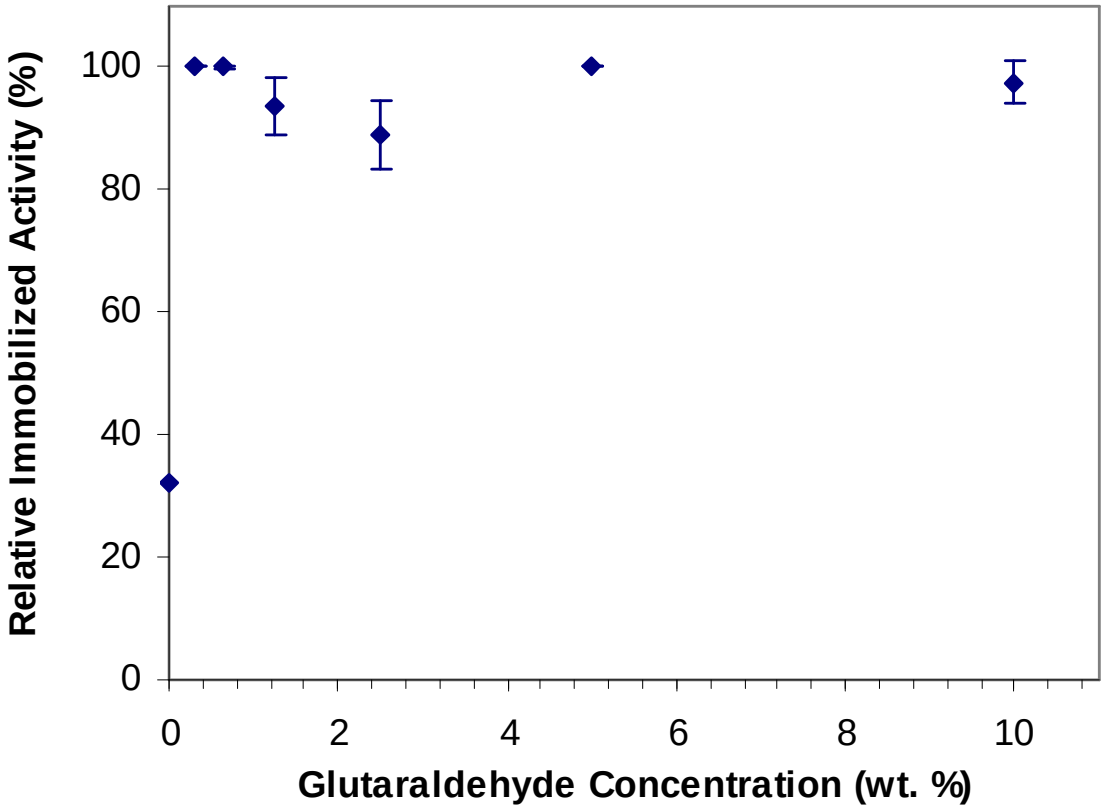

Figure 4-2. Immobilized activity after activation of N-CSMG with glutaraldehyde solutions of varying concentrations. The error bars indicate the standard deviation from the average of at least three results.

Figure 4-2 shows that when the amino-modified silica is activated with 20 mL of glutaraldehyde solution per gram of wet silica gel, no significant increase in immobilized enzyme activity is seen with increasing glutaraldehyde concentrations up to 10%. The lowest, non-zero, glutaraldehyde concentration studied was a 0.31 weight percent solution. The lack of significant variation of immobilized activity seen with even the lowest concentration is likely due to the relative abundance of glutaraldehyde in solution compared to available amino groups on the silica surface. A 20 mL volume of the 0.31% (w/w) solution contains approximately 0.625 mmols glutaraldehyde while a gram of wet N-CSMG, with a dry weight of 90 mg, contains approximately 0.35 mmols of amino groups. Even with this low glutaraldehyde concentration, there is approximately a 1.8 molar ratio of glutaraldehyde to surface amino groups. Increasing the glutaraldehyde concentration further had no effect on the immobilized activity because the system was already over saturated. A 2.5 wt.% glutaraldehyde solution was used in further studies for activation of the silica gel.

It is interesting to note that N-CSMG untreated with glutaraldehyde yields a relative immobilized activity of approximately 32 percent. This immobilization may occur through the formation of a salt-bridge between the basic, amino-modified surface and acidic side-chains of aspartic or glutamic acid; a well established interaction seen in proteins (King, Hansen et al. 1991; Dunten, Sahintoth et al. 1993; Sapse, Rothchild et al. 2002).

4.2.3 Optimization of Invertase concentration

The optimum invertase solution concentration for immobilization was determined by varying it between 0 to 20 g/L. For each concentration, 20 mL of

invertase solution (in 50 mM acetate, pH 4.5) was added to 500 mg (wet weight) of glutaraldehyde-activated N-CSMG gel (GA-N-CSMG).

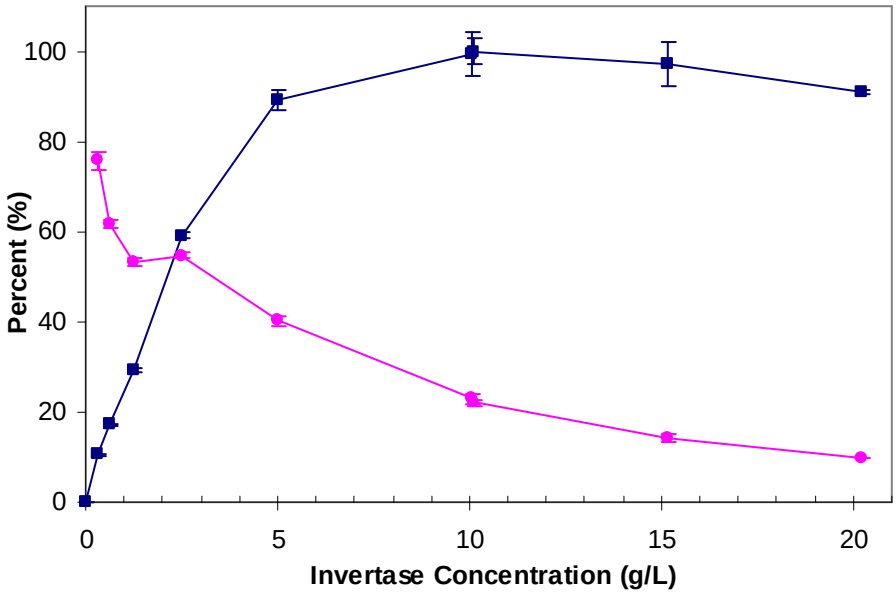

Figure 4-3. Relative immobilized activity (■) and immobilization efficiency (●) variation with invertase solution concentration. The relative activity plateaus with a 10 g/L invertase solution.

As shown in Figure 4-3, the optimum immobilized activity was achieved with a 10 g/L invertase solution concentration and no further increase in immobilized activity seen with higher enzyme concentrations. However the immobilization efficiency, obtained by a ratio of activity immobilized to the activity in the original enzyme solution, was only 23% when using 20 mL of a 10 g/L invertase solution with 500 mg of wet glutaraldehyde-activated N-CSMG. The immobilization was further optimized by varying the volume of the 10 g/L invertase solution between 1 and 20 mL and the results are shown in Figure 4-4. A solution volume of 10 mL yielded the maximum immobilization efficiency of 71% and provided 90% of the maximum immobilized activity, which was obtained with 20 mL of 10 g/L invertase solution.

All further immobilization of invertase onto GA-N-CSMG was done using 500 mg of wet, glutaraldehyde-activated gel with 10 mL of a 10 g/L enzyme solution.

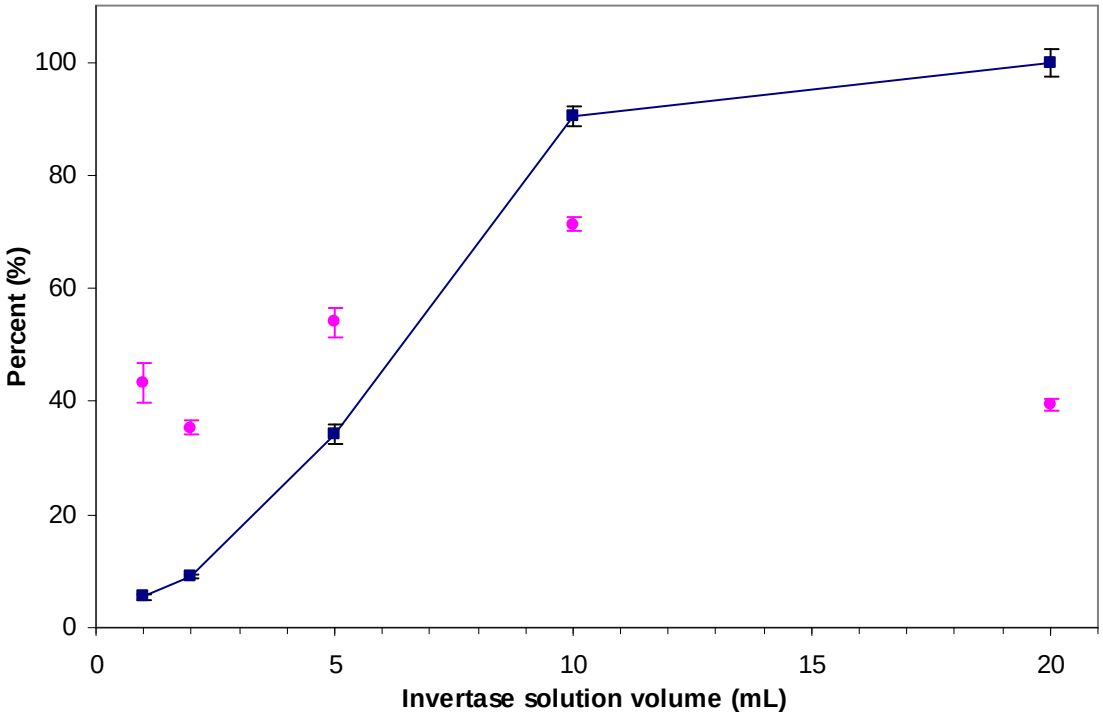

Figure 4-4. Optimization of 10 g/L invertase solution volume yielded a maximum immobilization efficiency (●) of 71% and relative immobilized activity (■) of 90% at an enzyme solution volume of 10 mL.

4.2.4 Effect of pH on invertase activity

Variation of pH can have a significant effect on enzyme stability with most enzymes showing a strong dependence of activity on pH. The pH-dependant activity profiles of both the immobilized and free invertase were determined at room temperature with a 50 g/L sucrose solution in 50 mM buffer. An acetate buffer was used for pHs 4, 4.5, and 5; phosphate buffer was used for pHs 2, 3, 6 and 7. The pH-dependent activity profiles of both free and immobilized invertase are shown in Figure 4-5. Free invertase showed maximum activity at pH 5.0 while the immobilized invertase was most active at pH 4.0. A possible explanation for the shift in pH is that the enzyme experiences a local pH which is greater than that of the bulk

solution because of the basic-functionalized silica surface. With ionic surface groups, like the amino group, there is an uneven distribution of hydrogen ions between the surface and bulk solution (Chaplin and Bucke 1992; Shuler and Kargi 1992). A higher local pH for the immobilized invertase would also explain the greater loss in activity seen, compared to free invertase, at pH greater than 4.5. It is also possible that immobilization has resulted in a conformational change which, while active, results in a higher invertase activity at a lower pH.

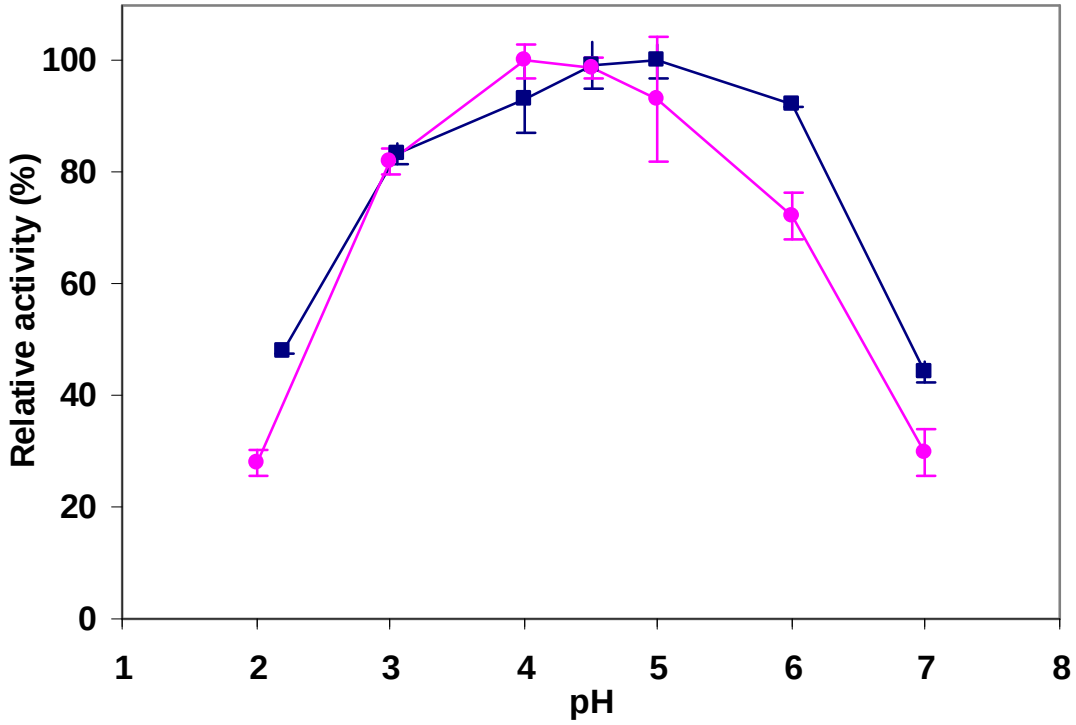

Figure 4-5. Activity profiles of free (■) and immobilized (●) invertase with pH variation.

4.2.5 Effect of temperature on invertase activity

The effect of temperature on both free and immobilized invertase activity was determined by measuring the hydrolysis of sucrose at temperatures ranging from 25-75°C. A 50 g/L sucrose solution, buffered with 50 mM acetate at pH 4.5, was used for activity determination. Both the immobilized and free enzymes show a very

similar temperature profile as seen in Figure 4-6. This indicates that immobilization of invertase on GA-N-CSMG does not significantly alter the enzyme's temperature stability.

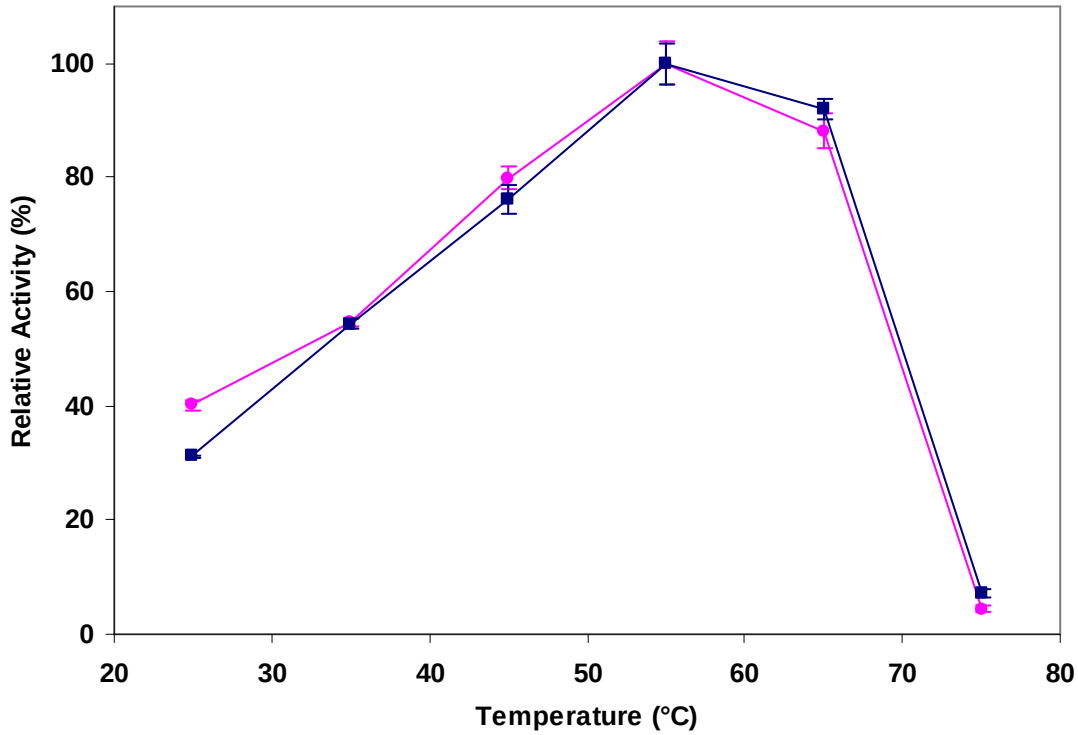

Figure 4-6. Effect of temperature on initial activities of free (■) and immobilized (●) invertase.

In Figure 4-7, the same data is plotted on an Arrhenius plot which provides a relation between the log of enzyme activity and inverse temperature. At the lower temperatures (T), higher inverse temperatures (T^{-1}), the plot is linear as enzymatic activity increases with increasing temperature. As the temperature is increased further enzyme denaturization occurs and a corresponding drop in enzymatic activity is observed. The slope of the line, in the region where temperature dependent denaturization does not occur, is used to determine the activation energy of the enzyme mediated reaction using Equation (16).

$$\ln k = \ln A - \frac{E_a}{RT} \tag{16}$$

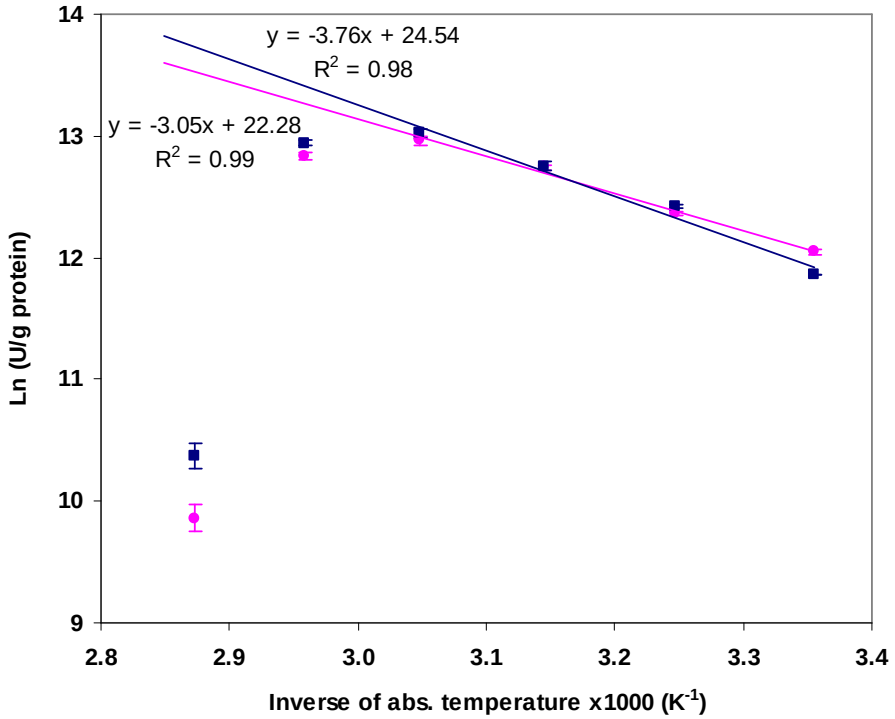

Figure 4-7. Arrhenius plot of immobilized (●) and free (■) invertase activity, Ln(Units per gram), as a function of inverse temperature.

Table 4-1. Comparison of activation energy and pre-exponential factor of free and immobilized invertase.

	Activation Energy (kJ/mol)	Pre-exponential factor (U/g protein)
Free invertase	31.3 ± 3.1	24.5 ± 1.2
Immobilized	25.4 ± 1.5	22.3 ± 0.6

The immobilized enzyme shows a decreased energy of activation at 25.4 kJ/mol compared to 31.3 kJ/mol for free invertase. Literature studies have indicated that a decrease in activation energy can be correlated to intraparticle diffusion of the substrate (Miyamoto, Fujii et al. 1973). The appearance of activation energy diffusion effects, for immobilization of invertase on GA-N-CSMG, is an indication that the immobilization is occurring within a porous matrix. In the case of a

nonporous matrix, activation energies of the free and immobilized enzyme would be in closer agreement with each other (Bahar and Tuncel 2002). The pre-exponential factor, also called the frequency factor, is proportional to the probability of a collision resulting in a substrate to product reaction. As seen in Table 4-1, this factor is very similar for both the immobilized and free invertase.

4.2.6 Michaelis-Menten kinetic parameters

The Michaelis-Menten kinetic parameters of both free and immobilized invertase were determined by measuring the initial reaction rates at various initial substrate concentrations. For this set of experiments, the initial sucrose concentration was varied between 8 wt % and 50 wt% with the pH fixed at 4.5 and temperature at 45 °C. A Lineweaver-Burk plot, shown in Figure 4-8, was used to determine V_{max} and K_m using Equation (17).

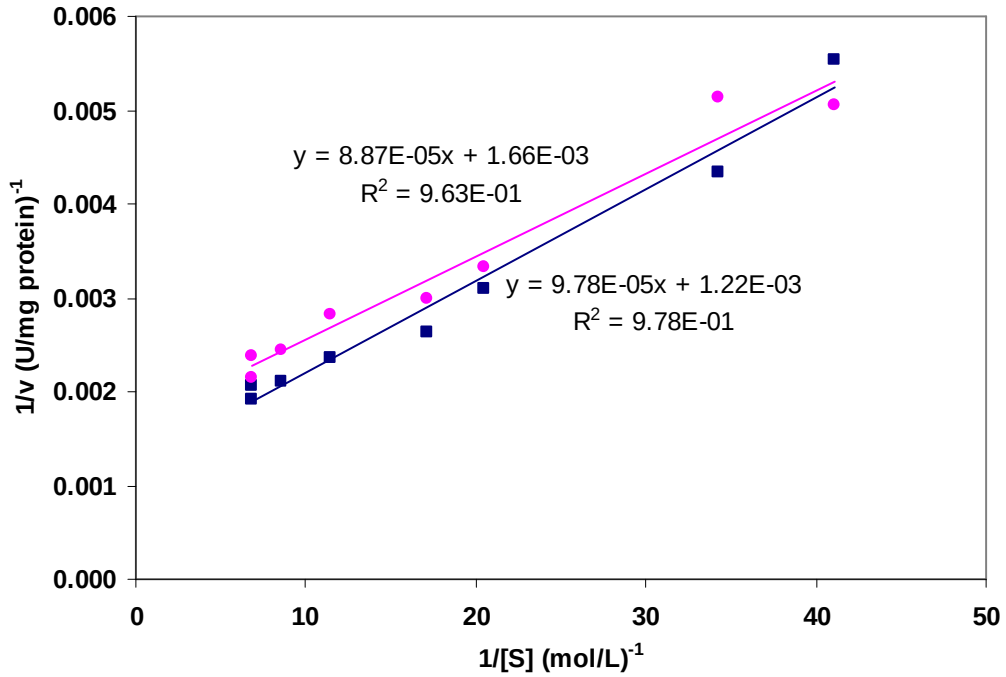

Figure 4-8. Lineweaver-Burk plot of change in the initial activity of free (■) and immobilized (●) invertase as a function of substrate concentration.

$$V_{\max} = \frac{1}{\text{intercept}}$$
$$K_m = \frac{\text{slope}}{\text{intercept}} \qquad (17)$$

The quantity K_m^{-1} is a measure of the stability of the ES complex or, in other words, enzyme affinity for its substrate. As seen in Table 4-2, the immobilized invertase exhibited a higher affinity for sucrose (lower K_m gives a larger K_m^{-1}) than free invertase while the maximum reaction rate, V_{max}, is decreased compared to that of the free enzyme. A catalytic efficiency, which is the ratio of V_{max} to K_m, was calculated to be similar for both the immobilized and free invertase. The slight increase in substrate affinity is able to compensate for a decreased V_{max} for immobilized invertase, providing a catalytic efficiency equal to that of the free enzyme.

Table 4-2. Michaelis-Menten kinetic parameter of free and immobilized invertase.

	V_{max} (U/mg)	K_m (mol/L)	Catalytic Efficiency (V_{max}/K_m)
Free	$(8.2 \pm 1.0) \times 10^{2}$	$(8.0 \pm 1.0) \times 10^{-2}$	$(1.0 \pm 0.2) \times 10^{4}$
Immobilized	$(6.0 \pm 0.6) \times 10^{2}$	$(5.4 \pm 0.7) \times 10^{-2}$	$(1.1 \pm 0.2) \times 10^{4}$

The efficiency factor, η, can be calculated from the reaction rates of the immobilized and free invertase,

$$\eta = \frac{v_{immob}}{v_{free}} = 0.73 \qquad (18)$$

where v_{immob} is the reaction rate of the immobilized invertase and v_{free} that of free invertase. GA-N-CSMG gives an efficiency factor of 0.73 for the immobilization of invertase. It has been shown that as the effectiveness factor, a ratio of immobilized to

free enzyme activity, decreases below unity, the activation energy measured approached the arithmetic mean of the activation energies of diffusion and reaction (De Whalley 1964).

There are several reasons that can explain the difference in behavior of the free and immobilized invertase. First, the immobilized invertase is located in an environment that is quite different from the environment of free enzyme in the bulk solution. The dependence of immobilized invertase on diffusion of substrate into the matrix interior is also quite different from free invertase, which interacts freely with the bulk solution. In addition, the attachment of invertase to GA-N-CSMG likely causes some change in conformation. A conformational change may explain why the K_m of immobilized invertase is only 67 percent that of the free. In this instance, immobilization of invertase actually increases its substrate affinity. Most cases show a decrease in substrate affinity due to conformation changes (Bahar and Tuncel 2002).

4.2.7 FTIR analysis of invertase immobilization

Infrared spectra were used to verify the immobilization procedure. Shown in Figure 4-9 are spectra obtained for unmodified silica gel, N-CSMG, GA-N-CSMG, and the immobilized invertase. As expected, C-H stretching vibration frequency is seen at 2936 cm^{-1} for all spectra except the silica gel with contributions from the organosilane, glutaraldehyde, and the enzyme (Monteiro and Airoldi 1999; Airoldi and Monteiro 2000). The corresponding simple bending vibrations occur at 1407 cm^{-1} for the GA-N-CSMG and immobilized invertase spectra. Free aldehyde presence is seen on GA-N-CSMG at 1718 cm^{-1} and does not appear in any other spectra. The

amine-glutaraldehyde reaction produces an imine N=C bond, Schiff-base, seen at 1647 cm^{-1} while an ethylenic C=C bond formed by resonance stabilization of the imine appears at 1563 cm^{-1} (Airoldi and Monteiro 2003). Associated with Si-O-Si bonds are the bands appearing in the range 1050-1070 cm^{-1} (Coates 2000).

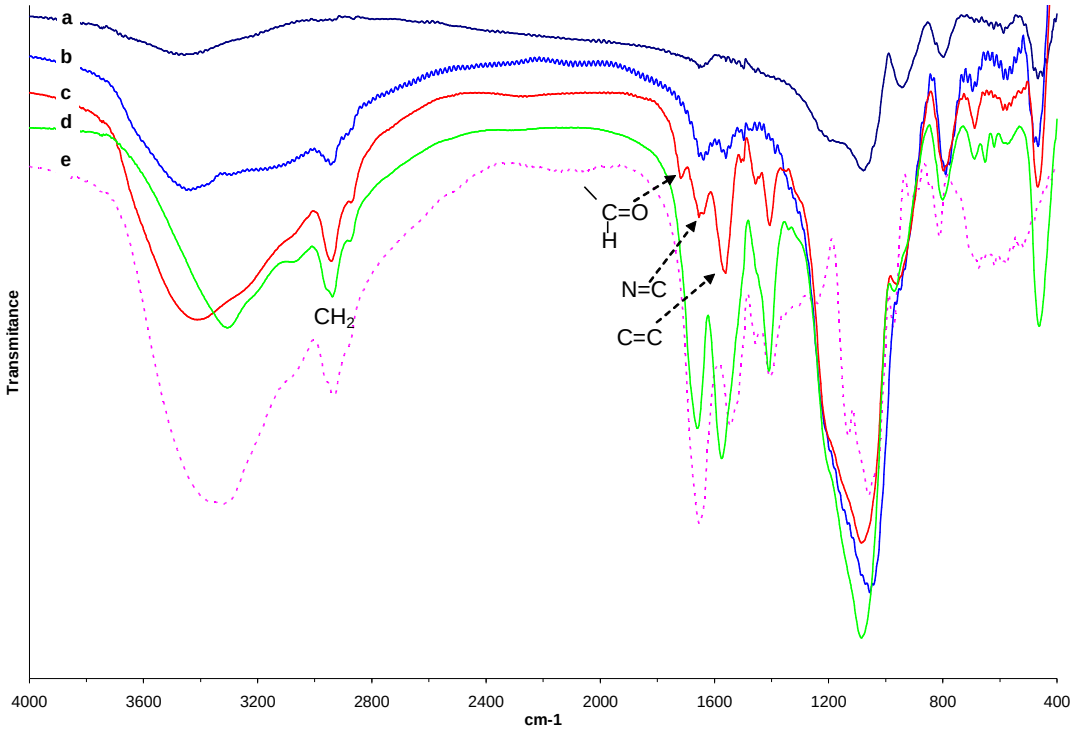

Figure 4-9. FTIR analysis of a) unmodified silica gel, b) N-CSMG, c) GA-N-CSMG, d) immobilized invertase, and e) free invertase.

4.2.8 Thermogravimetric analysis (TGA) of immobilized invertase loading

TGA analysis was used to verify the high enzyme loadings indicated by the observed immobilized activity. Figure 4-10 shows the TGA profiles obtained for silica (silicic acid gelled without surface modification), N-CSMG (amino-modified silica), GA-N-CSMG (N-CSMG activated with glutaraldehyde), and the immobilized invertase (invertase immobilized onto GA-N-CSMG). As the reactor temperature is increased organic groups within the silica gel are vaporized and carried away on a

stream of air. The final residual weight is a measure of the abundance of silicon dioxide (SiO_2).

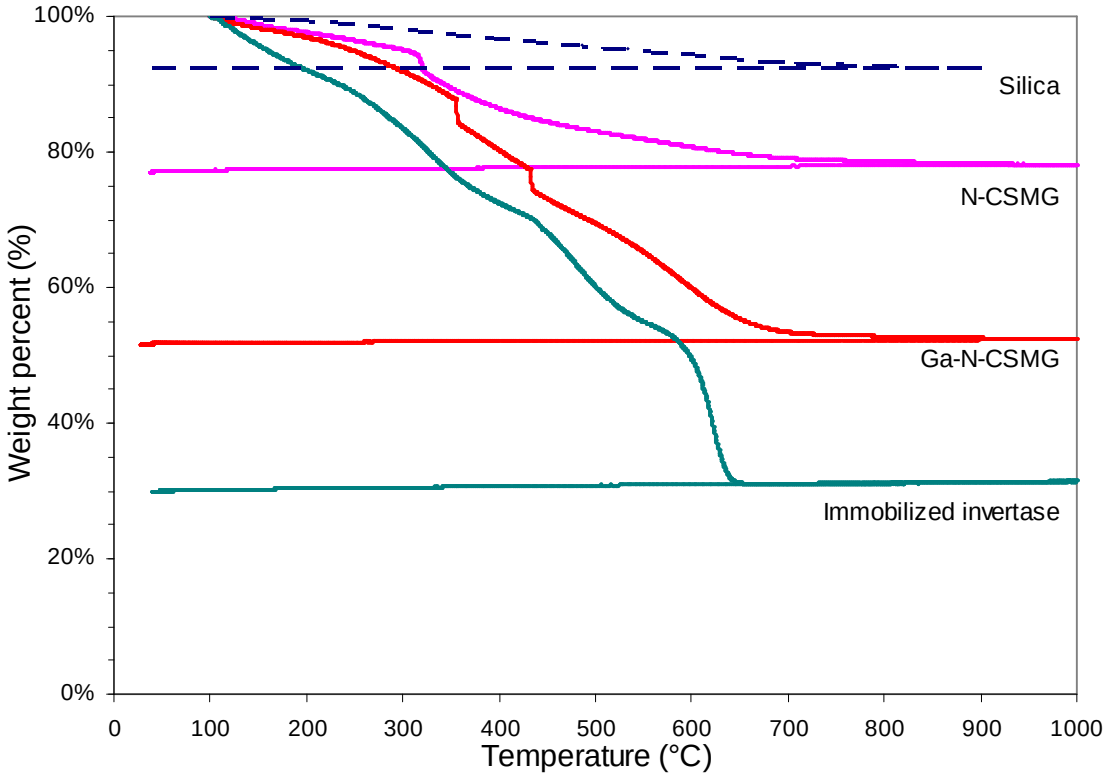

Figure 4-10. Thermogravimetric profiles for silica gel without modification (—Silica), amino-modified silica (—N-CSMG), glutaraldehyde-activated silica (—Ga-N-CSMG) and invertase-immobilized silica (—).

Loading (g/g SiO_2) of the various groups can be determined, by comparison of the residual weights, and the molar loading is determined, with the known molecular weights, as provided in Table 4-3. TGA has confirmed that the N-CSMG is able to achieve a very high loading of invertase with a maximum loading of 1.39 grams invertase per gram of SiO_2. This invertase loading corresponds to a loading of 723 mg invertase per gram of GA-N-CSMG.

Table 4-3. Functional group and invertase loading of silica gel as determined by TGA.

	Loading	
	g/g SiO_2	**mmol/g SiO_2**
Silanol	8.18×10^{-2}	4.54
Amino	0.212	3.64
Glutaraldehyde	0.634	7.54
Invertase	1.39	5.2×10^{-3}

The invertase loading obtained with the GA-N-CSMG is significantly greater than other published results. A comparison of the GA-N-CSMG loading with various other materials is shown in Table 4-4. With a loading of 723 mg/g matrix, GA-N-CSMG is able to immobilize a three-fold greater weight of invertase than the material with the next highest loading – lactam-amide graft polymer with 225 mg/g. The lactam-amide graft polymer exhibited only a 15 percent retention of enzyme activity. GA-N-CSMG, with an immobilized invertase activity of 340.9 ± 8.8 U/mg protein and 345.4 ± 11.6 U/mg protein for free invertase, provides almost 99 percent recovery of enzymatic activity.

Table 4-4. Comparison of invertase immobilization loading and the retained activity of GA-N-CSMG with other materials.

Carrier	Invertase Loading (mg /g matrix)	Retained activity (%)	Reference
GA-N-CSMG	**723**	**98.7 ± 4.1**	
Organosilane	3.51	--	(Airoldi and Monteiro 2003)
Sepabeads	--	90	(Mateo, Torres et al. 2003)
Pectin	--	57	(Gomez and Villalonga 2000)
Celite Polyacrylamide	3 10	92 81	(Mansour and Dawoud 2003)
Poly(*p*-chloromethylstyrene) beads	19	80	(Bahar and Tuncel 2002)
Lactam-amide graft copolymer	225	15	(De Queiroz, Vargas et al. 2002)

The efficiency of immobilization on GA-N-CSMG can also be analyzed by determining the degree of surface coverage. The Stokes radii of proteins is determined from sedimentation experiments and the Stokes-Einstein equation (Gosting 1956)

$$a = \frac{kT}{6\pi\eta D} \tag{19}$$

where a is the Stokes radius in Å, k is the Boltzmann constant, T is the absolute temperature, η is the viscosity, and D is the diffusion coefficient. Uversky generated a calibration curve for the dependence of a protein's Stokes radius on the molecular weight based on published results (Uversky 1993)

$$\log(R_S) = -(0.254 \pm 0.002) + (0.369 \pm 0.001)\log(MW) \tag{20}$$

where R_S is the Stokes radius in Å and MW is the protein molecular weight in Daltons. Applying this equation to the 270 kDa invertase and 649 m^2/g GA-N-CSMG, a loading efficiency based on surface coverage can be determined. The results presented in Table 4-5 assume that the invertase preparation used for immobilization is 100% pure.

Table 4-5. Surface coverage efficiency GA-N-CSMG surface coverage efficiency by invertase immobilization.

Molecular Weight	270,000 Da
Stokes radius	5.63 nm
Molecular footprint	99.4 nm^2
GA-N-CSMG surface area	649 m^2/g
Theoretical loading per g GA-N-CSMG	2.93 g/g
Actual loading per g GA-N-CSMG	0.723 g/g
Loading efficiency	24.7 %

Although a relatively high loading of invertase has been accomplished compared to other published results, there is still considerable room for improvement.

Based on the molecular footprint, calculated from the Stokes radius, and the measured surface area, a theoretical maximum loading of 2.93 grams invertase per gram GA-N-CSMG is achievable. The obtained loading of 0.723 g/g GA-N-CSMG is less than 25 percent of the theoretical maximum. Likely reasons for the low loading efficiency are the inaccessibility to surface areas by the enzyme due to the presence of small, micropores and the blockage of pore entrances (Raman, Ward et al. 1993; Baruque, Baruque et al. 2001).

Table 4-6. Comparison of GA-N-CSMG-immobilized invertase activity with various other matrix materials.

Matrix	Particle size (μm)	Activity (U/g matrix)	Temp, pH, [S]	Reference
GA-N-CSMG	**7 – 200**	**246,000**	45°C, pH 4.5, 0.146 M	
Corn grits	100 – 200	36,000	40°C, pH 4.5, 0.400 M	(Monsan, Combes et al. 1984)
Porous silica	--	11,500	45°C, pH 4.5, 0.146 M	(Vicente 2000)
Aminopropyl silica	--	3,700	45°C, pH 4.5, 0.146 M	(Rosa, Vicente et al. 2000)
Polystyrene	300	3,050	25°C, pH 4.5, 0.146 M	(Mansfeld and Schellenberger 1987)
Magnetic silica	20 – 45	469	55°C, pH 4.5, 0.292 M	(Goetz, Remaud et al. 1991)

Table 4-6 provides a comparison of immobilized activities of GA-N-CSMG with some published results under similar reaction conditions. The highest activity seen in literature for immobilized invertase is 36,000 U/g for immobilization on corn stover (Monsan, Combes et al. 1984), a result almost seven-fold lower than that of the GA-N-CSMG. For a silica-based matrix, the highest activity in literature is 11,500

U/g (Vicente 2000), again significantly lower than that obtained using the N-CSMG material.

4.2.9 SEM analysis of GA-N-CSMG after invertase immobilization

Visualization of N-CSMG before and after glutaraldehyde treatment, and after invertase immobilization, shows the evolution of the particle morphology with the processing steps as seen in the SEM images of Figure 4-11. The surface modifications, combined with effects of the mechanical stirring used, creates silica particles with a rougher appearance and finer particle size. A significant change in appearance is seen in moving from the N-CSMG to invertase immobilization. While the N-CSMG has a smooth surface on the micron scale, the immobilized invertase material shows significant porosity. This is likely created through the breaking of GA-N-CSMG into finer particles, by mechanical stirring, and then interacting to form into clusters. These interactions may occur between aldehyde groups of different particles or through the immobilization of a signal enzyme on two different silica particles. The end result is a material that is not only mesoporous, but also contains larger pores that would increase the rate of diffusion, of substrate and product, to and from the immobilized enzyme, respectively.

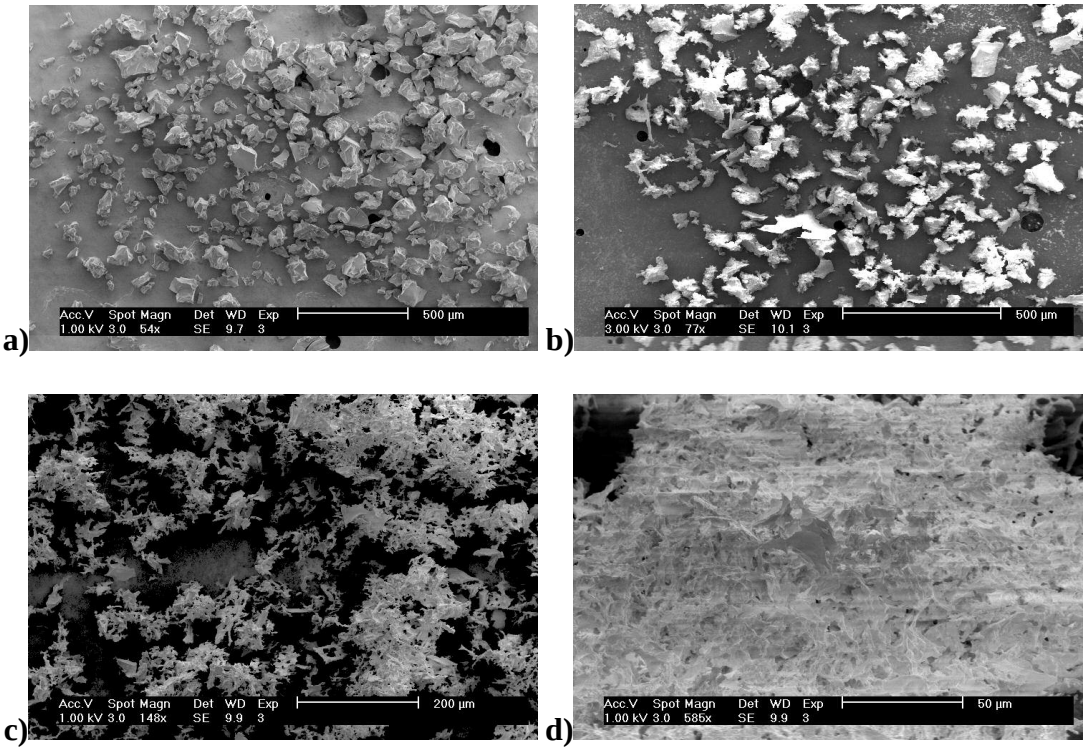

Figure 4-11. SEM images of (a) N-CSMG, (b) GA-N-CSMG, and (c) low and (d) high magnification of GA-N-CSMG-immobilized invertase.

4.3 Conclusions

Using ISTN's N-CSMG protocol and optimized immobilization steps, immobilized invertase activities of more than 246,000 U/g of GA-N-CSMG have been achieved with a 50 g/L substrate concentration (pH 4.5, 45 °C). This is a significant increase in immobilized activity when compared to published results. TGA analysis has confirmed the high loading of invertase at 0.723g invertase per gram GA-N-CSMG. While the weight of invertase immobilized is significantly improved compared to other published results, it is still less than 25 percent of the theoretical maximum based on the enzyme's Stokes radius. Also, the immobilized invertase exhibited a maximum reaction rate, V_{max}, only 73 percent of free invertase, an increase in substrate affinity, K_m^{-1}, compensated for this and no significant difference in catalytic efficiency is seen.

The vastly improved immobilization of enzymes on GA-N-CSMG would provide a significant advantage in many processes. In the next chapter we discuss a bioreactor fabricated, with the immobilization of the enzyme thermolysin on GA-N-CSMG, for the production of a pharmaceutical product.

Chapter 5: Production of Low Molecular Weight Protamine

5.1 Background

Protamine is commonly used clinically as an antagonist to heparin, an anticoagulant. However, protamine has been shown to induce some adverse reactions in patients, including some fatalities due to cardiac arrest (Horrow 1985; Horrow 1985; Weiss, Nyhan et al. 1989). The discovery of specific sequences within larger protein molecules which are accountable for the transduction abilities of proteins could potentially have significant implications for a broad range of biomedical applications.

Recently, Professor Victor Yang and his research group at the University of Michigan reported the development of low molecular weight protamine (LMWP) fragments as nontoxic substitutes for protamine in clinical heparin neutralization (Chang, Lee et al. 2001; Chang, Liang et al. 2001; Lee, Chang et al. 2001). These LMWP peptides, which display a high arginine fraction in their amino acid compositions, retain the ability to neutralize heparin yet have significantly less toxicity in vivo (Liang, Zhen et al. 2003). LMWP has also been shown to be equally potent, as protamine, in neutralization of low molecular weight heparins (LMWH), but with the benefit of markedly reduced toxicity. In addition, LMWP can be used to enable the sustained release of protein drugs such as insulin (Park, Liang et al. 2003). Sustained release systems for insulin are currently available in a complex form with protamine. However, when it is replaced with low molecular weight protamine, an extended release can be obtained since the cationic charge density in one molecule of

peptide is higher than in protamine, which leads to a more compact complex formation with insulin.

LMWP peptides have exhibited a significantly reduced level of immunogenecity and antigenicity, which are the two principal events of protamine-induced immunotoxicity (Chang, Lee et al. 2001; Chang, Liang et al. 2001; Lee, Chang et al. 2001). Furthermore, researchers from the Industrial Science & Technology Network, Inc. (ISTN), in collaboration with Professor Yang's group, discovered that LMWP was almost equally potent as TAT in mediating cell translocation of any attached species (Park, Liang et al. 2003). Low molecular weight protamine carries significant structural similarities to the protein transduction domain (PTD) of HIV-TAT protein. PTDs are small basic peptides that have been used to translocate proteins, polynucleotides, and even nanoparticles through cell membranes (Console, Marty et al. 2003). Hybridization with the TAT peptide has allowed the translocation of a variety of biologically active species, including liposomes (Torchilin, Rammohan et al. 2001), proteins (Futaki, Nakase et al. 2002), peptides, DNA (Torchilin, Levchenko et al. 2003) and nanoparticles (Futaki, Nakase et al. 2002). Poor cell uptake of active drugs has been one factor for insufficient treatment efficacy, especially against tumors (Schuster, Garg et al. 1991; Iznaga-Escobar, Mishra et al. 2004). LMWP, much like TAT, can ferry those active agents into various target cells and improve their therapeutic efficacies. Also, as a small peptide, LMWP itself could have tremendous benefits for drug therapy, as small peptides normally possess improved bioavailability compared to large protein drugs (Carriere, Neves et al. 2001). Because of all these benefits in therapeutic treatments, the

commercial potential of LMWP in biomedicine is remarkably promising. Drug delivery and heparin neutralization are two markets that provide immediate and clear commercialization opportunities for LMWP. According to Frost and Sullivan, the drug delivery market is expected to grow from $19 billion in 2000 to $41 billion in 2007 (Challener 2003).

An advantage of using LMWP as transmembrane carrier is its easier production and lower cost. Production of LMWP is achieved by thermolysin-catalyzed digestion of native protamine. For the production of such bioactive compounds, an enzyme-mediated reaction is often preferred over a chemical synthesis route because of its simplicities, selectivity, and specificity, as well as its moderate reaction conditions. Furthermore, the immobilization of thermolysin onto a nanoporous support will allow for continuous flow production of LMWP.

The enzymatic digestion of native protamine yields a series of LMWP species. The current preparation method utilizes a heparin affinity column to separate LMWP into five fractions termed TDSP1 to TDSP5 (see Figure 5-1), according to the ascending order of their elution ionic strength which correlates with an ascending order in arginine units ranging from 5 to 10. Literature evidence indicates a correlation between the number of arginine units in the peptide sequence to cell membrane transduction ability with an optimum value from 6 to15 arginine units (Henry 2003). Indeed, work by Futaki et. al. clearly indicated the effect of the length of arginine chain on the cell internalization (Futaki, Suzuki et al. 2001). In their work, peptides composed of even number (4–16) residues of arginine were prepared and tested. The Gly-Cys-amide segment was attached to their C termini for

fluorescein labeling. Considerable difference was recognized on the translocation efficiency and intracellular localization among these peptides. R4 showed extremely low translocation activity while R6 and R8 exhibited the maximum internalization and accumulation in the nucleus. The degree of internalization decreased as the chain length was further increased. It has been proposed that the uptake of arginine-rich peptide is mediated by the guanidine head group in the arginine through the formation of a hydrogen bond between arginine and lipid phosphate in the membrane (Calnan, Tidor et al. 1991; Wender, Mitchell et al. 2000; Futaki, Suzuki et al. 2001). The five LMWP groups, TDSP1-5, contain arginine units of 4, 5, 6, 9, and 10, respectively.

In this work, a continuous flow reactor using thermolysin immobilized on nanoporous silica was developed for the production of TDSP5. Enzyme encapsulation or immobilization has been commonly utilized for easy removal from a reaction, dispersion into insoluble liquid medium, and stabilization under various environments. By using a nanoporous silica support, the pore morphology, surface ligand groups, and the inherent large surface area can be exploited to achieve high enzyme loadings and, therefore, a reactor of high enzymatic activity can be developed.

5.1.1 Advantage of using thermolysin for preparation of LMWP

Conventional peptide synthesis uses the standard (9-fluorenylmethyl) chloroformate (Fmoc) solid-phase chemistry. This chemical synthesis, however, generates a heterogeneous peptide mixture which requires extensive purification. In addition, especially for producing highly polar (basic or acidic) peptides, the synthesis employs the additional steps of protecting and deprotecting of inhibitory

functional groups of amino acid (for example, capping the guanidyl group in arginine), which substantially increases the risk of heterogeneity in the final product. In contrast, the thermolysin digestion method in our approach has the common enzyme-substrate specificity, and therefore, can produce consistent peptide sequences with simplicity and of high quality. Prepared peptides sequences can then be separated and purified by routine heparin-affinity chromatography. The most significant advantage of the LMWP system would be the production of peptides in mass quantities unachievable by conventional peptide synthesis methods.

Protamine digestion can be accomplished using free thermolysin. A 10 mg/mL protamine solution, buffered at pH 7.5 by 50 mM TRIS/HCl, is incubated at 37 °C with 1% (w/w) thermolysin and 2mM calcium chloride. The digestion is allowed to proceed for 30 minutes and then stopped by addition of ethylenediaminetetraacetic acid (EDTA) and cooling in an ice bath. The desired peptide is then obtained by standard purification methods.

5.1.2 Purification and recovery of LMWP

The option of integrating both reaction and separation into one flow reactor is the primary benefit of NEED. Whenever possible, the pore surface of the silica support should be modified with ligands that have a high affinity to the reactants, but not to the product. Such a preferred retention of reactants will achieve the product separation and at the same time increase yield. Such an ideal scenario is difficult to achieve with the protamine digestion reaction because the only differences between the reactant and product species are their molecular weights and, correspondingly, variations in charge.

LMWP purification is done with the use of HiTrap Heparin columns from Amersham Biosciences which have approximately 10 mg heparin/mL gel, according to product specifications. Heparin, which is negatively charged, absorbs the positively charged protamine and its digested fragments. As mentioned earlier, protamine shows high affinity for heparin binding. The digested fragments, which have slight differences in size and charge density, show varying binding strengths with the heparin column. When eluted using a sodium chloride concentration gradient, the various fragments are released at different ionic strengths and can thus be separated from each other. After recovery of the peptide (TDSP5), the solution must be desalted by either ultra-filtration or dialysis. Dialysis typically requires the treatment of a given sample volume with approximately 1,000 times its volume in buffer over a period of 24 to 48 hours.

Prior to this work, LMWP purification was done using a 5 mL HiTrap Heprain column containing a total of approximately 50 mg heparin. The column was placed between two Alltech 526 HPLC Pumps and a Linear UVIS 200 detector equipped with a flow-through cell. A 1 mL sample loop was connected to a 2-position, 6-port sample injector. The HPLC system was connected to a PeakSimple Chromatography Data System (Model 202) and the data analyzed by PeakSimple software.

LMWP was purified by diluting 0.2 mL of the digested protamine solution with deionized water to 1 mL and loading this solution into the sample loop. Then, the salt gradient and data collection were initiated by switching the sample injector from the “LOAD” to “INJECT” position. Figure 5-1 shows the elution profile

obtained by this set-up. The peak labeled "TDSP5" is the desired fragment and is obtained at yields of less than 0.4 mg per cycle. Any further mention of LMWP will specifically refer to the TDSP5 fragment.

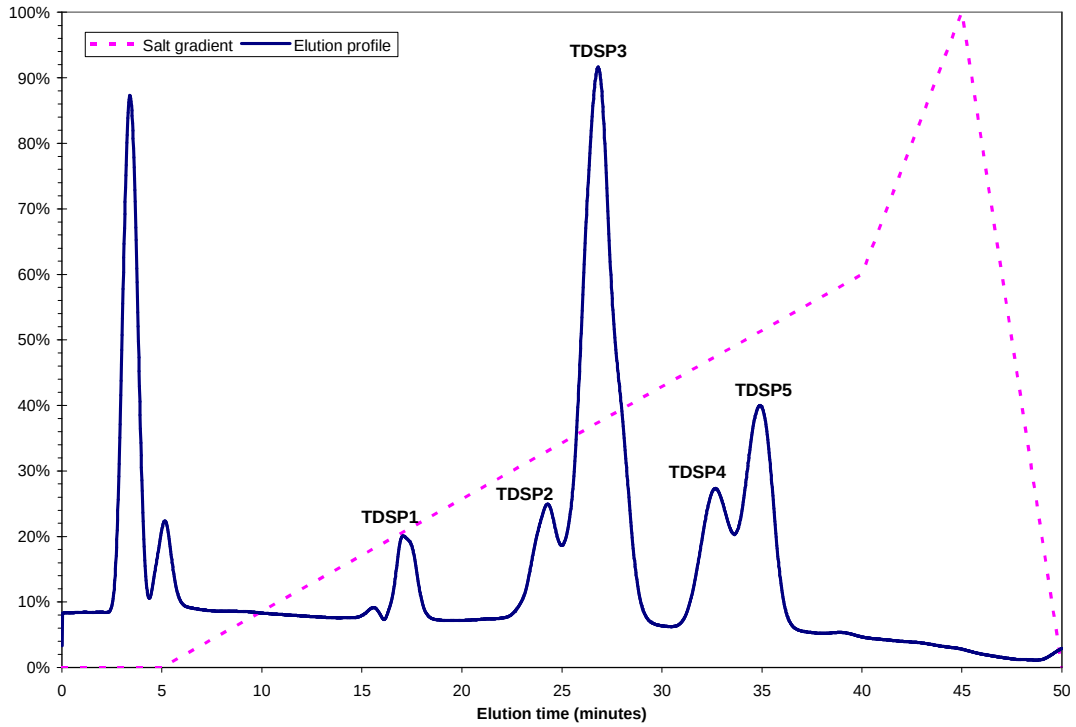

Figure 5-1. Elution profile of protamine fragments using a heparin column and NaCl gradient. The elution profile was obtained at an absorbance wavelength of 215 nm. Solution flow rate was 1.5 mL per minute with a 5 mL heparin column. The sample loading was 1 mL of a 2.2 mg digest/mL. Buffer A was 50 mM TRIS/HCl (pH 7.5) and Buffer B was 50 mM TRIS/HCl/2 M NaCl (pH 7.5).

The resolution between two peaks of a chromatogram is often used as a measure of the separation efficiency, as shown in Figure 5-2. Peak widths, W_1 and W_2, are determined at the intersection of the base line with lines tangent to the curve at the inflection point. The elution volumes, V_1 and V_2, are the solution volumes that pass through the column from the time of sample injection to the time at which the peaks elute from the column. A resolution of 1.0 indicates that 98% purity has been achieved at 98% peak recovery. At R_s = 1.5, 100% purity and recovery is obtained.

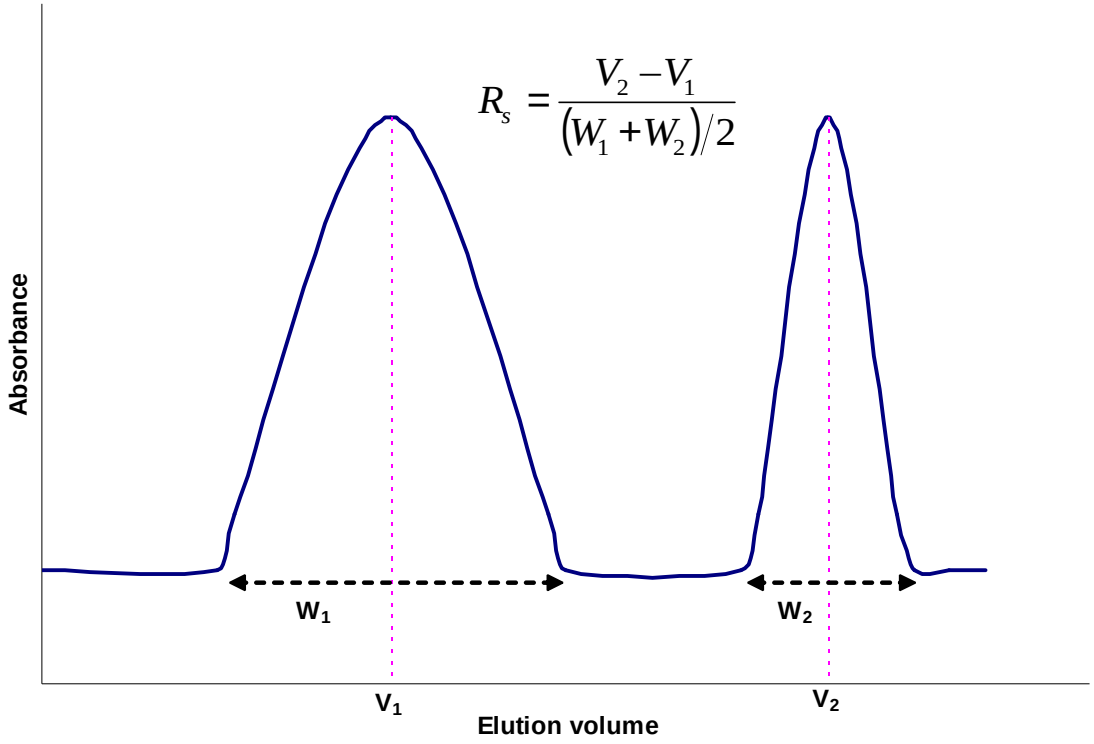

Figure 5-2. Determination of peak resolution (R_s) from elution profiles.

The peak resolution for the purification of LMWP is determined by looking at peaks TDSP4 and TDSP5. Figure 5-3 shows a magnification of the TDSP4 and TDSP5 elution profiles from Figure 5-1. Since the peptide of interest is TDSP5, the efficiency of the purification will be determined by the obtained peak resolution between TDSP5 and the closely eluting TDSP4. Purification of LMWP with a HiTrap heparin column and the salt gradient shown in Figure 5-1 gives a peak resolution of:

$$R_s = \frac{2(V_2 - V_1)}{(W_1 + W_2)} = \frac{2(34.87 - 32.68)\text{min}}{(2.90 + 2.48)\text{min}} \frac{1.5mL/\text{min}}{1.5mL/\text{min}} = 0.81 \qquad (21)$$

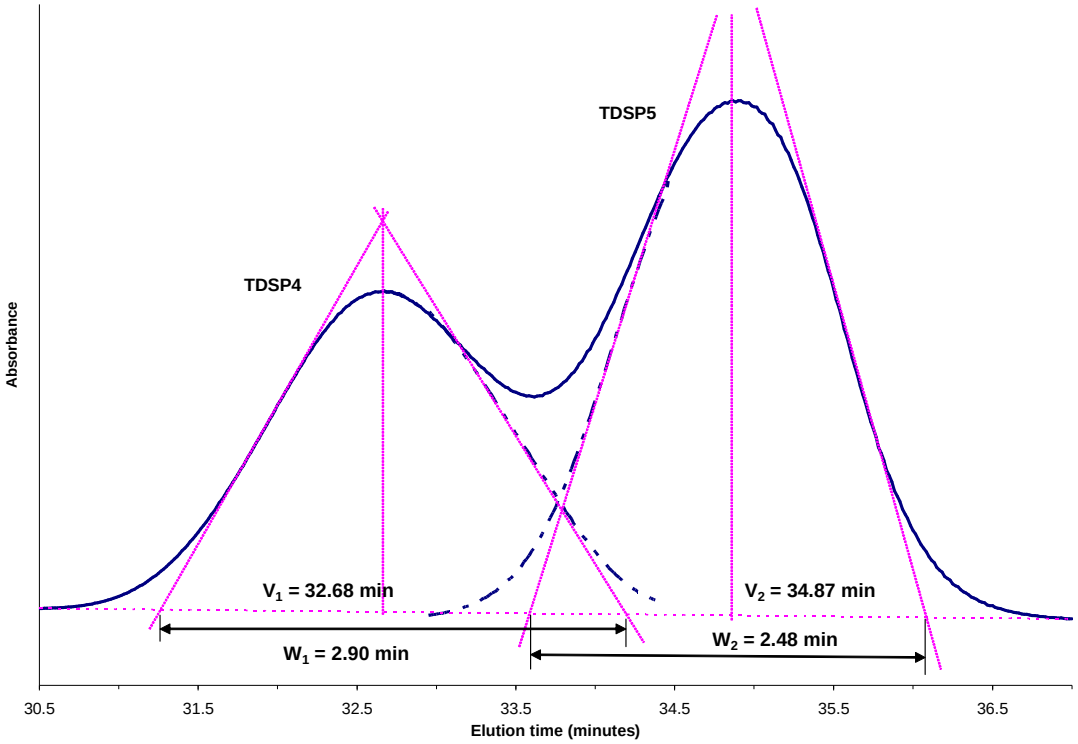

Figure 5-3. Determination of peak resolution for LMWP purification by a linear salt gradient.

This peak resolution of 0.81 yields a TDSP5 product of only 95.8% purity at a recovery of 96.7 percent, as determined through integration of the area between peak profiles and the base line. This purity of less than 96 percent is very low considering that the product is intended for pharmaceutical use. Therapeutic drugs are required in many cases to be 99.997% pure (Wheelwright 1991). In order to scale-up the production of LMWP, the peak resolution must first be improved to provide higher purity and yield.

Assuming that the peaks follow a Gaussian distribution, the peak resolution is proportional to the product of three terms, the selectivity (α), efficiency (N), and a capacity factor (k'), as follows:

$$R_s = \frac{1}{4}\frac{\alpha - 1}{\alpha}\sqrt{N}\frac{k'}{1+k'} \tag{22}$$

The capacity factor is a measure of the degree of retardation of a component; a higher capacity factor corresponds to greater retention. The capacity factor of the n^{th} component is determined by the elution volume (V_n) and total mobile phase volume in the chromatography column (V_t) as shown in Equation (23). When V_t is unknown, the component capacity factor is proportional to the elution volume V_n.

$$k'_n = \frac{V_n - V_t}{V_t} \tag{23}$$

In the peak resolution equation (22), k' is an average of the component capacity factors of the peaks in interest. This capacity factor is not the same as the column loading capacity.

In a chromatogram, selectivity is a measure of the separation between two peaks with good selectivity providing a greater separation. As shown in Equation (24), selectivity is determined as a ratio of the capacity factors of two components. This equation is approximately equal to a ratio of the component elution volumes when V_t is unknown.

$$\alpha = \frac{k'_{n+1}}{k'_n} \approx \frac{V_{n+1}}{V_n} \tag{24}$$

The third factor of the peak resolution equation (22) is the efficiency (N). This term is a measure of the number of theoretical plates for a column and provides a quantification of peak broadening caused by diffusion within the column. The efficiency is calculated from the component elution volume, V_n, and peak width, w_n, as shown in Equation (25).

$$N = 16\left(\frac{V_n}{w_n}\right)^2 \quad (25)$$

The requirements of high purity and high recovery, for this valuable peptide, necessitate a process with high resolution and high selectivity. The optimization of LMWP production was accomplished by looking at two aspects of the process: 1) the chromatographic scheme and 2) sample preparation. The following section of this chapter details the optimization and scale-up of LMWP purification.

5.2 Optimization and Scale-up of LMWP Purification

Optimization of LMWP purification was done using a Pharmacia LKB Fast Performance Liquid Chromatography (FPLC) System. This system consisted of a UV-M II detector, two P-500 pumps, LCC-501 Plus Controller, FRAC-100 fraction collector, a MV-7 motor valve, and REC102 recorder. The system was also equipped with a 50 mL Superloop loading column from Amersham Biosciences. The column was filled with free thermolysin, digested protamine solution. Switching the MV-7 motor valve from the LOAD to INJECT position directs buffer flow into the top of the column. This forces a moveable piston in the column downward which pushes the sample solution into the chromatography column. Elution profiles were recorded at a wavelength of 214 nm.

The first step in optimization the purification of LMWP is to improve the peak resolution between the TDSP4 and TDSP5 components. As shown in the previous section of this chapter, the resolution between two peaks is dependant on the selectivity (24), efficiency (25), and capacity factor (23) of the process. Each of these factors is related to the component elution volumes as shown by their respective

equations. Modification of the salt gradient is one method of affecting a change in the elution volumes. At lower salt concentrations, the elution volume is increased and this also increases the selectivity, efficiency, and capacity factors.

Figure 5-4 shows a sample of the elution profiles obtained during optimization of the process. The selectivity, efficiency, and capacity factors determined from these profiles are given in Table 5-1. Compared to the other profiles, the optimized profile, in Figure 5-4d, shows a significantly higher selectivity (*k'*) and improved efficiency; this accounts for the improvement in peak resolution ($R_s > 2$). For comparison, a peak resolution of 1.5 provides 100 percent peak purity and recovery.

Table 5-1. Peak resolution (R_s) as determined from elution profiles that were obtained with varying salt gradients.

Elution Profile	Selectivity (*k'*)	Efficiency (α)	Capacity factor (*N*)	Peak resolution (R_s)
Figure 5-4a	34.1	1.1	1777	0.95
Figure 5-4b	32.3	1.2	502	0.99
Figure 5-4c	41.3	1.5	182	1.2
Figure 5-4d	179	1.6	621	2.2

During process optimization, in addition to peak resolution, it is also important to consider the sample loading and cycle time; higher sample loadings and shorter cycle times result in increased production rates. Previous to this study, LMWP purification was accomplished using 0.2 mL sample volume and an 80 minute cycle time. The optimized profile purifies 5 mL of sample with a 60 minute cycle time - yielding greater than 30 times increased productivity per minute. The optimized profile is also functional for continuous operation as shown in Figure 5-5.

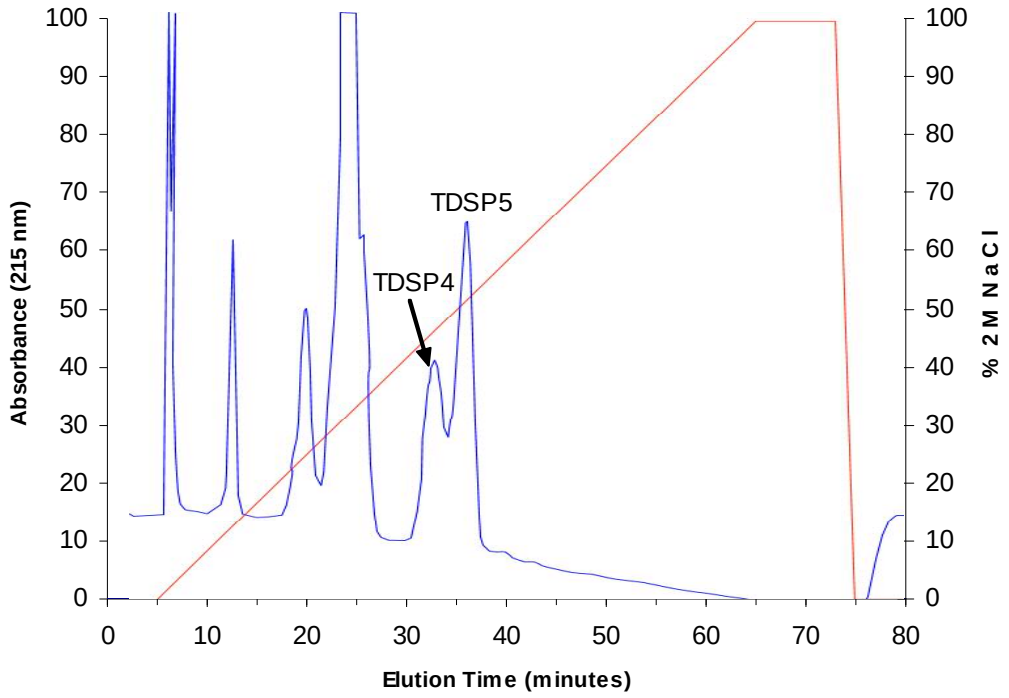
Absorbance (215 nm)
% 2 M NaCl
Elution Time (minutes)
TDSP5
TDSP4
0
10
20
30
40
50
60
70
80
90
100

a)

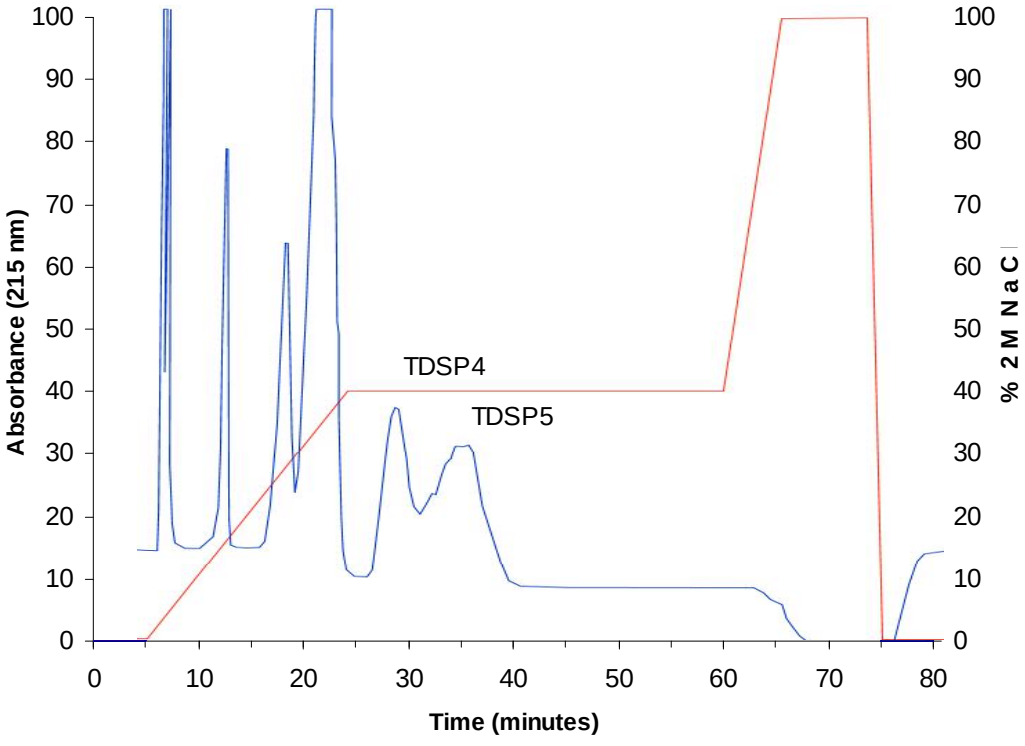
Absorbance (215 nm)
% 2 M NaCl
Time (minutes)
TDSP4
TDSP5
0
10
20
30
40
50
60
70
80
90
100

b)

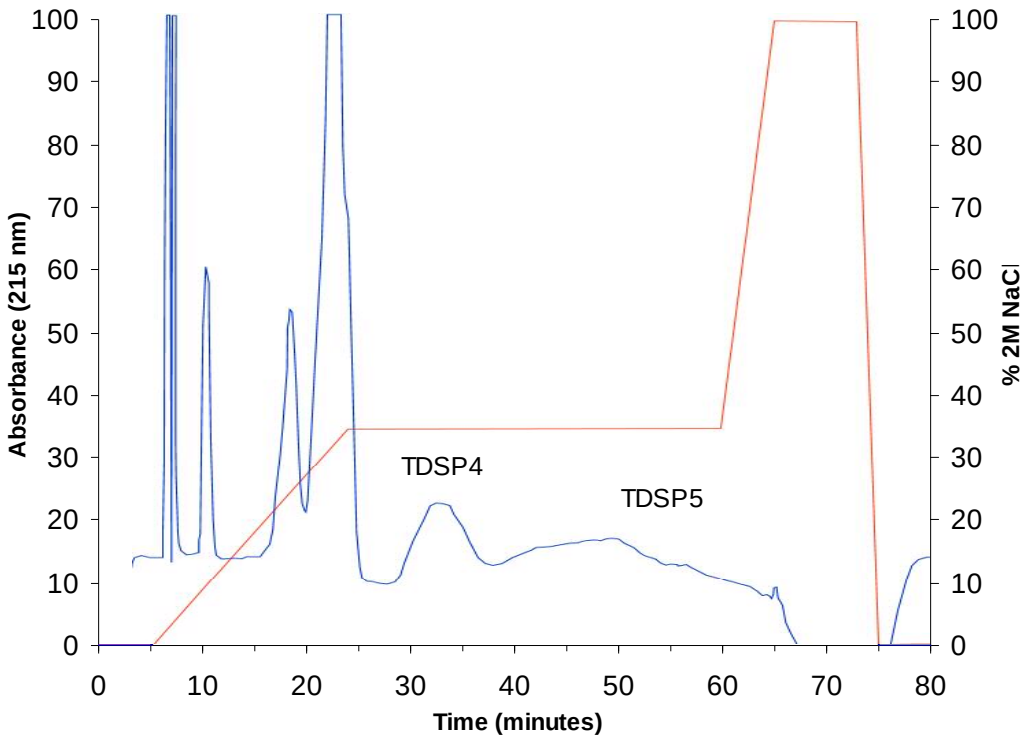

c)

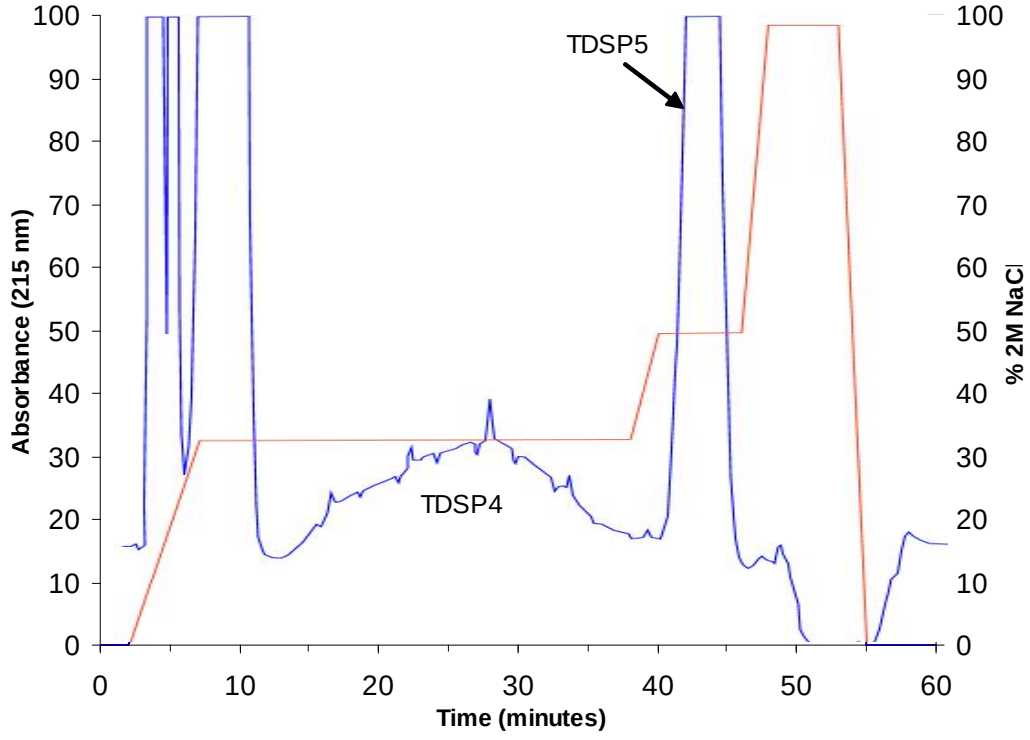

d)

Figure 5-4. LMWP elution profiles with gradients that are a) linearly increasing, and holding at b) 40%, c) 35%, and d) 33% salt concentration.

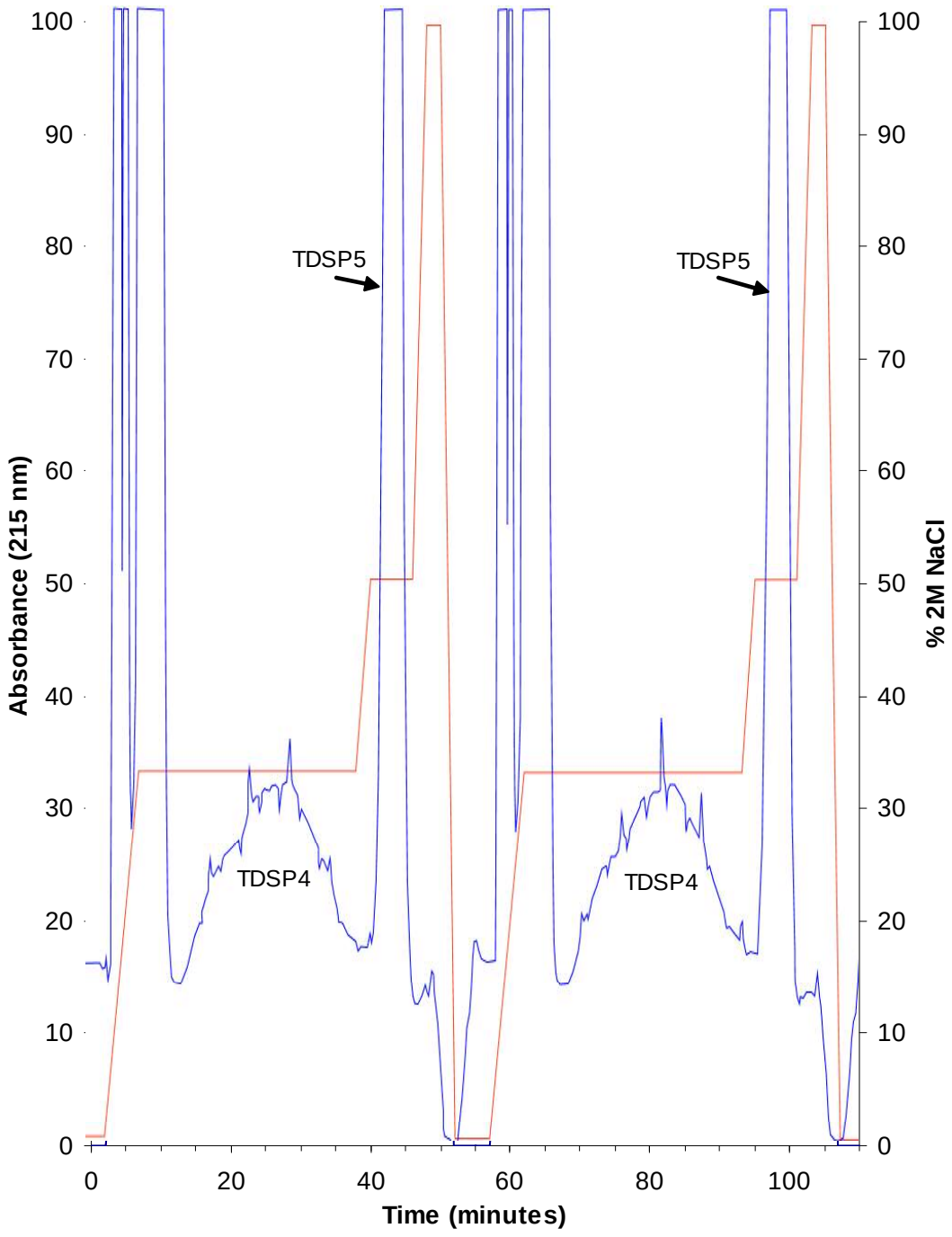

Figure 5-5. Purification of LMWP by optimized, continous-cyclying elution.

5.3 Immobilization of thermolysin on nanoporous silica

As mentioned earlier, a number of methods have been developed for peptide synthesis. Growth in the areas of protein synthesis and genetic engineering has resulted in the need for more efficient methods of separation and purification. Although synthesis methods, such as solid phase synthesis using t-Bloc or F-moc strategies have improved considerably, the reaction products are still composed of various sequences which must be separated from the desired product. This is especially true for therapeutic peptides that must meet stringent purity requirements. Although these methods can be used to prepare highly specific sequences, they are process intensive and limited in terms of large-scale production. Using thermolysin to hydrolyze protamine into peptide fragments, however, can be applied on a large scale to produce LMWP.

As mentioned in Chapter 4, the immobilization of invertase on silica gels has shown significantly improved immobilized activity in comparison with published results. This know-how, developed from invertase immobilization, was applied to the immobilization of thermolysin. Thermolysin immobilization was accomplished by adding a 2 g/L thermolysin solution, buffered with TRIS/HCl at pH 7, to glutaraldehyde-activated silica gel. After extensive washings, the pH and temperature dependent profiles of free and immobilized thermolysin were determined.

Thermolysin activity was measured colormetrically using an azocasein (Sigma-Aldrich, Catalogue Number A-2765) substrate. This substrate consists of casein modified with a dye, which upon hydrolysis of the protein becomes soluble. Free and immobilized thermolysin were incubated with 4 mL of 5 wt. % azocasein. To determine the extent of reaction, 500 μL of 15% trichloroacetic acid (TCA) was

added to a 1 mL aliquot of the reaction solution. Addition of TCA induces the precipitation of undigested azocasein; the substrate becomes insoluble at low pH. The precipitate is removed from solution by centrifugation at 12,000g for 5 minutes. Enzymatic activity is then proportional to the dye remaining in solution; measured at a wavelength of 440 nm.

5.3.1 Effect of pH on the activity of immobilized thermolysin

The pH-dependant activity profiles of both the immobilized and free thermolysin were determined at 37 °C with a 0.5 wt. % azocasein solution in 50 mM buffer. An acetate buffer was used for pH 5; phosphate buffer was used for pH 6; TRIS/HCl was used for pH 7 and 8; and, TRIS/NaOH was used for pH 9.

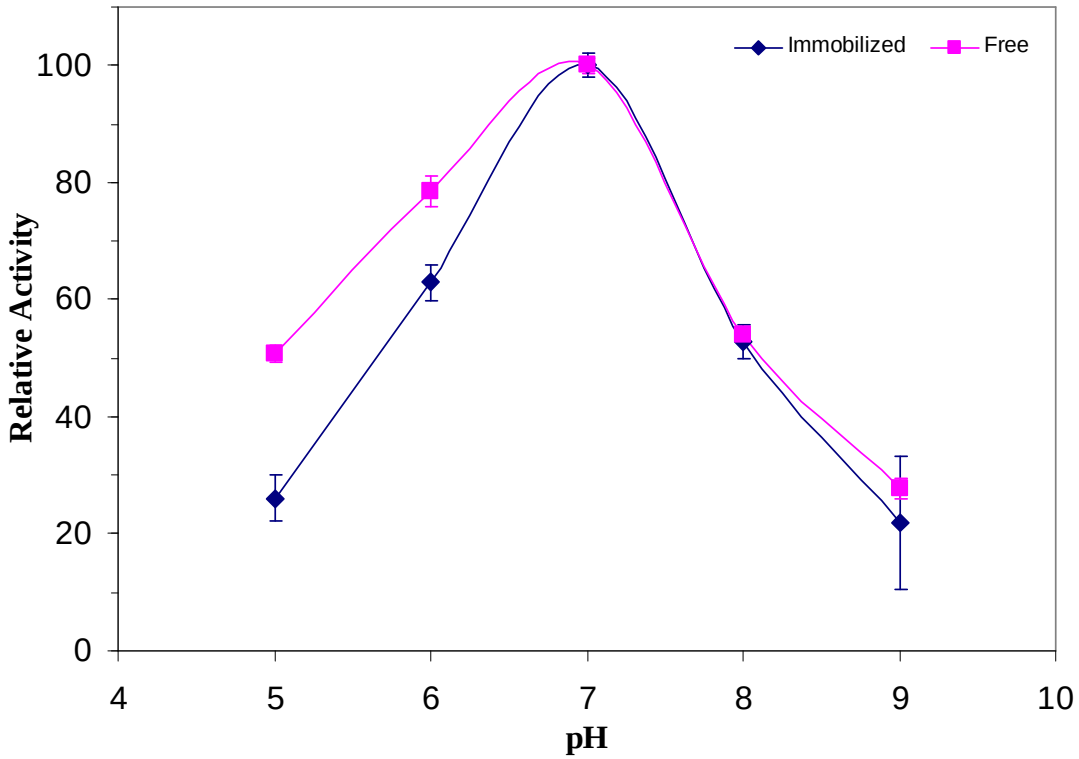

Figure 5-6. Relative activity profiles of free and immobilized thermolysin as a function of pH.

The pH activity profiles for free and immobilized thermolysin are shown in Figure 5-6. Both the free and immobilized thermolysin show a maximum activity at pH 7. There is a rapid drop-off in activity as the pH is changed away from neutral. The immobilized thermolysin follows a similar activity drop-off, as the free enzyme, for pH greater than 7. However at lower pH, the drop in immobilized thermolysin activity is significantly lower than that of the free enzyme.

5.3.2 Effect of temperature on the activity of immobilized thermolysin.

The effect of temperature on both free and immobilized thermolysin activity was determined by measuring the hydrolysis of azocasein at temperatures ranging from 25-85 °C. A 0.5 wt. % azocasein solution, buffered with 50 mM TRIS/HCl at pH 7, was used for activity determination. The substrate solution, 4 mL, was incubated in a temperature-controlled, circulating water bath (Precision, Cat. No. 51221039) for 10 minutes before addition of thermolysin. The extent of reaction was followed over time and the enzyme activity determined.

As seen in Figure 5-7, both the free and immobilized thermolysin preparations show increased activity at higher temperatures. Free thermolysin activity appears to increase only slightly from 25 to 35 °C. As the temperature in increased further, the activity increases linearly, at a higher rate, up to 85 °C. The immobilized thermolysin, on the other hand, shows only a slight increase in activity from 25 to 55°C. Above this temperature, immobilized thermolysin activity increases at a greater rate and linearly up to 85 °C.

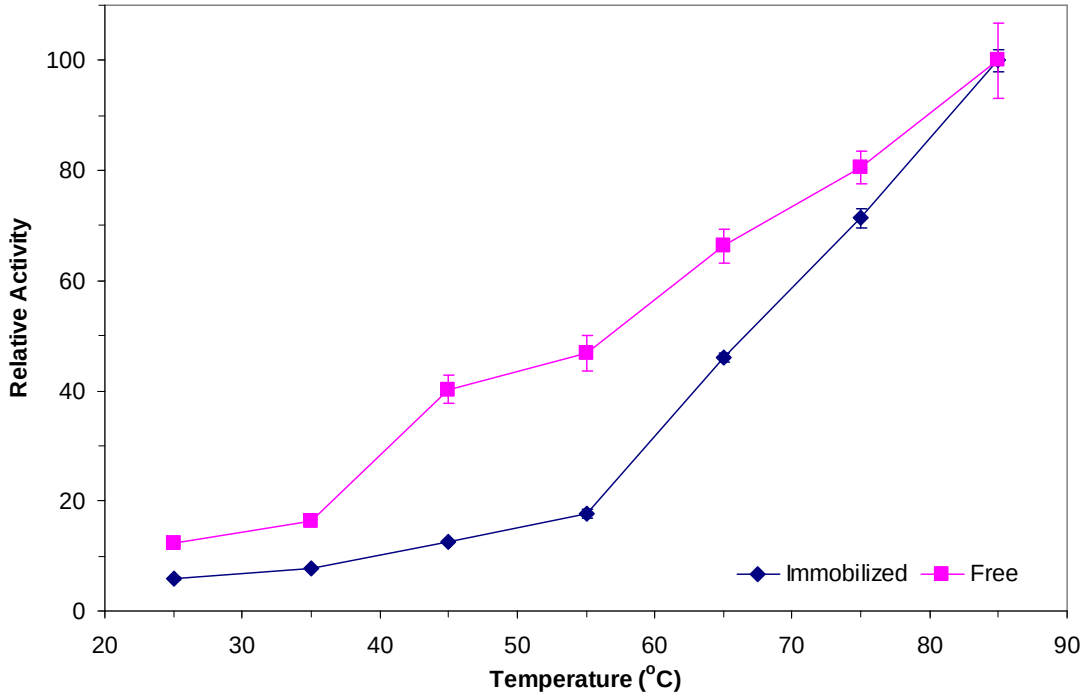

Figure 5-7. Relative activity profiles for free and immobilized thermolysin as a function of reaction temperature.

Azocasein was used to show the retention of thermolysin activity after immobilization on nanoporous silica. The immobilized thermolysin showed a similar pH activity profile to that of the free enzyme. Although some difference was seen in the temperature activity profiles, the trends were similar.

5.4 Digestion of protamine by immobilized thermolysin

The immobilized thermolysin activity was also measured for the hydrolysis of protamine. Immobilized thermolysin was introduced to a 10 mg/mL protamine solution buffered at pH 7.4 with 50 mM Tris/HCl/2 mM $CaCl_2$. The reaction was incubated in a 28.5°C water bath for specified times; then placed in ice and EDTA added to stop the reaction. After filtration with a 0.22 μm syringe filter, a sample of the protamine solution was injected into an HPLC gradient system for separation of

the individual peptides. The HPLC system was fitted with a 5mL Hi-Trap Heparin affinity column.

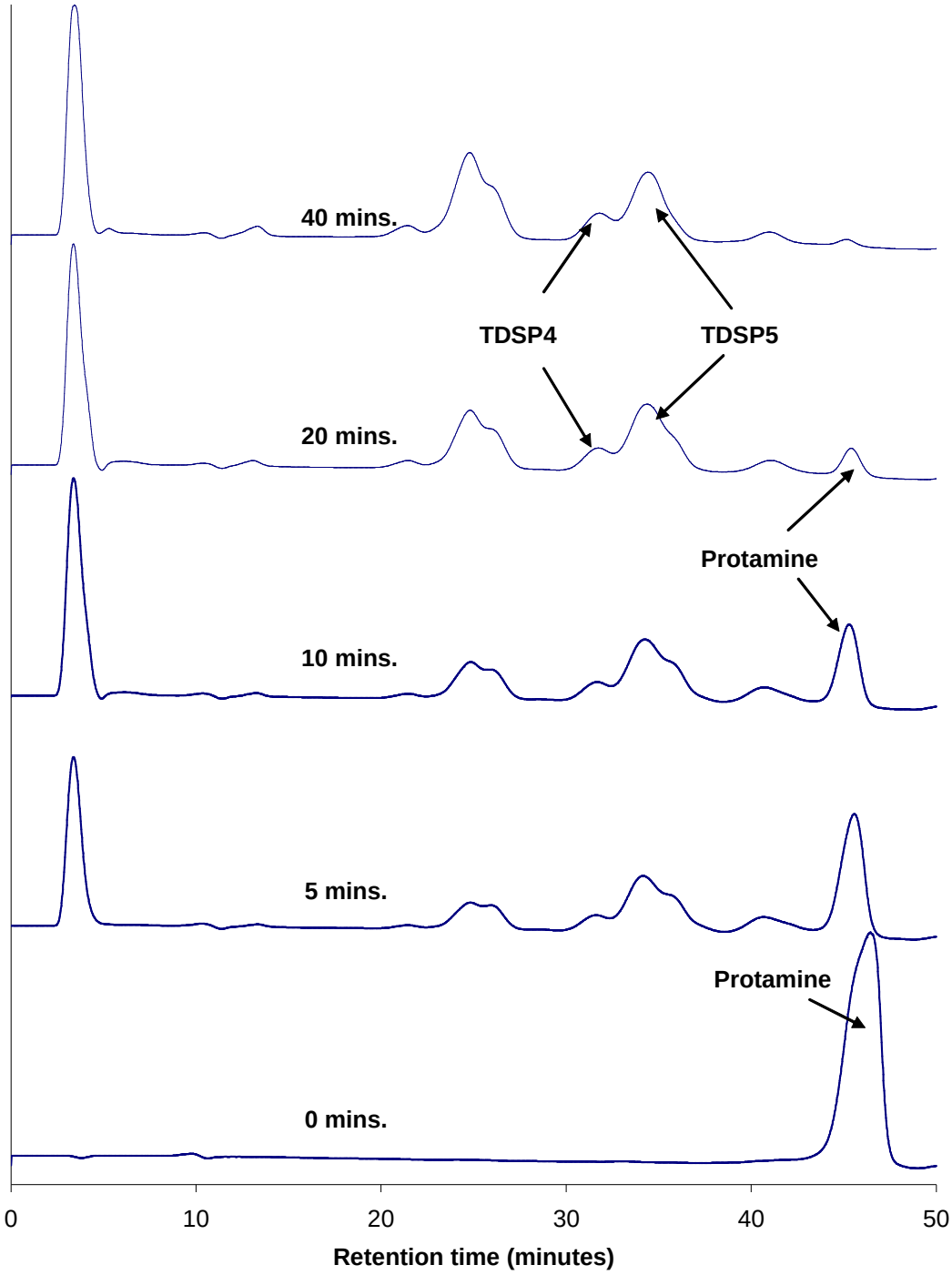

Figure 5-8. Elution profiles of protamine fragments digested by immobilized thermolysin with varying incubation times.

Hydrolysis of protamine by immobilized thermolysin, in a batch reactor, and the subsequent formation of smaller peptides, is shown in Figure 5-8. Clearly seen is the reduction of the protamine peak and development of the TDSP5 peak as the incubation time is increased from 0 to 40 minutes. The immobilized thermolysin also showed good retention of activity with multiple incubations in a protamine solution at 37°C over 40 minutes each. After completion of the reaction, the gel suspension was centrifuged to separate the immobilized enzyme and the hydrolysis products determined by heparin affinity. After washing with buffer solution, the immobilized thermolysin was introduced to a fresh protamine solution and the reaction repeated. Several of the HPLC runs are shown in Figure 5-9. The slight shift of peak position of the first run is due to a difference in initial state of the column and not indicative of a difference in peptides.

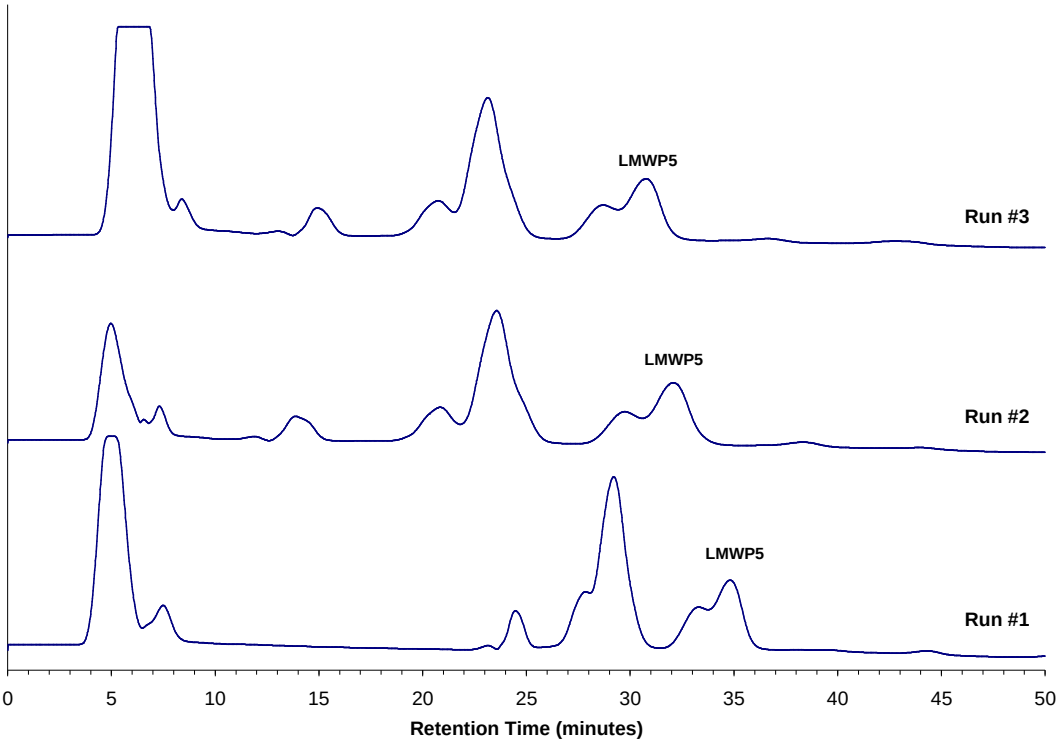

Figure 5-9. Elution profiles obtained from the repeated use of immobilized thermolysin.

Industrial reactors can be divided into three basic groups: the batch reactor, plug-flow reactor (PFR) and the continuous-stirred tank reactor (CSTR). Each of these reactor types offers certain advantages to the process. The batch reactor design equation (26) shows that the conversion, X, is a function of the moles of substrate charged to the reactor, N_{A0}, the reaction rate, r_A, the reactor volume, V, and the reaction time, t. A high conversion can be obtained by increasing the reaction time.

$$N_{A0}\frac{dX}{dt} = -r_A V \tag{26}$$

The batch reactor is generally used in small-scale processes, when expensive products are manufactured, and if a continuous process is unfeasible. While the batch reactor offers the best control of temperature and mixing, it suffers from down-time, during product discharging and substrate charging of the reactor, and is also labor intensive. The residence time of the substrate and enzyme in these reactors is the same, requiring subsequent separation in order to reuse the catalyst.

A PFR reactor that is filled with catalyst particles, or immobilized enzymes, is called a packed-bed reactor (PBR). Packed-bed reactors offer the highest conversion per weight of catalyst of any of the reactors. It operates as a continuous flow process but temperature can be difficult to control and it is also susceptible to channeling which reduces efficiency. In a PBR, the residence time of the substrate is much smaller than that of the enzyme providing the separation of the enzyme and its continuous use. In addition, PBR reactors provide a more reproducible process than the batch reactors which may produce products of varying purity from one batch to the next. The PBR design equation (27) shows that the conversion is a function of the reaction rate, r_A, the substrate flow rate, F_{A0}, and the catalyst weight, W.

$$F_{A0}\frac{dX}{dW} = -r_A \tag{27}$$

From the PBR design equation we see that the conversion is a function of the catalyst weight and reactor volume is only secondary. This illustrates the advantage of nanoporous silica with high enzyme loadings. As the enzyme loading on the silica matrix is increased, the reactor volume can be accordingly reduced.

The use of a PBR for protamine hydrolysis, by thermolysin, has several advantages. A flow reactor achieves a continuous operation requiring minimum labor. The flow reaction could be integrated with the separation by an affinity column to further streamline the separation and purification tasks. In addition there is the possibility of full automation with software controlled processes. The optimum design of such a system obviously requires the integration of several other devices with the enzyme reactor and involves extensive system engineering. However, the potential savings in labors and especially savings in processing time make it a worthwhile study. In this element of work the performance of the immobilized thermolysin system in a PBR mode was studied.

Because of the high enzyme loadings achieved, a relatively small reactor is sufficient to produce achieve the required conversion. A 0.22 μm syringe filter (Fisherbrand, Cat. No. 09-719A) was used to filter-off the immobilized thermolysin from a buffered suspension; loading approximately 45 mg of silica matrix containing 33 mg of immobilized thermolysin. The filter and immobilized thermolysin make-up a packed-bed reactor with a small height to diameter ratio, shown in Figure 5-10.

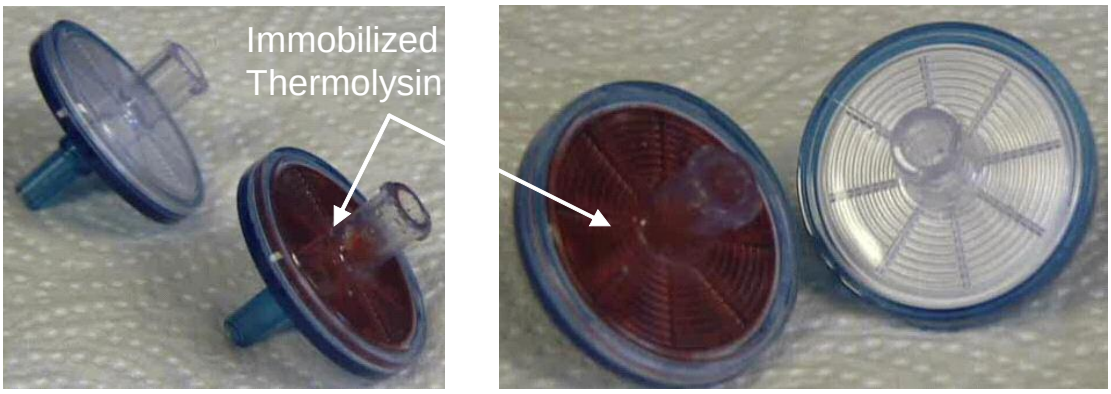

Figure 5-10. LMWP Bioreactor: Syringe filter loaded with silica particles containing immobilized thermolysin.

5.4.1 Production of LMWP using FPLC

The LMWP Bioreactor was fitted onto a Fast Performance Liquid Chromatography (FPLC) system for the production and purification of LMWP (see Figure 5-11). Figure 5-12 shows the flow profile of the FPLC system when the position valve is switched from the LOAD to INJECT position.

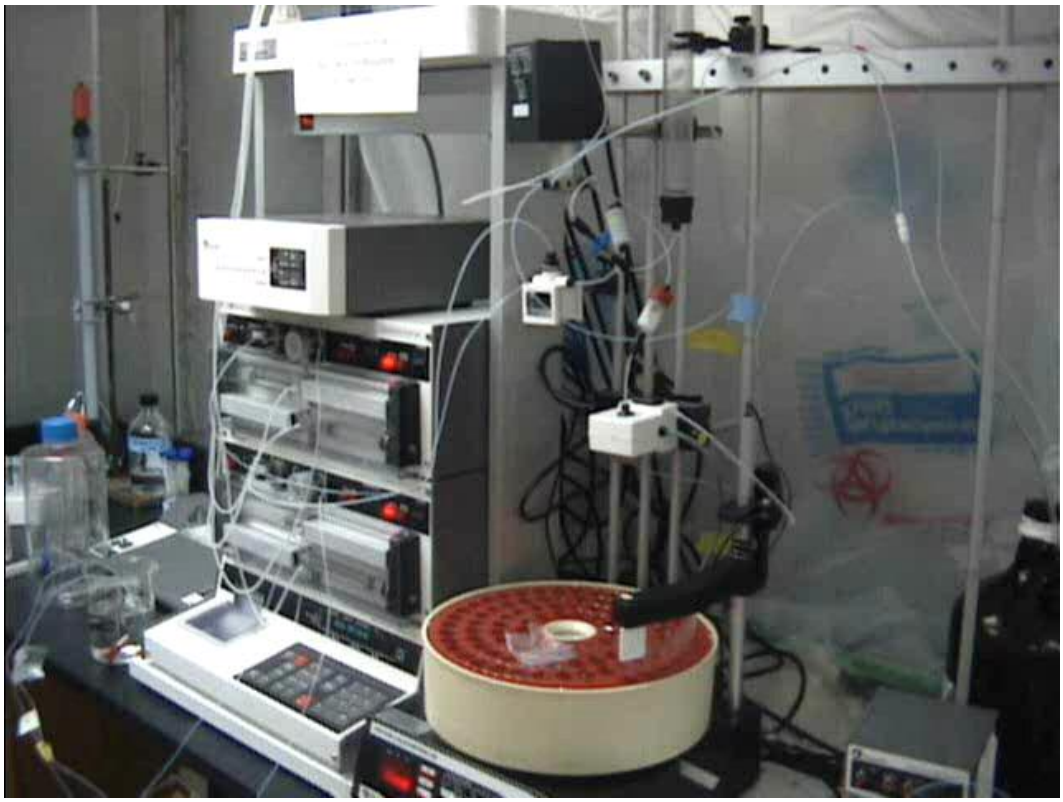

Figure 5-11. FPLC System for production and purification of LMWP.

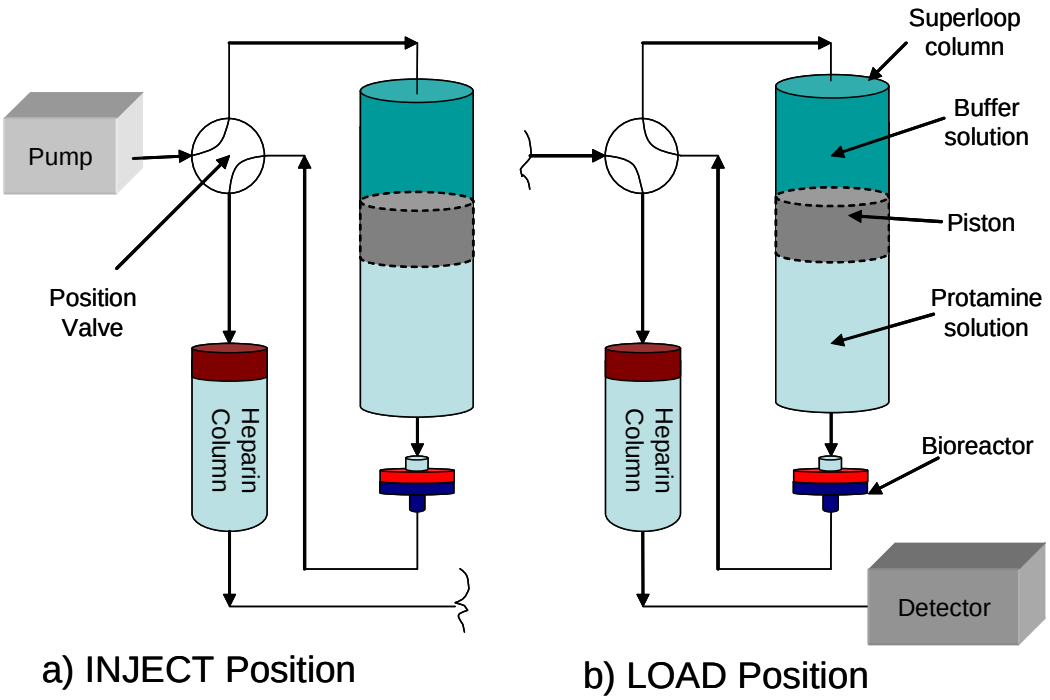

Figure 5-12. FPLC set-up for digestion of protamine by immobilized thermolysin.

With the position valve set at INJECT, the buffer flow from the pump is directed into the top of the Superloop column. This forces a moveable, water-tight piston downwards which forces protamine solution out of the column bottom. The protamine solution flows into the bioreactor, where it is hydrolyzed by the immobilized thermolysin, and then injected into a HiTrap Heparin column. The interaction between the protamine fragments and heparin results in the retention of the peptides within the column. Switching the position valve to the LOAD position then by-passes the superloop and directs the buffering solution directly into the chromatography column. A salt gradient is used to elute the peptides with the solution flowing into a UV detector for detection of the elution profiles.

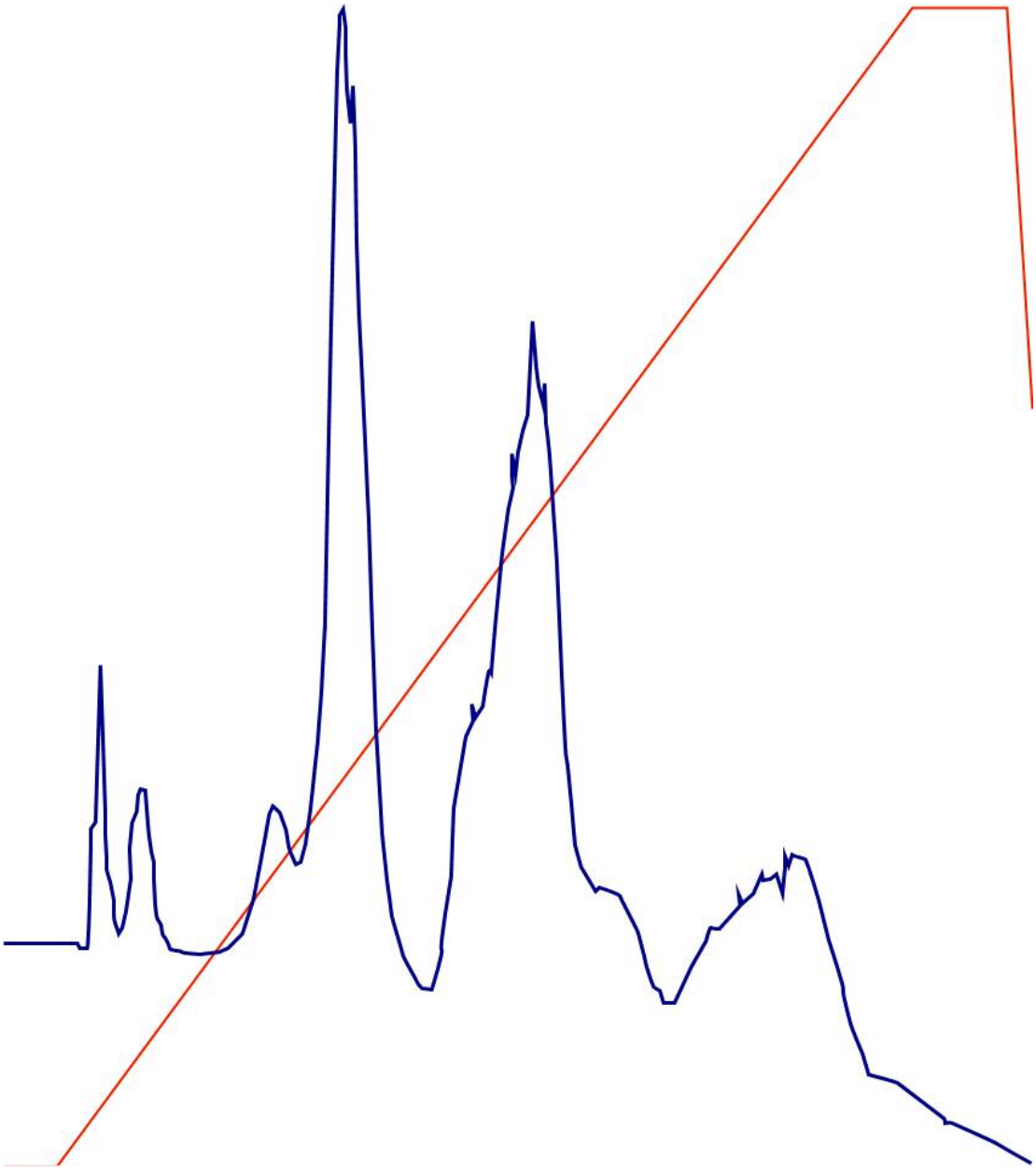

Figure 5-13. Elution profile of protamine digested by immobilized thermolysin reactor at 4 °C with a flow rate of 20 µL/min.

With this FPLC set-up, shown in Figure 5-12, the immobilized thermolysin reactor comes in contact with only the buffered protamine solution. The elution buffer, with its high salt content, completely bypasses the reactor. However, as will be seen in the next section, the enzymatic activity is retained even after exposure of the bioreactor to a high salt solution.

The extent of reaction can be controlled through adjustment of the protamine solution flow rate. Several protamine injection flow rates were tested and the elution profiles determined. Even at the low flow rate of 20 μL/min, a significant amount of native protamine still appears in the elution profile as shown in Figure 5-13. This is not surprising because of the reduced thermolysin activity at low temperatures. Since the FPLC is located in a cold room, the hydrolysis reaction occurs at 4°C. As shown in Figure 5-7, the immobilized thermolysin activity is significantly reduced at even 25°C.

As shown by equation (27), the conversion can be increased by further reduction of the flow rate, increasing the catalyst weight, and increasing the reaction rate. Further reduction of the flow rate is not feasible due to the resulting increase in the cycle time. The catalyst weight can be increased with a larger reactor and the reaction rate can be increased with an increase in temperature. The following section looks at protamine digestion with a HPLC system operating at higher temperatures.

5.4.2 Production of LMWP using HPLC

A High Performance Liquid Chromatography (HPLC) system, shown in Figure 5-14, was used to test the immobilized thermolysin reactor's performance at room temperature. The system consisted of two Alltech 526 HPLC pumps, a Linear UVIS 200 detector, and a two-position injection valve. Data acquisition was done by a PeakSimple Chromatography Data System, Model 202. A 1mL sample loop was connected to the sample injection port.

Figure 5-15 shows the direction of buffer flow for the INJECT and LOAD valve positions. In the INJECT position, the buffer is directed through the sample

loop which then carries the protamine solution through the thermolysin reactor. The reactor exit stream then flows into the chromatography column. When the valve is switched to the LOAD position, although the sample loop is bypassed, the reactor is still a part of the flow stream. With this configuration there is the possibility of enzymatic activity loss due to the high salt gradient.

Figure 5-14. High Performance Liquid Chromatography (HPLC) system.

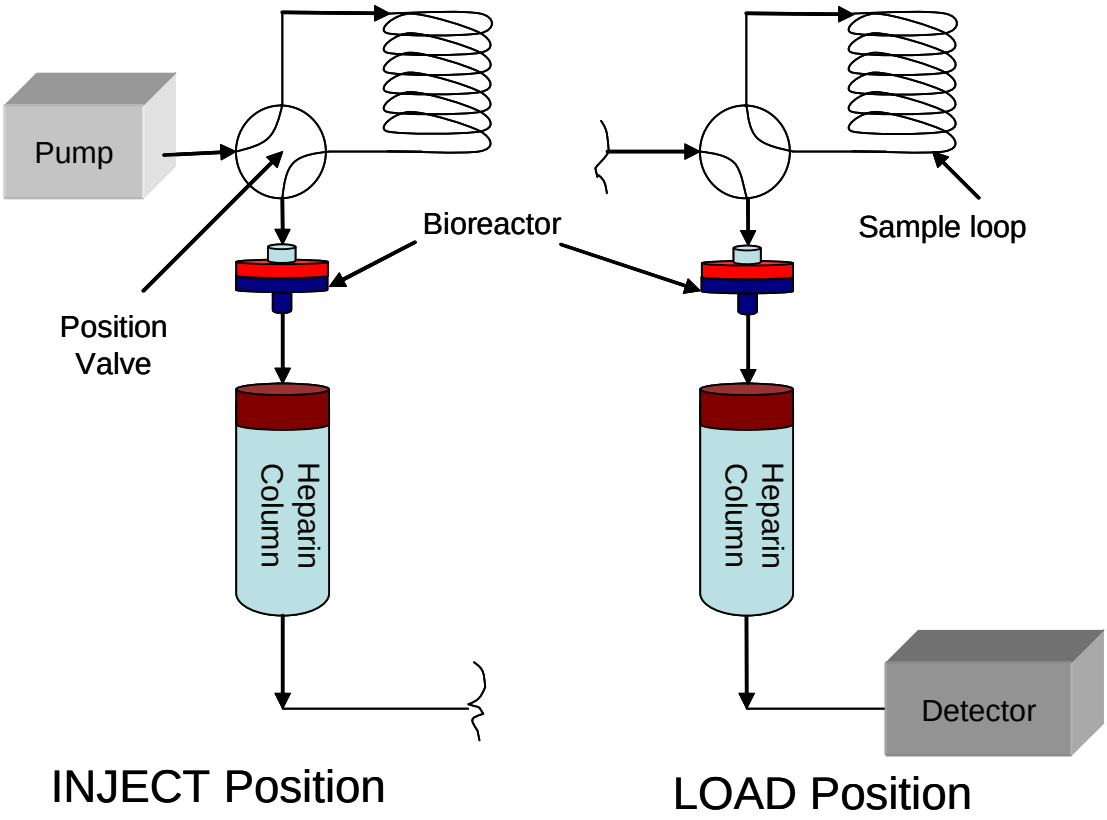

Figure 5-15. LMWP production and purification by an HPLC system.

The HPLC system was used to follow the hydrolysis of protamine by immobilized thermolysin at 25°C. First the sample loop was loaded with 1 mL of 2 mg/mL protamine solution. TRIS/HCl buffer, pH 7.5, was pumped through the loop at different flow rates with the position valve in the INJECT position. This forces the protamine solution through the immobilized thermolysin reactor and into the heparin column. The resulting elution profiles are shown in Figure 5-16.

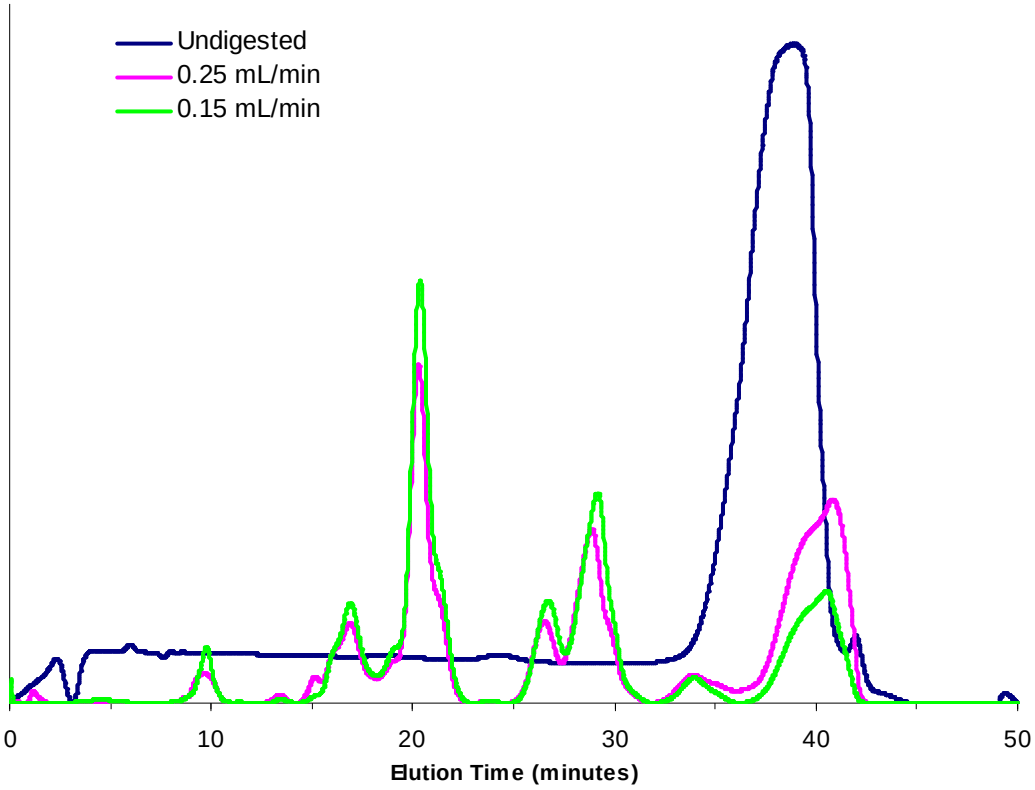

Figure 5-16. Digestion of protamine by immobilized thermolysin at 25°C.

The elution profiles clearly show the hydrolysis of protamine into smaller peptides by the immobilized thermolysin reactor. Two different flow rates, 0.25 mL/min and 0.15 mL/min, were used for the hydrolysis reaction. As the flow rate is decreased, the conversion of protamine to LMWP increases. Because the immobilized enzyme is only a thin layer in the reactor, the reaction time is relatively short with these flow rates. This serves as further evidence of the relatively high immobilized activity achieved in this work.

With the expectation that a higher temperature would yield greater enzymatic activity, the hydrolysis of protamine was also determined with varying reaction temperatures. Protamine solution was incubated at 25°C or 55°C before injecting into

the HPLC system. The resulting elution profiles in Figure 5-17 show the increased digestion of protamine at the higher temperature.

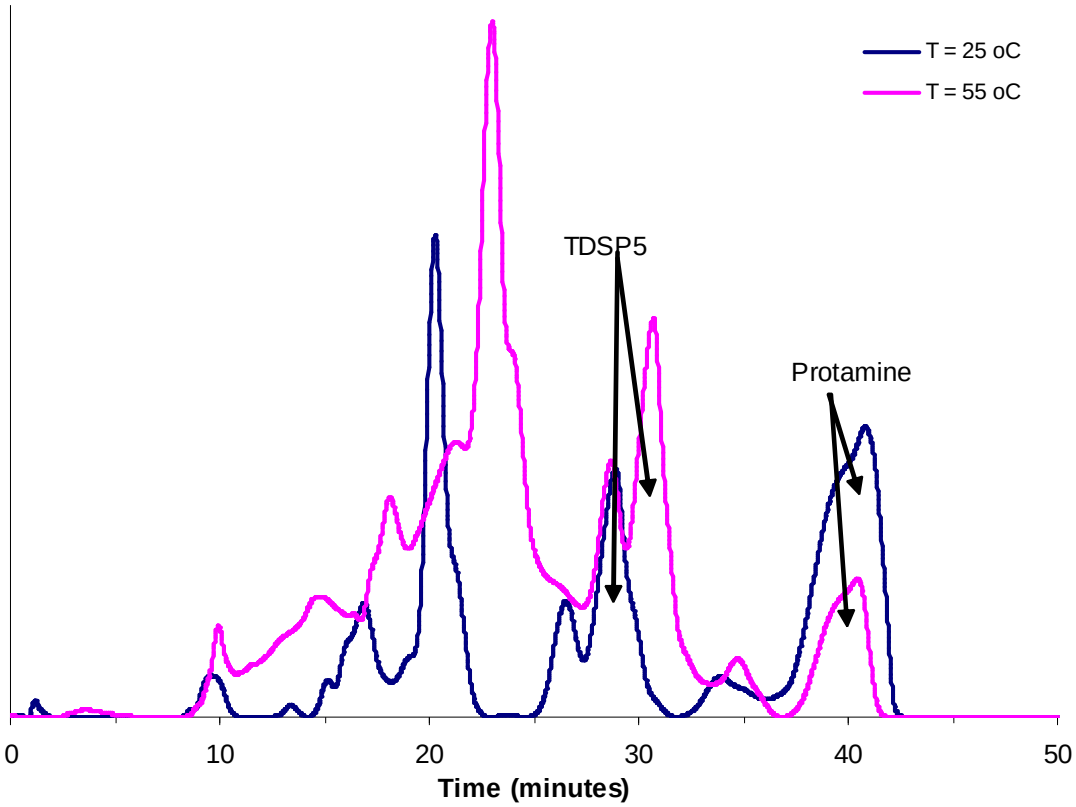

Figure 5-17. Protamine digestion by immobilized thermolysin at 25°C and 55°C.

The immobilized thermolysin reactor showed no apparent loss in activity after 20 cycles. This includes use of the reactor in the HPLC system where the salt gradient, which flows through the reactor, contacts the immobilized thermolysin. Retention of activity under a 2M NaCl solution shows that the immobilization method is stable and no leaching occurs. The system was eventually discarded due to the development of a leak in the housing and not because of a loss in enzymatic activity.

5.5 Summary

Using the protocol developed for the immobilization of invertase, thermolysin was immobilized on nanoporous silica. Enzymatic activity was characterized using

an azocasein substrate under varying pH and temperature. A small packed-bed reactor was created by packing the immobilized thermolysin into a syringe filter. The immobilized enzyme showed good retention of activity even after repeated exposure to 2M NaCl solutions. This combined with the optimization of the salt gradient for LMWP purification provides approximately a 30-fold improvement in productivity. High product purity is obtained as seen from the heparin affinity elution profile in Figure 5-18.

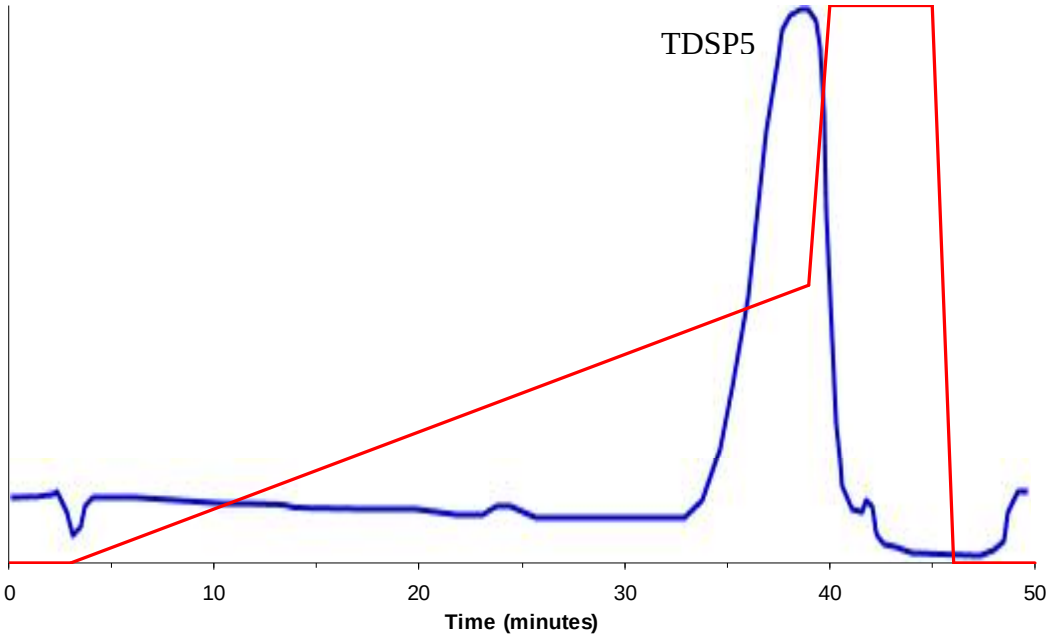

Figure 5-18. Determination of product purity by heparin affinity chromatography.

Chapter 6: Spherical Silica Composites

Earlier chapters have shown that the N-CSMG material is able to achieve a higher enzyme activity per gram of matrix than previously published results. The N-CSMG material, however, is made as a monolithic gel and then mechanically broken in smaller particles. This results in the generation of particles of irregular shape and a broad size distribution. Ideally, for a packed-bed reactor or chromatographic support, the matrix should have a regular shape and be of uniform size. Spherical particles are preferential because of improved packing; flow characteristics showing a minimum back-pressure; maximum surface to volume ratio providing a smaller diffusion path; and also because they are easier to model (Dasari, Prince et al. 1993).

6.1 Spherical N-CSMG Beads

Several methods have been described in literature for the fabrication of silica spheres. A well studied method for producing silica spheres, with diameters in the nanoscale, is the Stober process. In the Stober process, a dilute silica alkoxide solution is mixed with ammonia, which serves as a catalyst to induce condensation (Stober, Fink et al. 1968; Fox, Kokoropoulos et al. 1987; Jelinek, Dong et al. 1992). Particle formation can be tightly controlled by variation of the reactant concentrations (Giesche 1994), catalyst concentration (Liu, Xu et al. 2004), and reaction temperature (Chen, Dong et al. 1996). Modified Stober processes have also been developed for increased control of particle size (Dong 1998; Arkhireeva and Hay 2003).

Silica spheres have been produced containing various other components to yield a composite with unique properties. Tetraethoxysilane along with organoalkoxysilane have been used in a co-condensation process to produce

organically-modified silica spheres using the Stober process for heavy metal adsorption (Etienne, Sayen et al. 2002). Silica spheres have also been organically modified as nanofillers in polymeric systems (Arkhireeva and Hay 2004). Silica spheres have also been radioactively labeled to produce a marker (Flachsba.H and Stober 1969). A significant amount of research has also produced several silica composites of core-shell morphology with polystyrene (Gu, Kondo et al. 2004; Lu, McLellan et al. 2004; Zeng, Yu et al. 2004), block copolymers (Laruelle, Parvole et al. 2004), star polymers (Liu and Li 2004), magnetite (Tan, Wang et al. 2004), and gold (Osterloh, Hiramatsu et al. 2004), among many others (Hah, Um et al. 2004; Zhang and Li 2004; Zhao, Qin et al. 2004).

In addition to the Stober process, silica spheres have been produced by an emulsion system. Many of these processes produce silica beads which are surface modified in subsequent steps. Modification of silica using N-2-(aminoethyl)-3-aminopropyl (trimethoxy)silane has been shown to increase the chemical reactivity of silica for adsorption (Jesionowski 2002). Spherical particles, with a size of 50 nm, modified with 3-aminopropyl(triethoxy)silane have been produced using TEOS in a microemulsion process (Tan, Ye et al. 2004). Silica spheres with an amino loading of 2.3 mmol/g have been reported (Etienne, Lebeau et al. 2002). These particles however are in the nanoscale and not appropriate for bioreactors where a particle size of at least 50 microns is preferential. In addition, all of these published results use TEOS as the silica source.

6.1.1 Formation of amino-modified silica spheres by emulsion

Although there are published works that describe the formation of silica spheres using a sodium silicate source (Wang, Fu et al. 1993; Boissiere, Kummel et al. 2001; Kim, Seok et al. 2003; Chao, Lin et al. 2004), we found no literature evidence that micron-sized, amino-modified, spherical silica beads have been developed using sodium silicate. In this work, spherical N-CSMG beads were developed using sodium silicate, as the initial source of silica. As detailed in previous chapters, we first use an ion-exchange process to convert sodium silicate into silicic acid. The silicic acid serves as the water phase of the water-in-oil emulsion and 2-ethyl-1-hexanol is the oil phase. Silicic acid is added to the oil phase, with stirring, at a 1:15 volume ratio. Ethanol is added to the system, at a ethanol:silicic acid ratio of 2:1, as a cosolvent to improve the silicic acid/APTES compatibility. Under stirring, the silicic acid and ethanol solution form droplets within the oil phase. After five minutes of stirring to achieve a stable droplet size, APTES is added to the emulsion; it enters the oil phase and then diffuses into the droplets. Two events occur as 3-aminopropyl(triethoxy)silane enters the aqueous phase: 1) the ethoxy groups are hydrolyzed to form ethanol, leaving hydroxyl groups on the silane; and 2) the basic amino group causes an increase in droplet pH and induces gelation. This scheme is illustrated in Figure 6-1.

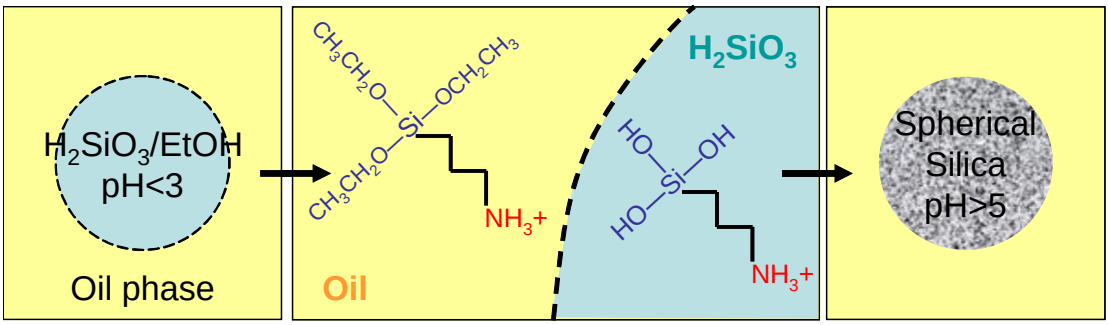

Figure 6-1. Emulsion scheme for formation of 3-aminopropyl(triethoxy)silane modified silica spheres.

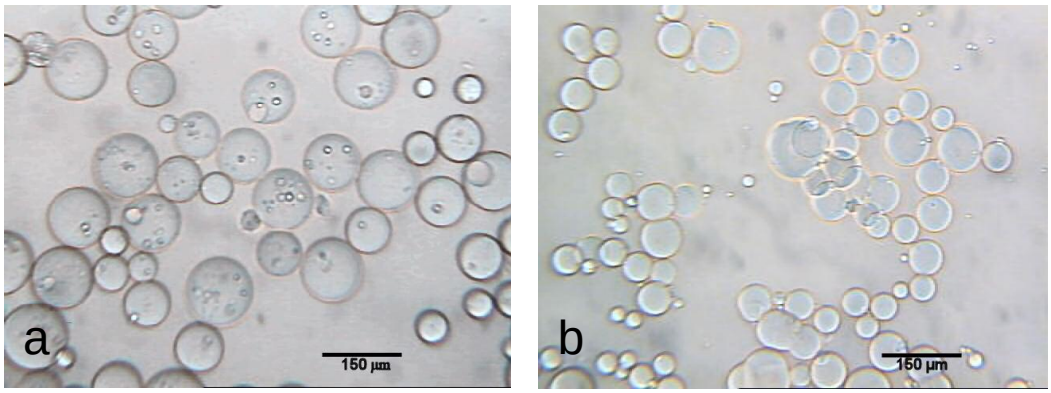

Figure 6-2. Micrographs of amino-modified silica spheres formed by a water-in-oil emulsion process at mixing rates of a) 690 RPM and b) 1040 RPM.

6.1.2 Control of spherical particle size

The silica sphere particle size can be controlled by variation of the stirring speed. In Figure 6-2 is shown the micrographs obtained by the emulsion process at two different stirring speeds. A correlation of pixel length to particle size, 1.5 µm per pixel, was determined through the imaging of a glass slide with cell-counting sections of known size. Size distribution of the spherical particles were then determined from the micrographs obtained for three different stirring rates. The particle size distribution is shown in Figure 6-3, with the average particle size and standard deviation, for each stirring rate along with a Gaussian distribution curve. From the curves and average particle size we can clearly see a decrease in particle size with increasing stirring rates. However, a narrower size distribution would be more ideal. In addition to the stirring rates, several other factors can be adjusted to obtain the

desired size distribution. Composition of the oil and water phases, surfactants, and even impeller shape can significantly affect the distribution (Pacek, Ding et al. 2001; Perez, Zambrano et al. 2002; Kraume, Gabler et al. 2004). The optimization of these factors will be an important aspect of future studies in further developing the amino-modified, spherical silica particles.

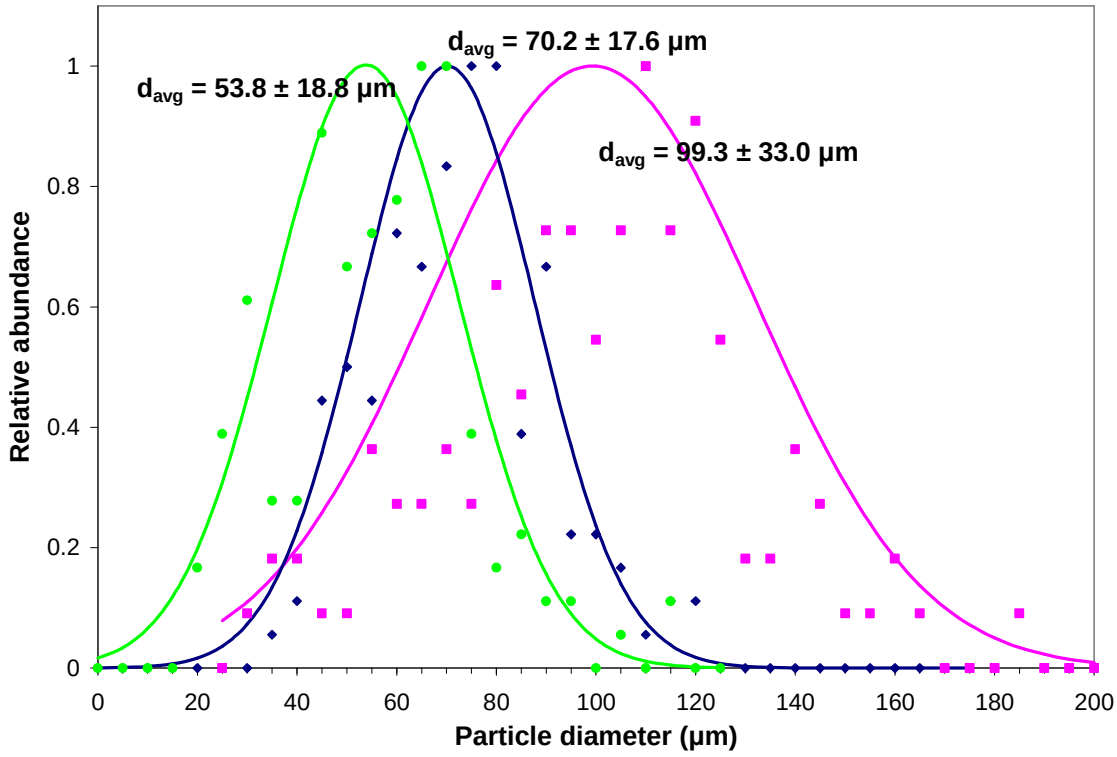

Figure 6-3. Particles size distribution obtained by the emulsion process with stirring rates of 690 (—), 860 (—), and 1040 (—) RPMs. The plotted curves represent the normal Gaussian distribution for the specified mean and standard deviation.

6.1.3 Amino-modified silica sphere morphology

In addition to particle size, it is also important to have control of particle morphology. As mentioned in previous chapter, an open morphology is vital in allowing the free diffusion of components between the bulk phase and particle interior. The morphology of spherical particles produced by the emulsion process was studied by scanning electron microscopy (SEM).

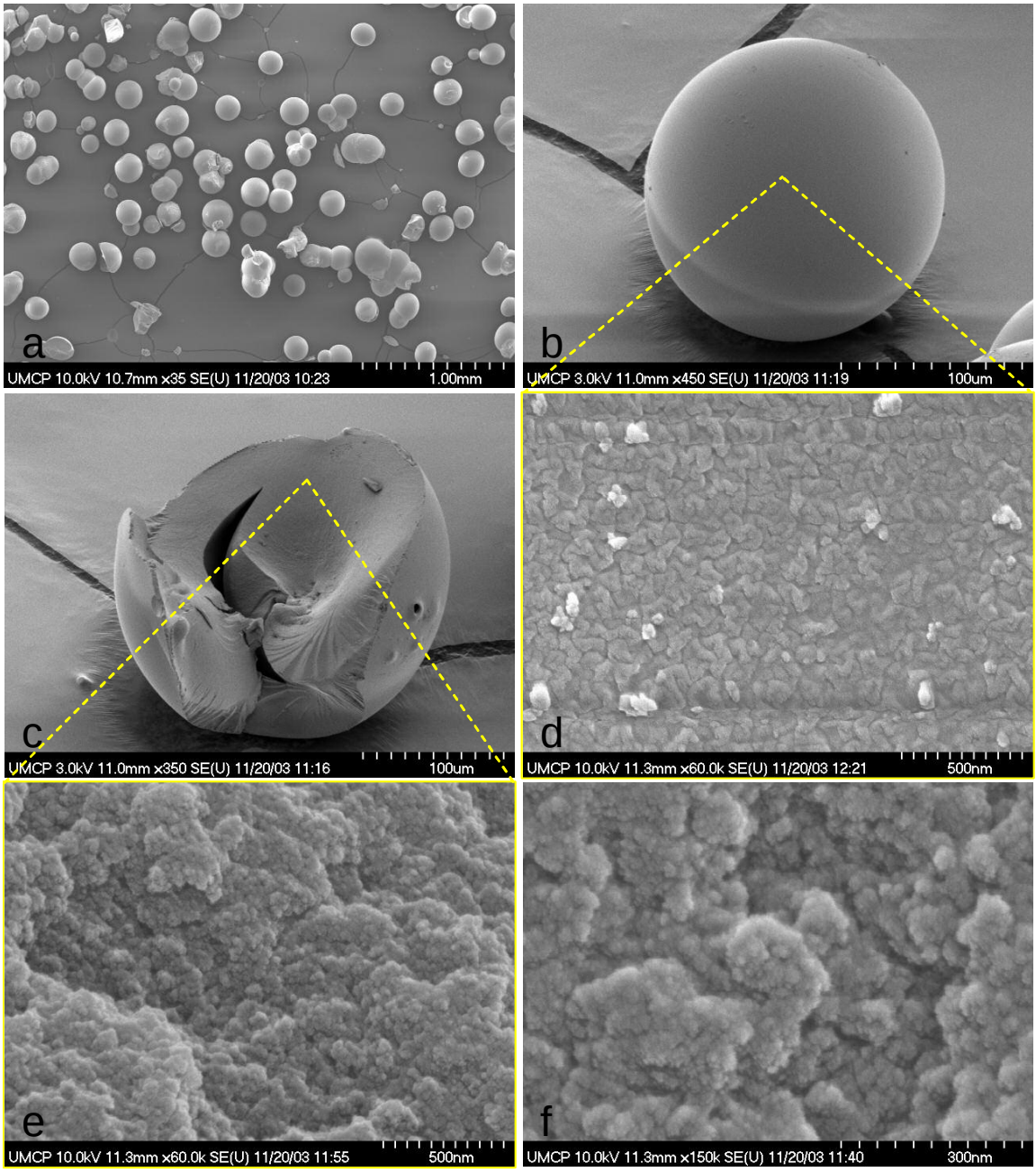

Figure 6-4. SEM images of a) spherical silica particles under low magnification; b) single spherical particle; c) fractured particle revealing the interior; d) high magnification of outer shell of the particles; e) 60k magnification of particle interior; and f) 150k magnification showing the porous interior.

A low magnification (x35) SEM image of spherical N-CSMG particles, produced with a stirring rate of 690 RPM, is presented in Figure 6-4(a). The images shown in Figure 6-4(b) and (c) are of an intact spherical particle and fractured particle, respectively. A closer inspection of the interior regions exposed in Figure

6-4(c) is shown in Figure 6-4(e) and (f). These images show a similar morphology to the N-CSMG material with some pores 50 nm in size. However, when then outer shell in Figure 6-4(b) is imaged the morphology is quite different as seen in Figure 6-4(d). Comparison of Figure 6-4(d) with Figure 6-4(e), both taken at the same magnification, clearly show this difference in morphology. The outer shell of the spherical particles appears to have a scale-like morphology and would likely pose a significant barrier to the diffusion of enzymes and other large molecules.

6.1.4 Adsorption of metal ions and small molecules

It is well know that amino functional groups are able to selectively adsorb metal ions, including copper, nickel, and cobalt (Tikhomirova, Fadeeva et al. 1991; Yoshitake, Yokoi et al. 2003). Although the outer morphology appears to be closed by SEM imaging, the spherical particles are able to adsorb cobalt, copper, and nickel ions as shown in Figure 6-5. The clear particles display a drastic change in color associated with the adsorption of these metal ions. If used in a water treatment system, the color change could be used as an indicator of when the material must be changed.

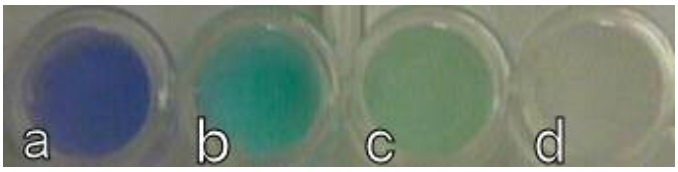

Figure 6-5. Adsorption of (a) cobalt, (b) copper, and (c) nickel by (d) spherical N-CSMG.

The Cu(II) adsorption capacity of the amino-modified silica spheres was determined colormetrically. A 25 mg sample of the silica particles was introduced to 10 mL of 1000 ppm Cu(II) solution initially at pH 4.5. The adsorption of Cu(II) was

followed through measurement of Cu(II) remaining in solution. A 300 μL aliquot of solution was removed and added to 60 μL of ammonia hydroxide solution. Chelation of copper ions by ammonia gives a blue color and the concentration is determined by absorbance measurement at a wavelength of 440 nm (see Appendix A-4). From the time profile of Cu(II) adsorption by N-CSMG and spherical N-CSMG, shown in Figure 6-6, it is clear that the spherical particles have an adsorption capacity less than half that of N-CSMG at 1.5 and 3.1 mmols/g, respectively.

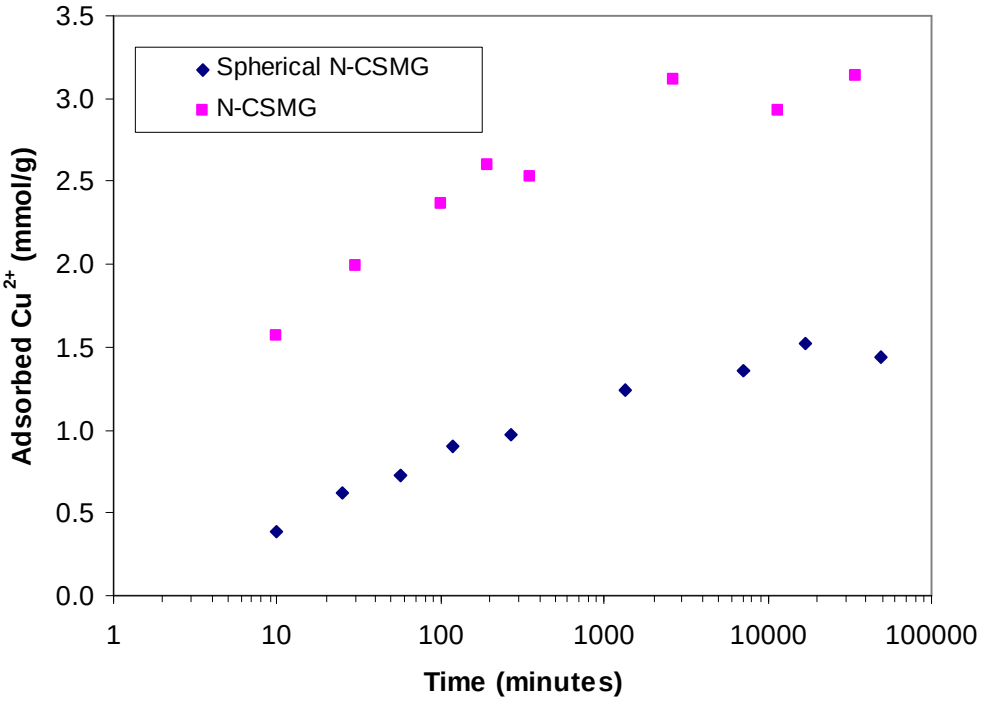

Figure 6-6. Adsorption of Cu(II) by N-CSMG and spherical N-CSMG particles from a 1000 ppm solution initially at pH 4.5.

The N-CSMG material is made with APTES homogenously mixed with the silicic acid; yielding a homogenous distribution of amino groups on the gel surface. However, the emulsion process of making amino-modified spherical particles depends on the diffusion of APTES into the silicic acid droplets. Gelation thus

occurs first at the water-oil interface, forming a solid shell, and progresses toward the center. The shell formation creates a greater barrier to APTES diffusion and results in a lower concentration of amino groups towards the particle center. Although the outer shell has a more closed morphology than the particle interior, it is permeable to glutaraldehyde which is a relatively small molecule. Fluorescence of the Shiff-base formed between glutaraldehyde and APTES is visualized in Figure 6-7 using confocal fluorescence microscopy. The image shows a bright band along the outer shell indicating a high concentration of Schiff bases and, thus, a higher density of amino groups. The core area, circled with a dashed line, shows a decreased amino density.

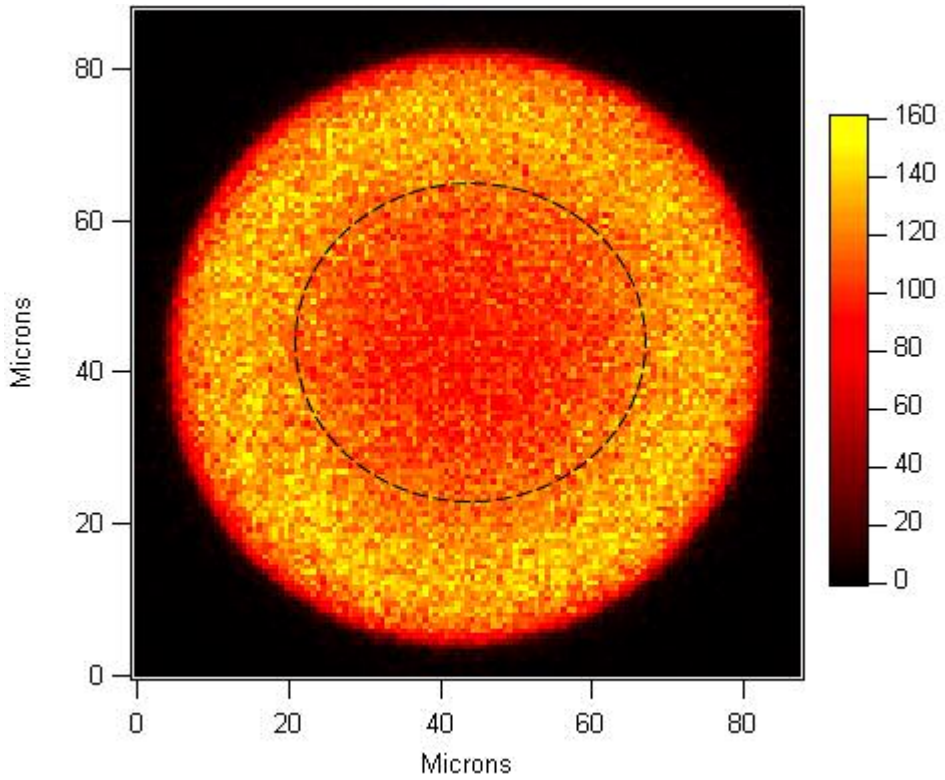

Figure 6-7. Fluorescence image of Schiff-base formed between glutaraldehyde and APTES showing the distribution of amino groups within the particle.

Although the spherical N-CSMG material can be activated with glutaraldehyde, it shows no ability to immobilize enzymes. After activation with

glutaraldehyde, the spherical particles were incubated with an invertase solution following the protocol for immobilization of invertase on N-CSMG. After washing the particles with buffer solution and incubating in sucrose solution, no immobilized invertase activity was detected. The closed morphology, shown in Figure 6-4(d), is likely one reason for the lack in immobilized activity. Since the enzyme is unable to diffuse through the outer shell, it is not immobilized on the interior surface area of the particle. The complete lack of immobilized activity also indicates that the enzyme is not immobilized on the outer shell of the spherical particles. This suggests that there is no significant amount of amino groups exposed on the outer surface. Because the amino group of APTES is hydrophilic and the triethoxy groups possess some hydrophobic nature, APTES likely behave as a surfactant with the orientation shown in Figure 6-8(a). If APTES were to orient as shown in Figure 6-8(b), then some degree of immobilized enzyme activity would be seen. The burying of the amino-head within the particle interior, combined with the outer shell's closed morphology, hinders the immobilization of enzymes on spherical N-CSMG particles made by this emulsion process.

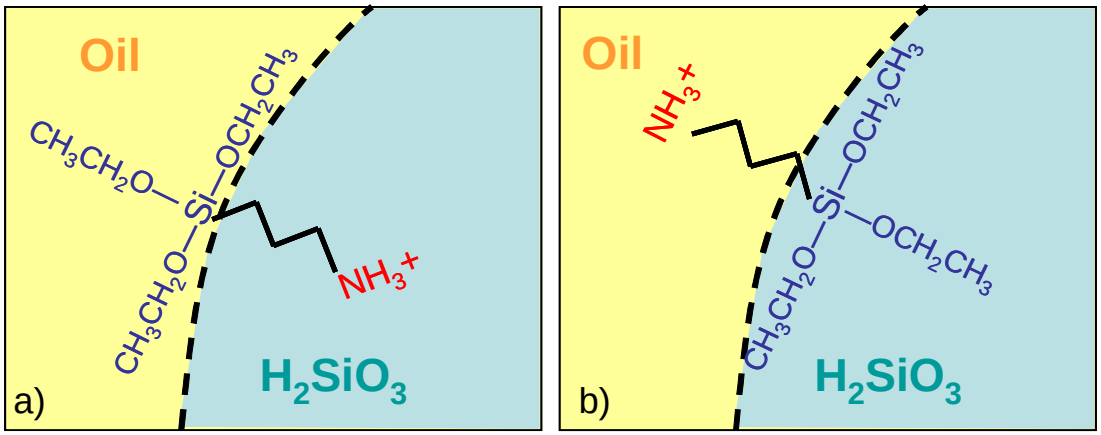

Figure 6-8. Possible orientations of APTES at the water-oil interface of emulsion.

6.2 Future Work

Using a water-in-oil emulsion process, we have developed spherical silica bead with an amino-modified surface. The amino loading of spherical beads is 1.5 mmols/g which, although significantly lower than the N-CSMG loading, is a higher loading than available in commercial products. Surface modification of the spherical beads relies on the diffusion of APTES into a silicic acid droplet. Because the APTES induces gelation of the droplets outer shell, a significant barrier to APTES diffusion is created. This leaves a core region with a relatively low loading of APTES. The loading can be significantly increased if APTES is homogenously mixed with silicic acid prior to gelation of the beads. Although they can be premixed and then introduced to the oil phase, the gelation occurs rapidly and this inhibits the control of particle size and shape. Although we have shown an ability to control particle size with adjustment of stirring rates, work still needs to be done in obtaining a narrower size distribution. This can be accomplished through the engineering of a mixer which provides a more uniform mixing profile. Another possibility is the addition of surfactants which can be used to tightly control the emulsion droplet size. Surfactants can also be used as a templating agent to improve the outer shell morphology.

The N-CSMG material has a hydrophilic nature and shows no adsorption of the pH dye Thymol Blue. However when treated with the surfactant sodium dodecyl sulfate (SDS) it becomes hydrophobic. The anionic head of SDS interacts with the cationic amino groups in N-CSMG creating a surface with the hydrophobic tails

pointing outward. After treatment with SDS, N-CSMG shows adsorption of Thymol Blue and exhibits the pH indicating characteristics of the dye as seen in Figure 6-9.

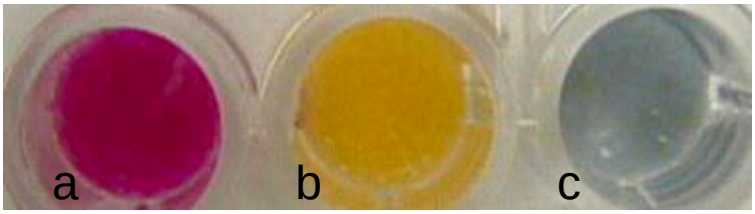

Figure 6-9. Indicating properties of Thymol blue adsorbed on SDS treated N-CSMG at a) pH 1.5, b) pH 7.0, and c) pH 11.5.

Amino-modified silica gels can be combined with a variety of other components to produce composites that respond to changes in their environment. One possibility that will be explored is a silica/chitosan composite. Chitosan is produced by the deactylation of chitin, one of the most abundant natural biopolymer - second only to cellulose. Chitin is an amino polysaccharide with the hydroxyl groups in the C-2 position replaced with acetamide groups. Each year approximately 100 billion tons of chitin is produced by crustaceans, mollusks, insects, fungi and other organisms and several million tons are harvested annually (Hejazi and Amiji 2003). This biomaterial has several attractive properties including biodegradability, biocompatibility, and bioactivity (Kurita 2001). It has been shown to have antimicrobial properties (Papineau, Hoover et al. 1991) and swelling properties sensitive to changing pH (Thanoo, Sunny et al. 1992). Silica-chitosan composites are receiving considerable interest for applications in catalysis (Molvinger, Quignard et al. 2004; Wei, Hao et al. 2004), gene delivery (Kumar, Hellermann et al. 2004), gastrointestinal drug delivery (Hejazi and Amiji 2003), tissue scaffolding (Chen, Zhou et al. 2004), water treatment (Wu and Wang 2003), and chromatography (Rashidova, Shakarova et al. 2004). With the relative abundance and low costs

associated with silica and natural biopolymers, there is a significant commercial interest in producing these composites with their unique properties (Bond and McAuliffe 2003).

Chapter 7: Summary

The present work was mainly concerned with the development of protocols for the immobilization of enzymes on nanoporous silica gels. Silicic acid was generated from sodium silicate using an ion-exchange process. Amino surface-modified, silica gels (N-CSMG) were then fabricated through the co-condensation of silicic acid with 3-aminopropyltriethoxysilane (APTES).

Thermogravimetric analysis (TGA) showed that a high amino loading of 3.6 mmol/g SiO_2 is achieved. Chelation of copper ions from solution indicated a loading of 3.1 mmol/g N-CSMG.

A significant hurdle to overcome in working with nanoporous materials is the shrinkage that accompanies drying of the gel. It was demonstrated in this work that the chemical modification of the gel surface, by glutaraldehyde, in the wet state can significantly reduce the shrinkage observed upon drying. Modified (GA-N-CSMG) and unmodified (N-CSMG) gels were air dried, freeze dried, and supercritically dried. In each case, the modified gel exhibited a significantly higher surface area. The aldehyde content of GA-N-CSMG was measured to be equivalent to 3.1 mmol glutaraldehyde per gram of GA-N-CSMG.

Immobilization of the enzyme invertase was optimized to finally yield 723 mg invertase per gram of silica matrix. The immobilized enzyme retained 99 percent of the free enzyme activity and exhibited similar activity profiles as a function of pH and temperature. An Arrhenius plot showed that the activation energy of the immobilized

invertase was approximately 5.9 KJ/mol lower than that of the free invertase, indicating the presence of some diffusion effects.

Comparison of Michaelis-Menten kinetic parameters showed that the immobilized invertase has a lower V_{max} than free invertase with an efficiency factor, η, of 0.73. However, a greater affinity for the sucrose substrate by the immobilized invertase is able to compensate for the lower reaction rate and the catalytic efficiencies of the immobilized and free invertase are found to be identical. The immobilization of invertase on GA-N-CSMG yielded an immobilized activity of 246,000 U/g matrix, significantly higher than previous published results.

The GA-N-CSMG material was also used to immobilize the enzyme thermolysin. Thermolysin was used to produce a peptide, Low Molecular Weight Protamine (LMWP), by the digestion of native protamine. Immobilized thermolysin was packed into a column to make a bioreactor for the continuous production of LMWP. This bioreactor exhibited good stability with no detectable leaching occurring over multiple uses. The immobilized thermolysin bioreactor was combined with an optimized purification scheme, using a heparin-affinity column, to provide more than 30 times increased productivity of LMWP compared to prior methods.

The final part of this work consisted of producing spherical N-CSMG particles of controlled size using an emulsion process. Particle size distribution was controlled by variation of stirring rates. While the particles had a porous interior region, the outer shell of the particles had a closed morphology. The closed morphology acted as a barrier to prevent the immobilization of enzymes, but it was permeable to metal ions and small molecules. Absorbance of cobalt, copper, and

nickel ions from solution by these particles resulted in a distinct color change. The spherical N-CSMG also adsorbed the hydrophobic, pH sensitive dye, Thymol blue, from solution with retention of pH sensitivity.

The composites developed in this work could provide significant improvements for a number of applications including sensors, bioreactors, and chromatography. Possible applications also exist in the drug delivery market for these composites.

Appendices

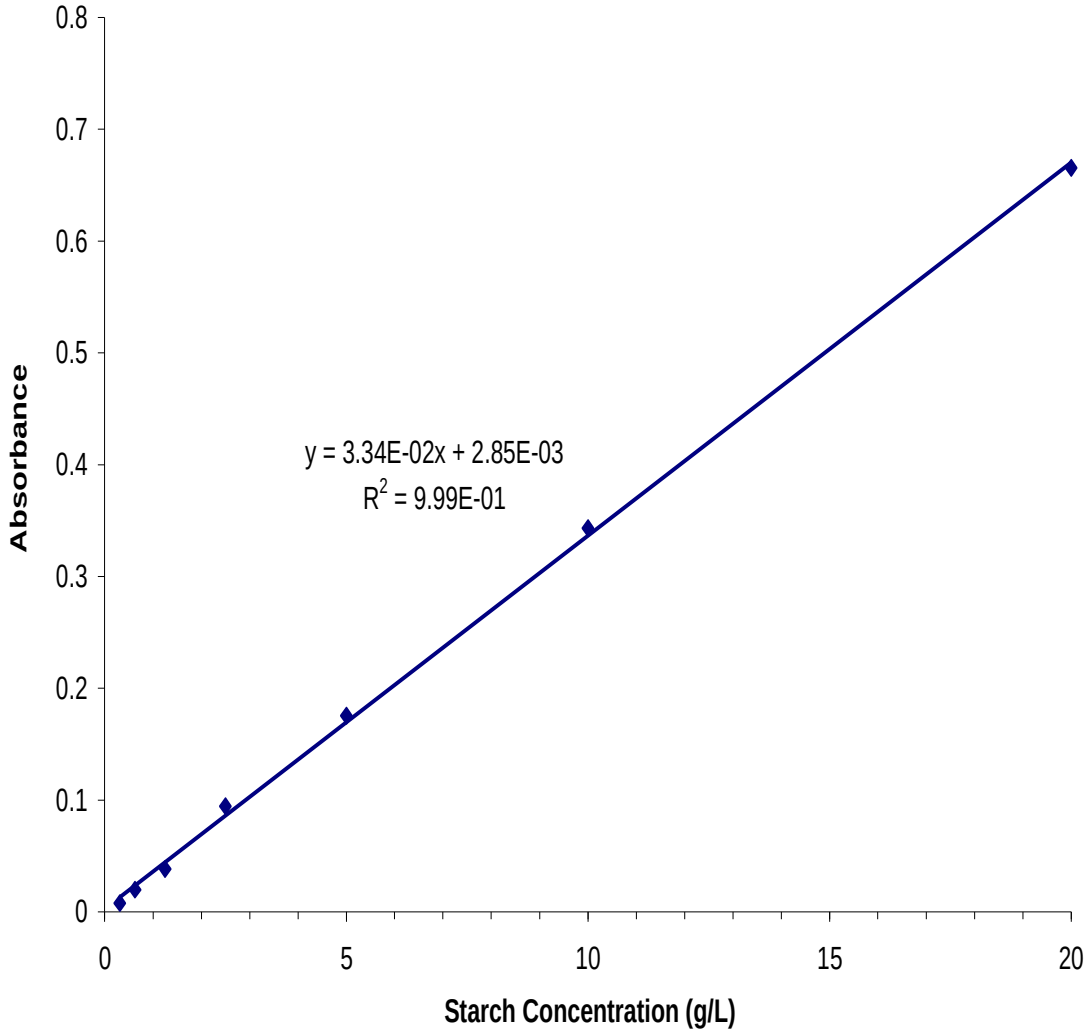

A. 1. Standard curve for determination of starch concentration using iodine-KI solution.

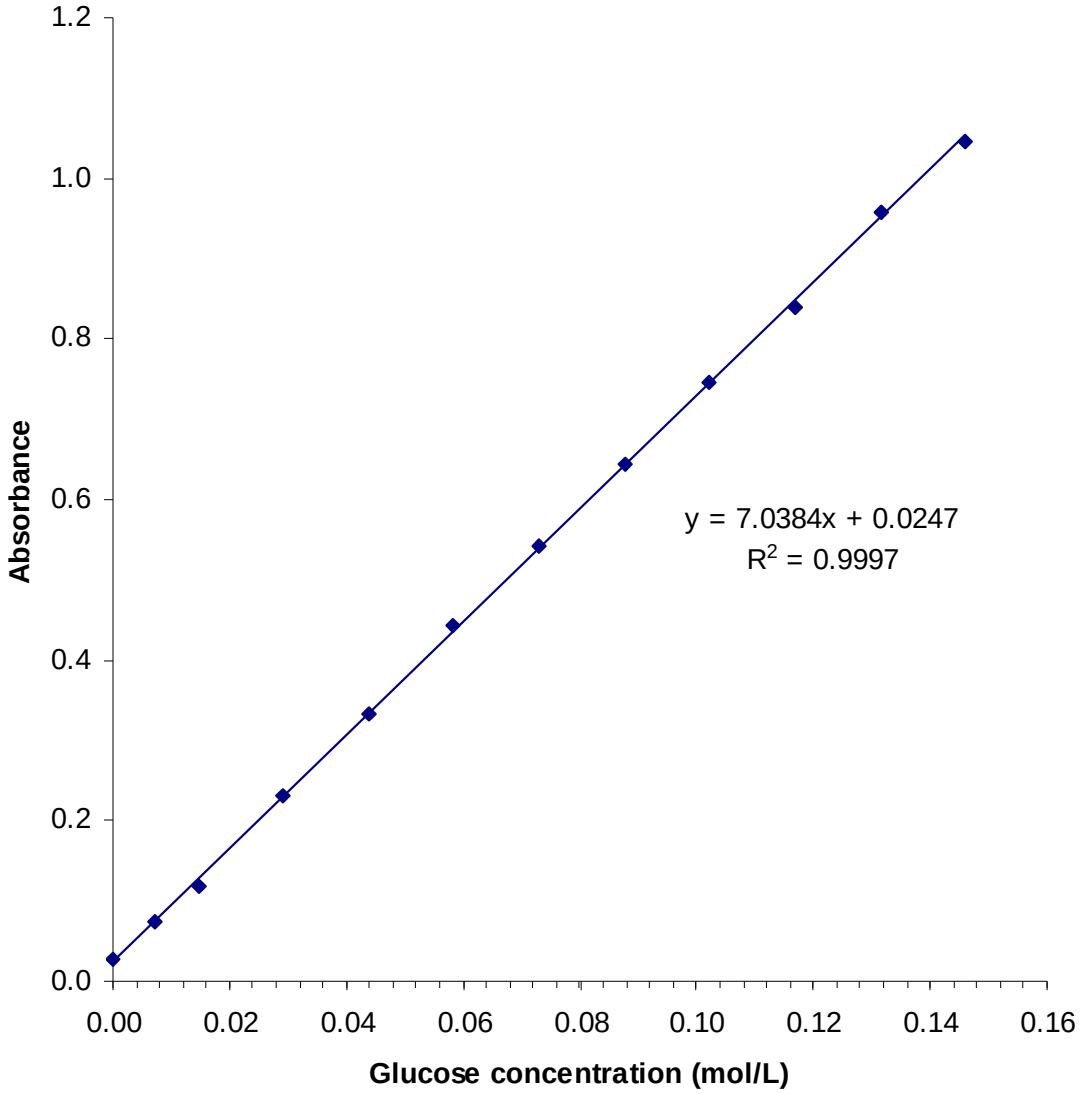

A. 2. Standard curve for determination of glucose concentration using dinitrosalicylic acid. DNS solution (5 mL) was introduced to 0.5 mL of test solution and heated at 100 °C for 30 minutes. After addition of 1 mL of 40 wt% sodium tartrate, the absorbance was measured at 575 nm.

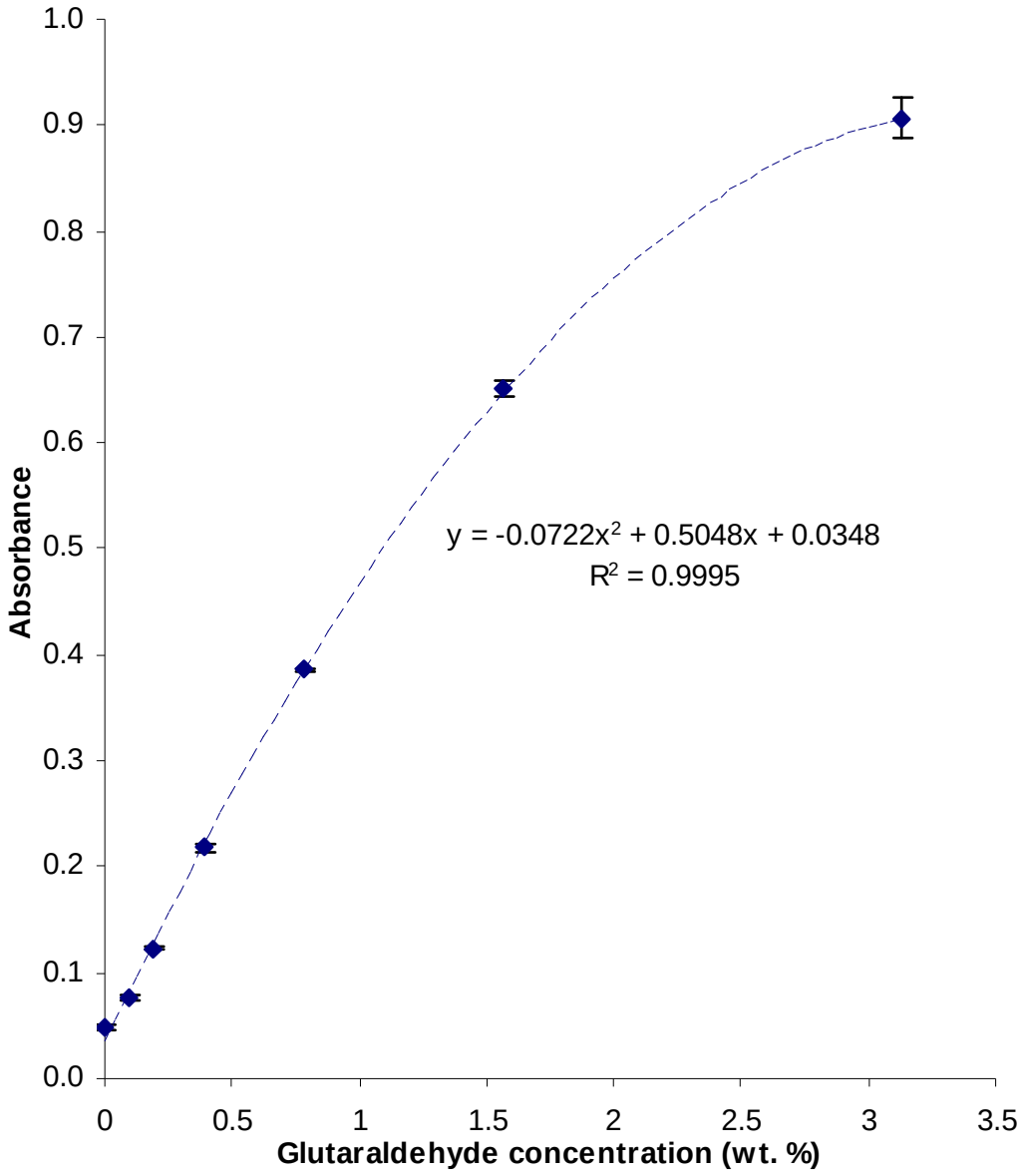

A. 3. Standard curve for aldehyde determination using DNS. DNS solution (1 mL) was introduced to 0.5 mL of test solution and heated at 100 °C for 15 minutes. After addition of 0.3 mL of 40 wt% sodium tartrate, the absorbance was measured at 575 nm.

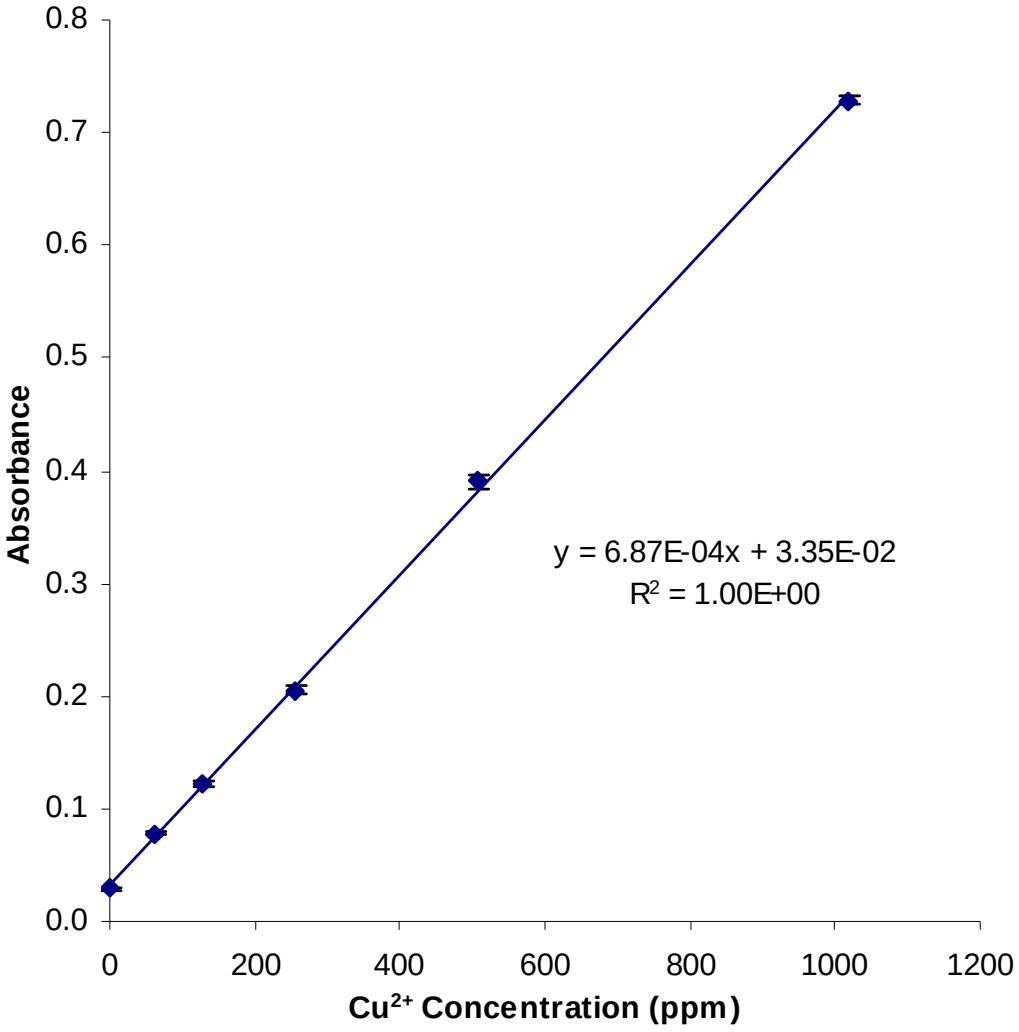

A. 4. Standard curve for determination of Cu^{2+} concentration. Copper containing solution (1 mL) was mixed with 0.2 mL NH_4OH and the absorbance measured at 610 nm.

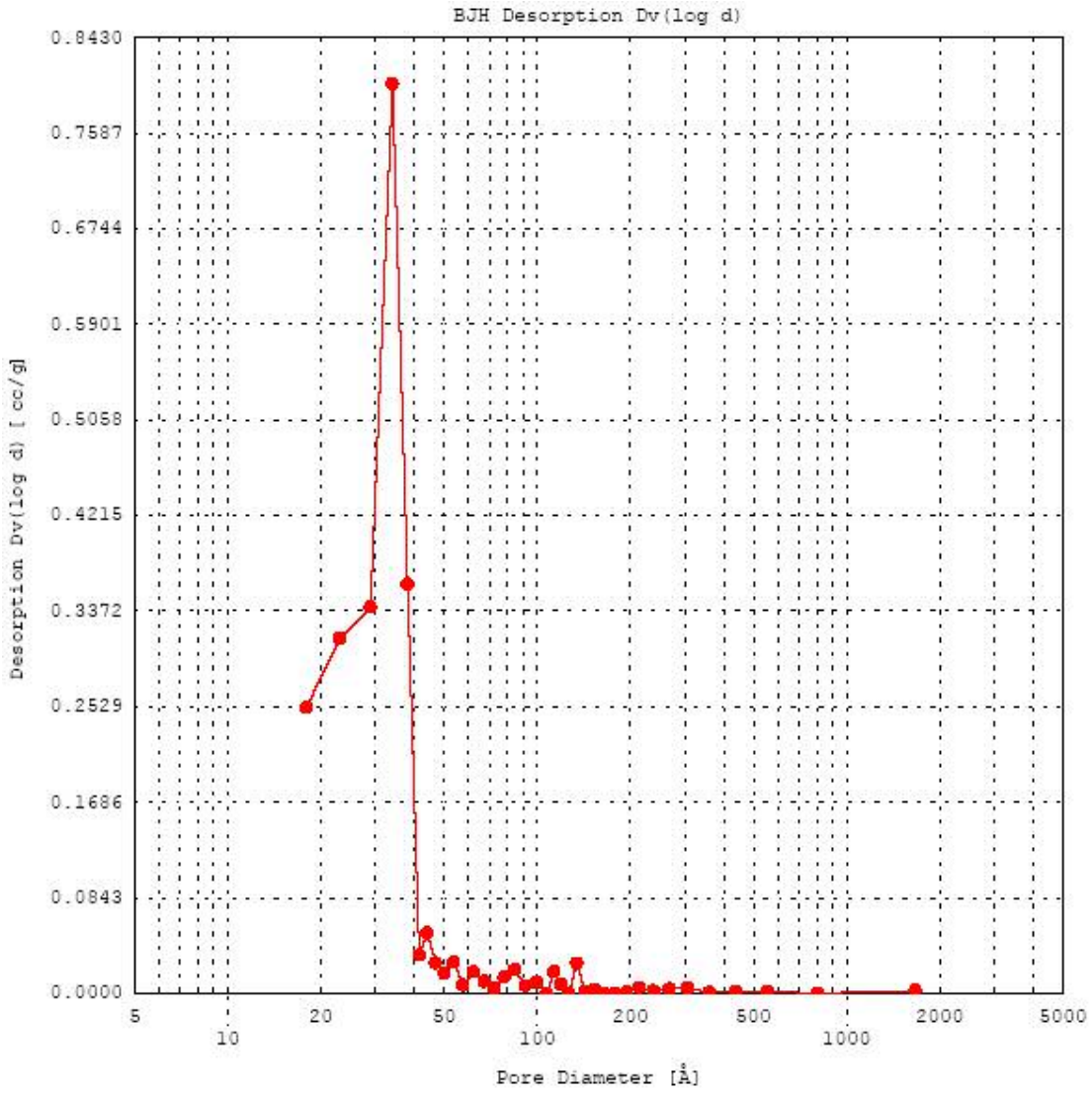

A. 5. Determination of freeze-dried GA-N-CSMG pore size distribution by nitrogen desorption.

GA-N-CSMG has an average pore size of 28 Å and a pore volume of 0.17 mL/gram for all pores of diameter smaller than 2354 Å.

Bibliography

Abourebyeh, H., F. Korber, et al. (1991). "Carrier Membrane as a Stationary Phase for Affinity-Chromatography and Kinetic-Studies of Membrane-Bound Enzymes." Journal of Chromatography-Biomedical Applications **566**(2): 341-350.

Airoldi, C. and O. A. C. Monteiro (2000). "Chitosan-organosilane hybrids - Syntheses, characterization, copper adsorption, and enzyme immobilization." Journal of Applied Polymer Science **77**(4): 797-804.

Airoldi, C. and O. A. C. Monteiro (2003). "Copper adsorption and enzyme immobilization on organosilane-glutaraldehyde hybrids as support." Polymer Bulletin **50**(1-2): 61-68.

Alimarin, I. P., V. I. Fadeeva, et al. (1987). "Concentration, Separation and Determination of Scandium, Zirconium, Hafnium and Thorium with a Silica-Based Sulfonic-Acid Cation-Exchanger." Talanta **34**(1): 103-110.

Alonso, D. O. V. and K. A. Dill (1991). "Solvent Denaturation and Stabilization of Globular-Proteins." Biochemistry **30**(24): 5974-5985.

Amanda, A. and S. K. Mallapragada (2001). "Comparison of protein fouling on heat-treated poly(vinyl alcohol), poly(ether sulfone) and regenerated cellulose membranes using diffuse reflectance infrared Fourier transform spectroscopy." Biotechnology Progress **17**(5): 917-923.

Arkhireeva, A. and J. N. Hay (2003). "Synthesis of sub-200 nm silsesquioxane particles using a modified Stober sol-gel route." Journal of Materials Chemistry **13**(12): 3122-3127.

Arkhireeva, A. and J. N. Hay (2004). "Synthesis of organically-modified silica particles for use as nanofillers in polymer systems." Polymers & Polymer Composites **12**(2): 101-110.

Aso, C. and Y. Aito (1962). "Studies on the Polymerization of Bifunctional Monomers .2. Polymerization of Glutaraldehyde." Makromolekulare Chemie **58**: 195-203.

Bahar, T. and A. Tuncel (2002). "Immobilization of invertase onto crosslinked poly(p-chloromethylstyrene) beads." Journal of Applied Polymer Science **83**(6): 1268-1279.

Baker, L., K. K. Meldrum, et al. (2003). "The role of estrogen in cardiovascular disease." Journal of Surgical Research **115**(2): 325-344.

Barboiu, M., C. Luca, et al. (1997). "Hybrid organic-inorganic fixed site dibenzo 18-crown-6 complexant membranes." Journal of Membrane Science **129**(2): 197-207.

Barrett, E. P., L. G. Joyner, et al. (1951). "The Determination of Pore Volume and Area Distributions in Porous Substances .1. Computations from Nitrogen Isotherms." Journal of the American Chemical Society **73**(1): 373-380.

Baruque, E. A., M. G. A. Baruque, et al. (2001). "Determination of the enzyme reaction rate in a differential fixed-bed reactor: A case study." Brazilian Journal of Chemical Engineering **18**(1): 1-11.

Bayramoglu, G., S. Akgol, et al. (2003). "Covalent immobilisation of invertase onto a reactive film composed of 2-hydroxyethyl methacrylate and glycidyl methacrylate: properties and application in a continuous flow system." Biochemical Engineering Journal **14**(2): 117-126.

Beck, F. and H. Suginome (1991). "Industrial Electroorganic Synthesis in Europe." Journal of Synthetic Organic Chemistry Japan **49**(9): 798-808.

Beck, J. S., J. C. Vartuli, et al. (1994). "Molecular or Supramolecular Templating - Defining the Role of Surfactant Chemistry in the Formation of Microporous and Mesoporous Molecular-Sieves." Chemistry of Materials **6**(10): 1816-1821.

Beck, J. S., J. C. Vartuli, et al. (1992). "A New Family of Mesoporous Molecular-Sieves Prepared with Liquid-Crystal Templates." Journal of the American Chemical Society **114**(27): 10834-10843.

Bergogne, L., S. Fennouh, et al. (2000). "Bio-encapsulation within sol-gel glasses." Molecular Crystals and Liquid Crystals **354**: 667-677.

Berman, K. and P. D. Boyer (1972). "Characteristics of Reversible Heat, Solvent, and Detergent Denaturation of Leucine Binding Protein." Biochemistry **11**(25): 4650-&.

Bernards, T. N. M., M. J. Vanbommel, et al. (1991). "Hydrolysis - Condensation Processes of the Tetra-Alkoxysilanes Tpos, Teos and Tmos in Some Alcoholic Solvents." Journal of Non-Crystalline Solids **134**(1-2): 1-13.

Blake, C. C. F., L. N. Johnson, et al. (1967). "Crystallographic Studies of Activity of Hen Ege-White Lysozyme." Proceedings of the Royal Society of London Series B-Biological Sciences **167**(1009): 378-&.

Blake, C. C. F., G. A. Mair, et al. (1967). "On Conformation of Hen Egg-White Lysozyme Molecule." Proceedings of the Royal Society of London Series B-Biological Sciences **167**(1009): 365-&.

Bois, L., A. Bonhomme, et al. (2003). "Functionalized silica for heavy metal ions adsorption." Colloids and Surfaces a-Physicochemical and Engineering Aspects **221**(1-3): 221-230.

Boissiere, C., M. Kummel, et al. (2001). "Spherical MSU-1 mesoporous silica particles tuned for HPLC." Advanced Functional Materials **11**(2): 129-135.

Bond, R. and J. C. McAuliffe (2003). "Silicon biotechnology: New opportunities for carbohydrate science." Australian Journal of Chemistry **56**(1): 7-11.

Boonstra, A. H. and T. N. M. Bernards (1989). "Hydrolysis Condensation-Reactions in the Acid Step of a 2-Step Silica Sol-Gel Process, Investigated with Si-29 Nmr at -75-Degrees-C." Journal of Non-Crystalline Solids **108**(3): 249-259.

Bowe, C. A. and D. F. Martin (2004). "Extraction of heavy metals by 2-mercaptoethoxy groups attached to silica gel." Journal of Environmental Science and Health Part a-Toxic/Hazardous Substances & Environmental Engineering **39**(6): 1479-1485.

Braco, L. (1995). "Biocatalysis and Biorecognition in Nonaqueous Media - Some Perspectives in Analytical Biochemistry." Mikrochimica Acta **120**(1-4): 231-242.

Branyik, T., G. Kuncova, et al. (1998). "Encapsulation of microbial cells into silica gel." Journal of Sol-Gel Science and Technology **13**(1-3): 283-287.

Brinker, C. J. and G. W. Scherer (1990). Sol-gel science : the physics and chemistry of sol-gel processing. Boston, Academic Press.

Brunauer, S., P. H. Emmett, et al. (1938). "Adsorption of gases in multimolecular layers." Journal of the American Chemical Society **60**: 309-319.

Burkett, S. L., S. D. Sims, et al. (1996). "Synthesis of hybrid inorganic-organic mesoporous silica by co-condensation of siloxane and organosiloxane precursors." Chemical Communications(11): 1367-1368.

Cabrera, K. (2004). "Applications of silica-based monolithic HPLC columns." Journal of Separation Science **27**(10-11): 843-852.

Calnan, B. J., B. Tidor, et al. (1991). "Arginine-Mediated Rna Recognition - the Arginine Fork." Science **252**(5009): 1167-1171.

Camperi, S. A., M. Grasselli, et al. (2004). "Preparation and characterisation of immobilised metal ion hollow-fibre polysulphone membranes. Their application in high-speed pectic enzyme fractionation." Process Biochemistry **39**(8): 1017-1024.

Carriere, M., C. Neves, et al. (2001). "Optimization of plasmids for gene delivery." Stp Pharma Sciences **11**(1): 5-10.

Carturan, G., R. Dal Toso, et al. (2004). "Encapsulation of functional cells by sol-gel silica: actual progress and perspectives for cell therapy." Journal of Materials Chemistry **14**(14): 2087-2098.

Challener, C. (2003). Drug delivery market looks to deliver results: strong growth is projected for the drug delivery market as companies emphasize an integrated approach to pharmaceutical development - Focus 2003: Active Pharmaceutical Ingredients - Industry Overview. Chemical Market Reporter, Schnell Publishing Company, Inc.

Chang, L. C., H. F. Lee, et al. (2001). "Low molecular weight protamine (LMWP) as nontoxic heparin/low molecular weight heparin antidote (I): Preparation and characterization." Aaps Pharmsci **3**(3): art. no.-17.

Chang, L. C., J. F. Liang, et al. (2001). "Low molecular weight protamine (LMWP) as nontoxic heparin/low molecular weight heparin antidote (II): In vitro evaluation of efficacy and toxicity." Aaps Pharmsci **3**(3): art. no.-18.

Chao, M. C., H. P. Lin, et al. (2004). "Controlling the morphology and mesostructural orderness of the mesoporous silica nanoparticles." Chemistry Letters **33**(6): 672-673.

Chao, M. C., H. P. Lin, et al. (2004). "Synthesis of SBA-1 mesoporous silica crystals with tunable pore size using sodium silicate and alkyltrimethylammonium surfactants." Chemistry Letters **33**(4): 374-375.

Chaplin, M. F. and C. Bucke (1992). Enzyme Technology. Cambridge, England, Cambridge University Press.

Cheetham, P. S. J. (1995). The applications of enzymes in industry. Handbook of enzyme biotechnology. London, Ellis**:** 420-40.

Chen, G., P. Zhou, et al. (2004). "Growth of human fetal lung fibroblasts on the natural biomaterial-chitosan scaffold." Acta Chimica Sinica **62**(10): 992-997.
Chen, S. L., P. Dong, et al. (1996). "Kinetics of formation of monodisperse colloidal silica particles through the hydrolysis and condensation of tetraethylorthosilicate." Industrial & Engineering Chemistry Research **35**(12): 4487-4493.
Chitnis, S. R. and M. M. Sharma (1997). "Industrial applications of acid-treated clays as catalysts." Reactive & Functional Polymers **32**(1): 93-115.
Cirpan, A., S. Alkan, et al. (2003). "Immobilization of invertase in conducting copolymers of 3-methylthienyl methacrylate." Bioelectrochemistry **59**(1-2): 29-33.
Coates, J. (2000). Interpretation of Infrared Spectra, A Practical Approach. Encyclopedia of Analytical Chemistry. R. A. Meyers. Chichester, John Wiley & Sons Ltd**:** 10815-10837.
Coltrain, B. K. and L. W. Kelts (1990). "The Chemistry of Hydrolysis and Condensation of Silica Sol-Gel Precursors." Abstracts of Papers of the American Chemical Society **200**: 218-Coll.
Conder, J. R. and B. O. Hayek (2000). "Adsorption kinetics and equilibria of bovine serum albumin on rigid ion-exchange and hydrophobic interaction chromatography matrices in a stirred cell." Biochemical Engineering Journal **6**(3): 215-223.
Console, S., C. Marty, et al. (2003). "Antennapedia and HIV transactivator of transcription (TAT) "protein transduction domains" promote endocytosis of high molecular weight cargo upon binding to cell surface glycosaminoglycans." Journal of Biological Chemistry **278**(37): 35109-35114.
Cserhati, T. and Z. Illes (1991). "Salting-out and Salting-in Effects in the Reversed-Phase Thin-Layer Chromatography of Dansylated Amino-Acids - Effect of Acids." Journal of Liquid Chromatography **14**(8): 1495-1510.
Dasari, G., I. Prince, et al. (1993). "High-Performance Liquid-Chromatography of Amino-Acids, Peptides and Proteins .124. Physical Characterization of Fluidized-Bed Behavior of Chromatographic Packing Materials." Journal of Chromatography **631**(1-2): 115-124.
De, G., D. Kundu, et al. (1993). "Ftir Studies of Gel to Glass Conversion in Teos Fumed Silica-Derived Gels." Journal of Non-Crystalline Solids **155**(3): 253-258.
De Queiroz, A. A. A., R. R. Vargas, et al. (2002). "Lactam-amide graft copolymers as novel support for enzyme immobilization." Journal of Applied Polymer Science **84**(4): 767-777.
De Whalley, H. C. S. (1964). ICUMSA Methods of Sugar Analysis. Amsterdam, Elsevier Publishing Company.
Dong, P. (1998). "Preparation of monodisperse silica spheres by growth of silica sol particles." Acta Physico-Chimica Sinica **14**(2): 109-114.
Duffours, L., T. Woignier, et al. (1996). "Irreversible volume shrinkage of silica aerogels under isostatic pressure." Journal of Non-Crystalline Solids **194**(3): 283-290.

Dunten, R. L., M. Sahintoth, et al. (1993). "Role of the Charge Pair Aspartic Acid-237-Lysine-358 in the Lactose Permease of Escherichia-Coli." Biochemistry **32**(12): 3139-3145.

Etienne, M., B. Lebeau, et al. (2002). "Organically-modified mesoporous silica spheres with MCM-41 architecture." New Journal of Chemistry **26**(4): 384-386.

Etienne, M., S. Sayen, et al. (2002). "Organically-modified mesoporous silica spheres with MCM-41 architecture as sorbents for heavy metals." Nanoporous Materials Iii **141**: 615-622.

Etienne, M. and A. Walcarius (2003). "Analytical investigation of the chemical reactivity and stability of aminopropyl-grafted silica in aqueous medium." Talanta **59**(6): 1173-1188.

EUFIC Chymosin and cheese making. EUFIC.org. http://www.eufic.org/gb/tech/tech02e.htm.

Fersht, A. (1999). Structure and mechanism in protein science : a guide to enzyme catalysis and protein folding. New York, W.H. Freeman.

Flachsba.H and W. Stober (1969). "Preparation of Radioactively Labeled Monodisperse Silica Spheres of Colloidal Size." Journal of Colloid and Interface Science **30**(4): 568-&.

Fox, J. R., P. C. Kokoropoulos, et al. (1987). "Steric Stabilization of Stober Silica Dispersions Using Organosilanes." Journal of Materials Science **22**(12): 4528-4531.

Fuentes, M., J. V. Maquiese, et al. (2004). "New cationic exchanger support for reversible immobilization of proteins." Biotechnology Progress **20**(1): 284-288.

Futaki, S., I. Nakase, et al. (2002). "Translocation of branched-chain arginine peptides through cell membranes: Flexibility in the spatial disposition of positive charges in membrane-permeable peptides." Biochemistry **41**(25): 7925-7930.

Futaki, S., T. Suzuki, et al. (2001). "Arginine-rich peptides - An abundant source of membrane-permeable peptides having potential as carriers for intracellular protein delivery." Journal of Biological Chemistry **276**(8): 5836-5840.

Gamradt, S. C. and J. R. Lieberman (2004). "Genetic modification of stem cells to enhance bone repair." Annals of Biomedical Engineering **32**(1): 136-147.

Giesche, H. (1994). "Synthesis of Monodispersed Silica Powders .2. Controlled Growth Reaction and Continuous Production Process." Journal of the European Ceramic Society **14**(3): 205-214.

Gill, I. and A. Ballesteros (2000). "Bioencapsulation within synthetic polymers (Part 1): sol-gel encapsulated biologicals." Trends in Biotechnology **18**(7): 282-296.

Goetz, V., M. Remaud, et al. (1991). "A Novel Magnetic Silica Support for Use in Chromatographic and Enzymatic Bioprocessing." Biotechnology and Bioengineering **37**(7): 614-626.

Goldstein, A. and J. O. Lampen (1975). "Beta-D-fructofuranoside fructohydrolase from yeast." Methods in Enzymology **42**: 504-11.

Gomez, L. and R. Villalonga (2000). "Functional stabilization of invertase by covalent modification with pectin." Biotechnology Letters **22**(14): 1191-1195.
Gordon, N. F., C. M. V. Moore, et al. (1990). "An Overview of Continuous Protein-Purification Processes." Biotechnology Advances **8**(4): 741-762.
Gosting, L. J. (1956). "Measurement and Interpretation of Diffusion Coefficients of Proteins." Advances in Protein Chemistry **11**: 429-554.
Groen, J. C., L. A. A. Peffer, et al. (2003). "Pore size determination in modified micro- and mesoporous materials. Pitfalls and limitations in gas adsorption data analysis." Microporous and Mesoporous Materials **60**(1-3): 1-17.
Gu, S. C., T. Kondo, et al. (2004). "Preparation of silica-poly styrene core-shell particles up to micron sizes." Journal of Colloid and Interface Science **272**(2): 314-320.
Gupta, M. N. (1992). "Enzyme Function in Organic-Solvents." European Journal of Biochemistry **203**(1-2): 25-32.
Hah, H. J., J. I. Um, et al. (2004). "New synthetic route for preparing rattle-type silica particles with metal cores." Chemical Communications(8): 1012-1013.
Handy, B., K. L. Walther, et al. (1991). In Preparation of Catalysts V. Studies in Surface Science and Catalysis. P. A. Jacobs, P. Grange and D. B. Amsterdam, Elsevier Science. **63:** 239.
Harris, B., R. G. Cooke, et al. (1998). "Sol-gel composites - A low cost manufacturing route." Industrial Ceramics **18**(1): 33-37.
Hejazi, R. and M. Amiji (2003). "Chitosan-based gastrointestinal delivery systems." Journal of Controlled Release **89**(2): 151-165.
Hench, L. L. and J. K. West (1990). "The Sol-Gel Process." Chemical Reviews **90**(1): 33-72.
Henry, C. M. (2003). "Breaching Barriers." Chemical & Engineering News **81**(34): 35-43, 55.
Horrow, J. C. (1985). "Adverse Reactions to Protamine." International Anesthesiology Clinics **23**(3): 133-144.
Horrow, J. C. (1985). "Protamine - a Review of Its Toxicity." Anesthesia and Analgesia **64**(3): 348-361.
Hossain, M. M. and D. D. Do (1985). "Fundamental-Studies of Glucose-Oxidase Immobilization on Controlled Pore Glass." Biotechnology and Bioengineering **27**(6): 842-851.
Huh, S., J. W. Wiench, et al. (2003). "Organic functionalization and morphology control of mesoporous silicas via a co-condensation synthesis method." Chemistry of Materials **15**(22): 4247-4256.
Huttl, R., K. Oehlschlager, et al. (1999). "Calorimetric investigations of the enzyme catalyzed sucrose hydrolysis." Thermochimica Acta **325**(1): 1-4.
Ikehata, K., I. D. Buchanan, et al. (2004). "Recent developments in the production of extracellular fungal peroxidases and laccases for waste treatment *." Journal of Environmental Engineering and Science **3**(1): 1-19.
Isaacs, I. J. (1996). "The strategy employed for purification of protein-based biopharmaceutical products." Australasian Biotechnology **6**(2): 88-92.

Iznaga-Escobar, N., A. K. Mishra, et al. (2004). "Factors affecting pharmacokinetics of monoclonal antibodies: A review article." Methods and Findings in Experimental and Clinical Pharmacology **26**(2): 123-127.

Jelinek, L., P. Dong, et al. (1992). "Study of the Stober Reaction .1. Properties of Colloidal Silica Spheres Prepared Via Alkoxide Hydrolysis." Langmuir **8**(9): 2152-2164.

Jesionowski, T. (2002). "Synthesis of organic-inorganic hybrids via adsorption of dye on an amino silane-functionalised silica surface." Dyes and Pigments **55**(2-3): 133-141.

Keeley, C. T. (1983). "Sodium-Silicate - the Key Ingredient in Detergent Agglomeration." Journal of the American Oil Chemists Society **60**(7): 1370-1372.

Khobragade, C. N. and S. G. Chandel (2002). "Comparative study of catalytic activity of immobilized invertase in sodium alginate gel on sucrose hydrolysis." Indian Journal of Chemical Technology **9**(6): 535-539.

Khushalani, D., G. A. Ozin, et al. (1999). "Glycometallate surfactants. Part 1: non-aqueous synthesis of mesoporous silica." Journal of Materials Chemistry **9**(7): 1483-1489.

Kickelbick, G. (2004). "Hybrid inorganic-organic mesoporous materials." Angewandte Chemie-International Edition **43**(24): 3102-3104.

Kim, J. H., H. J. Kang, et al. (2004). "One-step purification of poly-his tagged penicillin G acylase expressed in E-coli." Journal of Microbiology and Biotechnology **14**(2): 231-236.

Kim, M. S., S. I. Seok, et al. (2003). "Encapsulation of water-soluble dye in spherical sol-gel silica matrices." Journal of Sol-Gel Science and Technology **27**(3): 355-361.

King, S. C., C. L. Hansen, et al. (1991). "The Interaction between Aspartic Acid-237 and Lysine-358 in the Lactose Carrier of Escherichia-Coli." Biochimica Et Biophysica Acta **1062**(2): 177-186.

Kiralp, S., L. Toppare, et al. (2003). "Immobilization of invertase in copolymers of thiophene functionalized menthyl ester with pyrrole." Synthetic Metals **135**(1-3): 79-80.

Kistler, S. (1931). "Coherent Expanded Aerogels and Jellies." Nature **227**: 741.

Kistler, S. S. (1937). Method of producing aerogels. USA**:** 7.

Klemperer, W. G., V. V. Mainz, et al. (1988). Beter Ceramics Through Chemistry III. C. J. Brinker, D. E. Clark and D. R. Ulrich. Pittsburgh, PA, Materials Research Society. **121:** 15.

Koizumi, S. (2004). "Production of oligosaccharides by coupling engineered bacteria." Synthesis of Carbohydrates through Biotechnology **873**: 153-164.

Kraume, M., A. Gabler, et al. (2004). "Influence of physical properties on drop size distributions of stirred liquid-liquid dispersions." Chemical Engineering & Technology **27**(3): 330-334.

Kresge, C. T., M. E. Leonowicz, et al. (1992). "Ordered Mesoporous Molecular-Sieves Synthesized by a Liquid-Crystal Template Mechanism." Nature **359**(6397): 710-712.

Krishna, S. H. (2002). "Developments and trends in enzyme catalysis in nonconventional media." Biotechnology Advances **20**: 239-267.
Kruk, M., T. Asefa, et al. (2002). "Metamorphosis of ordered mesopores to micropores: Periodic silica with unprecedented loading of pendant reactive organic groups transforms to periodic microporous silica with tailorable pore size." Journal of the American Chemical Society **124**(22): 6383-6392.
Kumar, M. N. V. R., G. Hellermann, et al. (2004). "Nanoparticle-mediated gene delivery: state of the art." Expert Opinion on Biological Therapy **4**(8): 1213-1224.
Kupcu, S., M. Sara, et al. (1991). "Chemical Modification of Crystalline Ultrafiltration Membranes and Immobilization of Macromolecules." Journal of Membrane Science **61**: 167-175.
Kurita, K. (2001). "Controlled functionalization of the polysaccharide chitin." Progress in Polymer Science **26**(9): 1921-1971.
Lampen, J. O. (1971). The Enzymes. New York, NY, Academic Press.
Laruelle, G., J. Parvole, et al. (2004). "Block copolymer grafted-silica particles: a core/double shell hybrid inorganic/organic material." Polymer **45**(15): 5013-5020.
Laszlo, P. (1998). "Heterogeneous catalysis of organic reactions." Journal of Physical Organic Chemistry **11**(5): 356-361.
Lee, B., Y. Kim, et al. (2001). "Synthesis of functionalized porous silicas via templating method as heavy metal ion adsorbents: the introduction of surface hydrophilicity onto the surface of adsorbents." Microporous and Mesoporous Materials **50**(1): 77-90.
Lee, L. M., L. C. Chang, et al. (2001). "Low molecular weight protamine as nontoxic heparin/low molecular weight heparin antidote (III): Preliminary in vivo evaluation of efficacy and toxicity using a canine model." Aaps Pharmsci **3**(3): art. no.-19.
Li, G. T., S. Bhosale, et al. (2004). "Template synthesis of functionalized polystyrene in ordered silicate channels." Chemical Communications(15): 1760-1761.
Li, Z. Y., Z. L. Wu, et al. (2003). "New methods in immobilization: Biocapsulation by epoxy-amine resins and silicone elastomers." Chinese Journal of Organic Chemistry **23**(2): 150-154.
Liang, J. F., L. Zhen, et al. (2003). "A less toxic heparin antagonist - Low molecular weight protamine." Biochemistry-Moscow **68**(1): 116-120.
Lim, M. H. and A. Stein (1999). "Comparative studies of grafting and direct syntheses of inorganic-organic hybrid mesoporous materials." Chemistry of Materials **11**(11): 3285-3295.
Liu, R. L., Y. Xu, et al. (2004). "Liquid-state Si-29 NMR study on the chemical kinetics of Stober synthesis." Acta Chimica Sinica **62**(1): 22-27.
Liu, Y. L. and S. H. Li (2004). "Poly(dimethyl siloxane) star polymers having nanosized silica cores." Macromolecular Rapid Communications **25**(15): 1392-1395.
Lu, Y., J. McLellan, et al. (2004). "Synthesis and crystallization of hybrid spherical colloids composed of polystyrene cores and silica shells." Langmuir **20**(8): 3464-3470.

Mahmoud, M. E., M. M. El-Essawi, et al. (2004). "Characterization of surface modification, thermal stability, and metal selectivity properties of silica gel phases-immobilized dithiocarbamate derivatives." Journal of Liquid Chromatography & Related Technologies **27**(11): 1711-1727.

Mahmoud, M. E., M. S. Masoud, et al. (2004). "Synthesis, characterization and selective metal binding properties of physically adsorbed 2-thiouracil on the surface of porous silica and alumina." Microchimica Acta **147**(1-2): 111-115.

Majors, R. E. (2003). "A review of HPLC column packing technology." American Laboratory **35**(20): 46-+.

Mansfeld, J. and A. Schellenberger (1987). "Invertase Immobilized on Macroporous Polystyrene - Properties and Kinetic Characterization." Biotechnology and Bioengineering **29**(1): 72-78.

Mansour, E. H. and F. M. Dawoud (2003). "Immobilization of invertase on celite and on polyacrylamide by an absorption procedure." Journal of the Science of Food and Agriculture **83**(5): 446-450.

Mateo, C., R. Torres, et al. (2003). "Epoxy-amino groups: A new tool for improved immobilization of proteins by the epoxy method." Biomacromolecules **4**(3): 772-777.

Michaelis, L. and M. L. Menton (1913). "The kinetics of invertin action." Biochem Z **49**: 333-369.

Miller, G. L. (1959). "Use of Dinitrosalicylic Acid Reagent for Determination of Reducing Sugar." Analytical Chemistry **31**(3): 426-428.

Miyamoto, K., T. Fujii, et al. (1973). "Intraparticle Diffusion in Reaction Catalyzed by Immobilized Glucoamylase." Journal of Fermentation Technology **51**(8): 566-574.

Molvinger, K., F. Quignard, et al. (2004). "Porous chitosan-silica hybrid microspheres as a potential catalyst." Chemistry of Materials **16**(17): 3367-3372.

Monsan, P. and D. Combes (1988). "Enzyme Stabilization by Immobilization." Methods in Enzymology **137**: 584-598.

Monsan, P., D. Combes, et al. (1984). "Invertase Covalent Grafting onto Corn Stover." Biotechnology and Bioengineering **26**(7): 658-664.

Monteiro, O. A. C. and C. Airoldi (1999). "Some studies of crosslinking chitosan-glutaraldehyde interaction in a homogeneous system." International Journal of Biological Macromolecules **26**(2-3): 119-128.

Moreno, J. M. and J. V. Sinisterra (1994). "Immobilization of Lipase from Candida-Cylindracea on Inorganic Supports." Journal of Molecular Catalysis **93**(3): 357-369.

Mori, Y. and T. J. Pinnavaia (2001). "Optimizing organic functionality in mesostructured silica: direct assembly of mercaptopropyl groups in wormhole framework structures." Chemistry of Materials **13**(6): 2173-2178.

Moss, G. P. (January 23, 2004). Enzyme Nomenclature. London, International Union of Biochemistry and Molecular Biology. http://www.chem.qmul.ac.uk/iubmb/enzyme/.

Nair, B. N., W. J. Elferink, et al. (1996). "Sol-gel synthesis and characterization of microporous silica membranes .1. SAXS study on the growth of polymeric structures." Journal of Colloid and Interface Science **178**(2): 565-570.
Nakagawa, K., K. Haraguchi, et al. (1998). "Concentration of some metal ions using 2-(5-bromo-2-pyridylazo)-5-(N-propyl-N-sulfopropylamino)phenol and C-18-bonded silica gel." Analytical Sciences **14**(2): 317-320.
Narayanan, S. R. (1994). "Preparative Affinity-Chromatography of Proteins." Journal of Chromatography A **658**(2): 237-258.
Nassar, M. M., O. A. Fadali, et al. (1999). "Thermal studies on paper treated with flame-retardant." Fire and Materials **23**(3): 125-129.
Nefedov, B. K. (1992). "Physicochemical Properties of High-Silica Zeolites (Review)." Chemistry and Technology of Fuels and Oils **28**(1-2): 103-117.
Ober, C. K. and G. Wegner (1997). "Polyelectrolyte-surfactant complexes in the solid state: Facile building blocks for self-organizing materials." Advanced Materials **9**(1): 17-&.
Osterloh, F., H. Hiramatsu, et al. (2004). "Alkanethiol-induced structural rearrangements in silica-gold core-shell-type nanoparticle clusters: An opportunity for chemical sensor engineering." Langmuir **20**(13): 5553-5558.
Overberger, C. G., S. Ishida, et al. (1962). "Intra-Intermolecular Polymerization of Glutaraldehyde." Journal of Polymer Science **62**(173): S1-&.
Pacek, A. W., P. Ding, et al. (2001). "The effect of volume fraction and impeller speed on the structure and drop size in aqueous/aqueous dispersions." Chemical Engineering Science **56**(10): 3247-3255.
Pajonk, G. M. (2003). "Some applications of silica aerogels." Colloid and Polymer Science **281**(7): 637-651.
Pang, J. B., K. Y. Qiu, et al. (2002). "Recent progress in research on mesoporous materials I: Synthesis." Journal of Inorganic Materials **17**(3): 407-414.
Pannier, A. K. and L. D. Shea (2004). "Controlled release systems for DNA delivery." Molecular Therapy **10**(1): 19-26.
Papineau, A. M., D. G. Hoover, et al. (1991). "Antimicrobial Effect of Water-Soluble Chitosans with High Hydrostatic-Pressure." Food Biotechnology **5**(1): 45-57.
Park, Y. J., J. F. Liang, et al. (2003). "Low molecular weight protamine as an efficient and nontoxic gene carrier: in vitro study." Journal of Gene Medicine **5**(8): 700-711.
Perez, M., N. Zambrano, et al. (2002). "Surfactant-oil-water systems near the affinity inversion. XII. Emulsion drop size versus formulation and composition." Journal of Dispersion Science and Technology **23**(1-3): 55-63.
Perry, C. C. and X. C. Li (1991). "Structural Studies of Gel Phases .1. Infrared Spectroscopic Study of Silica Monoliths - the Effect of Thermal History on Structure." Journal of the Chemical Society-Faraday Transactions **87**(5): 761-766.
Phillips, D. C. (1967). "Hen Egg-White Lysozyme Molecule." Proceedings of the National Academy of Sciences of the United States of America **57**(3): 484-&.
Pizarro, C., M. A. FernandezTorroba, et al. (1997). "Optimization by experimental design of polyacrylamide gel composition as support for enzyme

immobilization by entrapment." Biotechnology and Bioengineering **53**(5): 497-506.
Raman, N. K., T. L. Ward, et al. (1993). "Catalyst Dispersion on Supported Ultramicroporous Inorganic Membranes Using Derivatized Silylation Agents." Applied Catalysis a-General **96**(1): 65-82.
Rashidova, S. S., D. S. Shakarova, et al. (2004). "Bionanocompositional chitosan-silica sorbent for liquid chromatography." Journal of Chromatography B-Analytical Technologies in the Biomedical and Life Sciences **800**(1-2): 49-53.
Rasmusse.Ke and Albrecht.J (1974). "Glutaraldehyde - Influence of Ph, Temperature, and Buffering on Polymerization Rate." Histochemistry **38**(1): 19-26.
Righetti, P. G. and T. Caravaggio (1976). "Isoelectric Points and Molecular-Weights of Proteins - Table." Journal of Chromatography **127**(1): 1-28.
Rosa, A. H., A. A. Vicente, et al. (2000). "A new application of humic substances: activation of supports for invertase immobilization." Fresenius Journal of Analytical Chemistry **368**(7): 730-733.
Sanchez, C., G. J. D. A. Soler-Illia, et al. (2001). "Designed hybrid organic-inorganic nanocomposites from functional nanobuilding blocks." Chemistry of Materials **13**(10): 3061-3083.
Sapse, A. M., R. Rothchild, et al. (2002). "The role of salt bridge formation in glucagon: An experimental and theoretical study of glucagon analogs and peptide fragments of glucagon." Molecular Medicine **8**(5): 251-262.
Sartori, G., F. Bigi, et al. (2004). "Catalytic activity of aminopropyl xerogels in the selective synthesis of (E)-nitrostyrenes from nitroalkanes and aromatic aldehydes." Journal of Catalysis **222**(2): 410-418.
Sayari, A. and S. Hamoudi (2001). "Periodic mesoporous silica-based organic - Inorganic nanocomposite materials." Chemistry of Materials **13**(10): 3151-3168.
Schellman, J. A. and R. B. Hawkes (1979). "Protein Stability from Thermal and Solvent Denaturation Curves." Hoppe-Seylers Zeitschrift Fur Physiologische Chemie **360**(8): 1015-1015.
Scherer, G. W. (1988). "Aging and Drying of Gels." Journal of Non-Crystalline Solids **100**(1-3): 77-92.
Schuster, J. M., P. K. Garg, et al. (1991). "Improved Therapeutic Efficacy of a Monoclonal-Antibody Radioiodinated Using N-Succinimidyl-3-(Tri-Normal-Butylstannyl)Benzoate." Cancer Research **51**(16): 4164-4169.
Selber, K., F. Tjerneld, et al. (2004). "Large-scale separation and production of engineered proteins, designed for facilitated recovery in detergent-based aqueous two-phase extraction systems." Process Biochemistry **39**(7): 889-896.
Shah, J., S. S. Kim, et al. (2004). "A versatile pathway for the direct assembly of organo-functional mesostructures from sodium silicate." Chemical Communications(5): 572-573.
Shuler, M. and F. Kargi (1992). Bioprocess Engineering. Englewood Cliffs, NJ, Prentice Hall.
Stepuro, I. I., E. A. Lapshina, et al. (1991). "Study of Heat Denaturation of Human Serum-Albumin in Aqueous Alcohol and Aqueous Salt-Solutions in the Presence of Organic-Ligands." Molecular Biology **25**(2): 275-284.

Stinson, S. C. (2000). "Fine Chemicals Fair." Chemical & Engineering News **78**(49): 35.
Stober, W., A. Fink, et al. (1968). "Controlled Growth of Monodisperse Silica Spheres in Micron Size Range." Journal of Colloid and Interface Science **26**(1): 62-&.
Suleman, Y. H. and E. M. S. Hamid (1997). "Chemically modified soluble sodium silicate as an adhesive for solid wood panels." Mokuzai Gakkaishi **43**(10): 855-860.
Sumner, J. B. (1926). "The isolation and crystallization of the enzyme urease." Journal of Biological Chemistry **69**: 435-441.
Tan, M. Q., Z. Q. Ye, et al. (2004). "Preparation and time-resolved fluorometric application of luminescent europium nanoparticles." Chemistry of Materials **16**(12): 2494-2498.
Tan, W. H., K. M. Wang, et al. (2004). "Bionanotechnology based on silica nanoparticles." Medicinal Research Reviews **24**(5): 621-638.
Tasleem, S., S. Durani, et al. (2004). "Salting-out coefficients and activity coefficients of alkali and alkaline earth metals in aqueous and aqueous organic mixed solvents." Journal of the Chemical Society of Pakistan **26**(1): 39-43.
Tewari, P. H., A. J. Hunt, et al. (1985). "Ambient-Temperature Supercritical Drying of Transparent Silica Aerogels." Materials Letters **3**(9-10): 363-367.
Thanoo, B. C., M. C. Sunny, et al. (1992). "Cross-Linked Chitosan Microspheres - Preparation and Evaluation as a Matrix for the Controlled Release of Pharmaceuticals." Journal of Pharmacy and Pharmacology **44**(4): 283-286.
Tharakan, J., F. Highsmith, et al. (1992). "Physical and Biochemical-Characterization of 5 Commercial Resins for Immunoaffinity Purification of Factor-Ix." Journal of Chromatography **595**(1-2): 103-111.
Tikhomirova, T. I., V. I. Fadeeva, et al. (1991). "Sorption of Noble-Metal Ions on Silica with Chemically Bonded Nitrogen-Containing Ligands." Talanta **38**(3): 267-274.
Tischer, W. and V. Kasche (1999). "Immobilized enzymes: crystals or carriers?" Trends in Biotechnology **17**(8): 326-335.
Tischer, W. and F. Wedekind (1999). "Immobilized enzymes: Methods and applications." Biocatalysis - from Discovery to Application **200**: 95-126.
Tong, A., Y. Akama, et al. (1990). "Selective Preconcentration of Au(Iii), Pt(Iv) and Pd(Ii) on Silica-Gel Modified with Gamma-Aminopropyltriethoxysilane." Analytica Chimica Acta **230**(1): 179-181.
Torchilin, V. P., T. S. Levchenko, et al. (2003). "Cell transfection in vitro and in vivo with nontoxic TAT peptide-liposome-DNA complexes." Proceedings of the National Academy of Sciences of the United States of America **100**(4): 1972-1977.
Torchilin, V. P., R. Rammohan, et al. (2001). "TAT peptide on the surface of liposomes affords their efficient intracellular delivery even at low temperature and in the presence of metabolic inhibitors." Proceedings of the National Academy of Sciences of the United States of America **98**(15): 8786-8791.

Torres, R., C. Mateo, et al. (2002). "Reversible immobilization of invertase on Sepabeads coated with polyethyleneimine: Optimization of the biocatalyst's stability." Biotechnology Progress **18**(6): 1221-1226.
Tyagi, R. and M. N. Gupta (1998). "Chemical modification and chemical cross-linking for protein/enzyme stabilization." Biochemistry-Moscow **63**(3): 334-344.
Uversky, V. N. (1993). "Use of Fast Protein Size-Exclusion Liquid-Chromatography to Study the Unfolding of Proteins Which Denature through the Molten Globule." Biochemistry **32**(48): 13288-13298.
Vansant, E. F., P. van der Voort, et al. (1995). Characterization and chemical modification of the silica surface. Amsterdam; New York, Elsevier.
Vicente, A. A. (2000). Preparacao de acucau invertido por meio de invertase imobiliizada emm silica. Araraquara-SP, Universidade Estadual Paulista.
Walcarius, A. and C. Delacote (2003). "Rate of access to the binding sites in organically modified silicates. 3. Effect of structure and density of functional groups in mesoporous solids obtained by the co-condensation route." Chemistry of Materials **15**(22): 4181-4192.
Wang, R., U. Narang, et al. (1993). "Affinity of Antifluorescein Antibodies Encapsulated within a Transparent Sol-Gel Glass." Analytical Chemistry **65**(19): 2671-2675.
Wang, W., X. A. Fu, et al. (1993). "Preparation of Submicron Spherical-Particles of Silica by the Water-in-Oil Microemulsion Method." Colloids and Surfaces a-Physicochemical and Engineering Aspects **81**: 177-180.
Weetall, H. H. (1993). "Preparation of Immobilized Proteins Covalently Coupled through Silane Coupling Agents to Inorganic Supports." Applied Biochemistry and Biotechnology **41**(3): 157-188.
Wei, W. L., S. J. Hao, et al. (2004). "Catalytic behavior of silica-supported chitosan-platinum-iron complex for asymmetric hydrogenation of ketones." Polymers for Advanced Technologies **15**(5): 287-290.
Weiss, M. E., D. Nyhan, et al. (1989). "Association of Protamine Ige and Igg Antibodies with Life-Threatening Reactions to Intravenous Protamine." New England Journal of Medicine **320**(14): 886-892.
Wender, P. A., D. J. Mitchell, et al. (2000). "The design, synthesis, and evaluation of molecules that enable or enhance cellular uptake: Peptoid molecular transporters." Proceedings of the National Academy of Sciences of the United States of America **97**(24): 13003-13008.
Wheelwright, S. M. (1991). Protein Purification: Design and Scale up of Downstream Processing. New York, Hanser Publishers.
Winter, M. (2003). WebElements, the periodic table on the WWW. UK, WebElements Ltd. http://www.webelements.com/webelements/elements/text/Si/key.html.
Woignier, T., F. Despetis, et al. (2000). "Mechanical properties of gel-derived materials." Journal of Sol-Gel Science and Technology **19**(1-3): 163-169.
Wu, J. M. and Y. Y. Wang (2003). "Immobilized chitosan as a selective absorbent for the nickel removal in water sample." Journal of Environmental Sciences-China **15**(5): 633-638.

Xu, L., Y. Q. Feng, et al. (2004). "Applications of ordered mesoporous materials in separation science." Chinese Journal of Analytical Chemistry **32**(3): 374-380.
Yan, S. B. (1996). "Review of conformation-specific affinity purification methods for plasma vitamin K-dependent proteins." Journal of Molecular Recognition **9**(3): 211-218.
Ying, J. Y., J. B. Benziger, et al. (1993). "Structural Evolution of Alkoxide Silica-Gels to Glass - Effect of Catalyst Ph." Journal of the American Ceramic Society **76**(10): 2571-2582.
Yokoi, T., H. Yoshitake, et al. (2004). "Synthesis of amino-functionalized MCM-41 via direct co-condensation and post-synthesis grafting methods using mono-, di- and tri-amino-organoalkoxysilanes." Journal of Materials Chemistry **14**(6): 951-957.
Yoshitake, H., T. Yokoi, et al. (2003). "Adsorption behavior of arsenate at transition metal cations captured by amino-functionalized mesoporous silicas." Chemistry of Materials **15**(8): 1713-1721.
Yu, N. Y., Y. J. Gong, et al. (2004). "One-pot synthesis of mesoporous organosilicas using sodium silicate as a substitute for tetraalkoxysilane." Microporous and Mesoporous Materials **72**(1-3): 25-32.
Zeng, Z., J. Yu, et al. (2004). "Preparation of epoxy-functionalized polystyrene/silica core-shell composite nanoparticles." Journal of Polymer Science Part a-Polymer Chemistry **42**(9): 2253-2262.
Zhang, S. C. and X. G. Li (2004). "Synthesis and characterization of CaCO3@SiO2 core-shell nanoparticles." Powder Technology **141**(1-2): 75-79.
Zhao, D., W. P. Qin, et al. (2004). "Laser selective spectroscopy of europium complex embedded in colloidal silica spheres." Chemical Physics Letters **388**(4-6): 400-405.
Zuhlke, J., D. Knopp, et al. (1995). "Sol-Gel Glass as a New Support Matrix in Immunoaffinity Chromatography." Fresenius Journal of Analytical Chemistry **352**(7-8): 654-659.